Detailed Weather and Terrain Analysis for Aircraft Noise Modeling

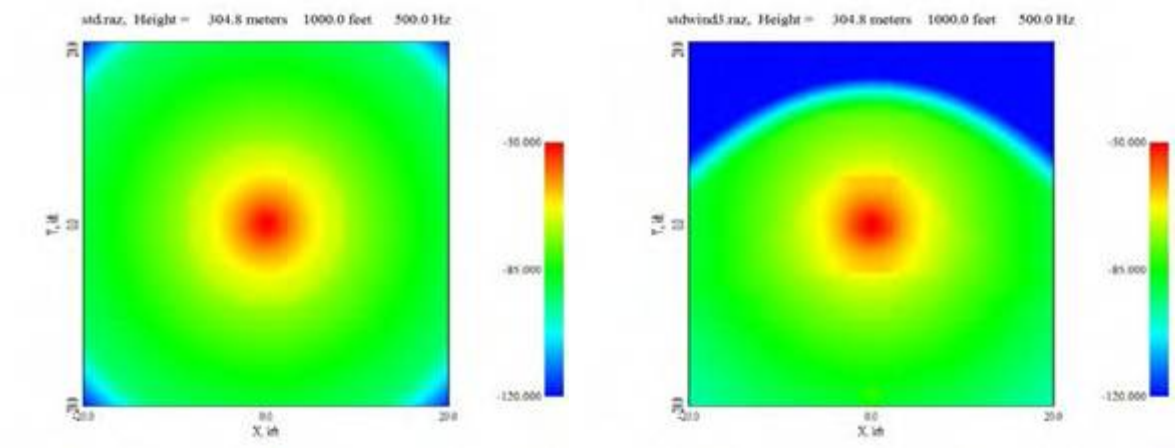

Final Contractor Report — April 2013

DOT-VNTSC-FAA-14-08

Wyle Report 13-01

Prepared for:

U.S. Department of Transportation

John A. Volpe National Transportation Systems Center

Cambridge, MA 02142-1093

Volpe

The National Transportation Systems Center

Notice

REPORT DOCUMENTATION PAGE

Form Approved
OMB No. 0704-0188

1. AGENCY USE ONLY (Leave blank)	2. REPORT DATE	3. REPORT TYPE AND DATES COVERED
	April 2013	Final Contractor Report

4. TITLE AND SUBTITLE
Detailed Weather and Terrain Analysis for Aircraft Noise Modeling

5a. FUNDING NUMBERS
FA4TCK MLB45

6. AUTHOR(S)
Kenneth J. Plotkin, Juliet A. Page, Yuriy Gurovich, Christopher M. Hobbs

5b. CONTRACT NUMBER
DTRT57-10-D-30014 DTRTV-T02002

7. PERFORMING ORGANIZATION NAME(S) AND ADDRESS(ES)
Wyle
Environmental and Energy Research and Consulting
200 12th Street South
Suite 900
Arlington, VA 22202

8. PERFORMING ORGANIZATION REPORT NUMBER
Wyle Report 13-01

9. SPONSORING/MONITORING AGENCY NAME(S) AND ADDRESS(ES)
U.S. Department of Transportation
Federal Aviation Administration
Office of Environment and Energy, AEE-100
Washington, DC 20591

U.S. Department of Transportation
John A. Volpe National Transportation Systems Center
Environmental Measurement and Modeling Division, RVT-41
Cambridge, MA 02142-1093

10. SPONSORING/MONITORING AGENCY REPORT NUMBER
DOT-VNTSC-FAA-14-08

11. SUPPLEMENTARY NOTES
FAA Program Manager: Hua "Bill" He (AEE, Office of Environment and Energy, Noise Division)

12a. DISTRIBUTION/AVAILABILITY STATEMENT

12b. DISTRIBUTION CODE

13. ABSTRACT (Maximum 200 words)

A study has been conducted supporting refinement and development of FAA's airport environmental analysis tools. Tasks conducted in this study are: (1) updated analysis of the 1997 KDEN noise model validation study with newer versions of INM and related tools; (2) analyze a sample of the 1997 KDEN validation data with simulation modeling; (3) develop algorithms for detailed weather modeling in FAA tools; (4) assess available validation data from studies at other airports; and (5) develop simplified terrain processing implementation, adapting the process successfully employed in simulation models.

14. SUBJECT TERMS
noise, aircraft noise, airport noise, INM, Integrated Noise Model, AEDT, Aviation Environmental Design Tool, noise prediction, computer noise model, weather modeling, airport environmental analysis, model validation, terrain processing

15. NUMBER OF PAGES
107

16. PRICE CODE

17. SECURITY CLASSIFICATION OF REPORT	18. SECURITY CLASSIFICATION OF THIS PAGE	19. SECURITY CLASSIFICATION OF ABSTRACT	20. LIMITATION OF ABSTRACT
Unclassified	Unclassified	Unclassified	

NSN 7540-01-280-5500

Standard Form 298 (Rev. 2-89)
Prescribed by ANSI Std. 239-18
298-102

SI* (MODERN METRIC) CONVERSION FACTORS

APPROXIMATE CONVERSIONS TO SI UNITS

Symbol	When You Know	Multiply By	To Find	Symbol
		LENGTH		
in	inches	25.4	millimeters	mm
ft	feet	0.305	meters	m
yd	yards	0.914	meters	m
mi	miles	1.61	kilometers	km
		AREA		
in^2	square inches	645.2	square millimeters	mm^2
ft^2	square feet	0.093	square meters	m^2
yd^2	square yard	0.836	square meters	m^2
ac	acres	0.405	hectares	ha
mi^2	square miles	2.59	square kilometers	km^2
		VOLUME		
fl oz	fluid ounces	29.57	milliliters	mL
gal	gallons	3.785	liters	L
ft^3	cubic feet	0.028	cubic meters	m^3
yd^3	cubic yards	0.765	cubic meters	m^3
		NOTE: volumes greater than 1000 L shall be shown in m^3		
		MASS		
oz	ounces	28.35	grams	g
lb	pounds	0.454	kilograms	kg
T	short tons (2000 lb)	0.907	megagrams (or "metric ton")	Mg (or "t")
oz	ounces	28.35	grams	g
		TEMPERATURE (exact degrees)		
°F	Fahrenheit	5 (F-32)/9 or (F-32)/1.8	Celsius	°C
		ILLUMINATION		
fc	foot-candles	10.76	lux	lx
fl	foot-Lamberts	3.426	$candela/m^2$	cd/m^2
		FORCE and PRESSURE or STRESS		
lbf	poundforce	4.45	newtons	N
lbf/in^2	poundforce per square inch	6.89	kilopascals	kPa

APPROXIMATE CONVERSIONS FROM SI UNITS

Symbol	When You Know	Multiply By	To Find	Symbol
		LENGTH		
mm	millimeters	0.039	inches	in
m	meters	3.28	feet	ft
m	meters	1.09	yards	yd
km	kilometers	0.621	miles	mi
		AREA		
mm^2	square millimeters	0.0016	square inches	in^2
m^2	square meters	10.764	square feet	ft^2
m^2	square meters	1.195	square yards	yd^2
ha	hectares	2.47	acres	ac
km^2	square kilometers	0.386	square miles	mi^2
		VOLUME		
mL	milliliters	0.034	fluid ounces	fl oz
L	liters	0.264	gallons	gal
m^3	cubic meters	35.314	cubic feet	ft^3
m^3	cubic meters	1.307	cubic yards	yd^3
mL	milliliters	0.034	fluid ounces	fl oz
		MASS		
g	grams	0.035	ounces	oz
kg	kilograms	2.202	pounds	lb
Mg (or "t")	megagrams (or "metric ton")	1.103	short tons (2000 lb)	T
g	grams	0.035	ounces	oz
		TEMPERATURE (exact degrees)		
°C	Celsius	1.8C+32	Fahrenheit	°F
		ILLUMINATION		
lx	lux	0.0929	foot-candles	fc
cd/m^2	$candela/m^2$	0.2919	foot-Lamberts	fl
		FORCE and PRESSURE or STRESS		
N	newtons	0.225	poundforce	lbf
kPa	Kilopascals	0.145	poundforce per square inch	lbf/in^2

*SI is the symbol for the International System of Units. Appropriate rounding should be made to comply with Section 4 of ASTM E380. (Revised March 2003)

DETAILED WEATHER AND TERRAIN ANALYSIS FOR AIRCRAFT NOISE MODELING

WR 13-01
April 2013

wyle

USDOT/RITA/VOLPE CENTER

Prepared for:
The Volpe National
Transportation Systems Center

Detailed Weather and Terrain Analysis for Aircraft Noise Modeling

Wyle Report 13-01
Contract No. DTRT57-10-D-30014
Task Order No. DTRTV-T02002
USDOT/RITA/VOLPE CENTER
Job No. T60121.03.01

April 2013

Prepared for:

The Volpe National Transportation Systems Center

55 Broadway
Kendall Square
Cambridge, MA 02142

Prepared by:

200 12th Street South
Suite 900
Arlington, VA 22202

Wyle
Environmental and Energy
Research & Consulting (EERC)

Authors:

Kenneth J. Plotkin
Juliet A. Page
Yuriy Gurovich
Christopher M. Hobbs

Contents

Section

Figures

Tables

1.0 Introduction

Excessive airport and aircraft noise produces stress and annoyance in local communities. National legislation, including the Aviation and Noise Abatement Act of 1978, addresses this problem by mandating the protection of the public's health and welfare through regulation of aircraft noise. The FAA has been charged with the responsibility of developing noise control regulations. In this effort, the FAA maintains tools for aircraft noise analysis. A study has been conducted supporting FAA's refinement and development of those tools.

Tasks conducted in this study are:

- Updated analysis of the 1997 KDEN noise model validation study with newer versions of INM and related tools (Section 2.0).
- Analyze a sample of the 1997 KDEN validation data with simulation modeling (Section 3.0).
- Develop algorithms for detailed weather modeling in FAA tools (Section 4.0).
- Assess available validation data from studies at other airports (Section 5.0).
- Develop simplified terrain processing implementation, adapting the process successfully employed in simulation models (Section 6.0).

Each of the sections is self contained, and may be read in any order with minimum prerequisite for earlier sections. Conclusions are presented in Section 7.0.

Intentionally left blank.

2.0 Denver International Airport Noise Analysis – INM

2.1 *INM5, INM6, and INM7 Analysis of Profile Point Modeled DIA Departure Operations*

In 1997 detailed noise measurements were conducted at Denver International Airport (DIA or KDEN). This dataset was examined with INM 5.2a using profile point analysis[2-1] and procedure step analysis.[2-2] This section contains analysis comparing the prior profile point results from INM 5.2a[2-3] with new analyses using INM 6.2[2-4] and INM 7.0c[2-5] for a variety of aircraft types. The analyses show significant improvement in the comparison of predicted and measured acoustic data at the noise monitoring locations with the later versions of INM (Figure 2-1).

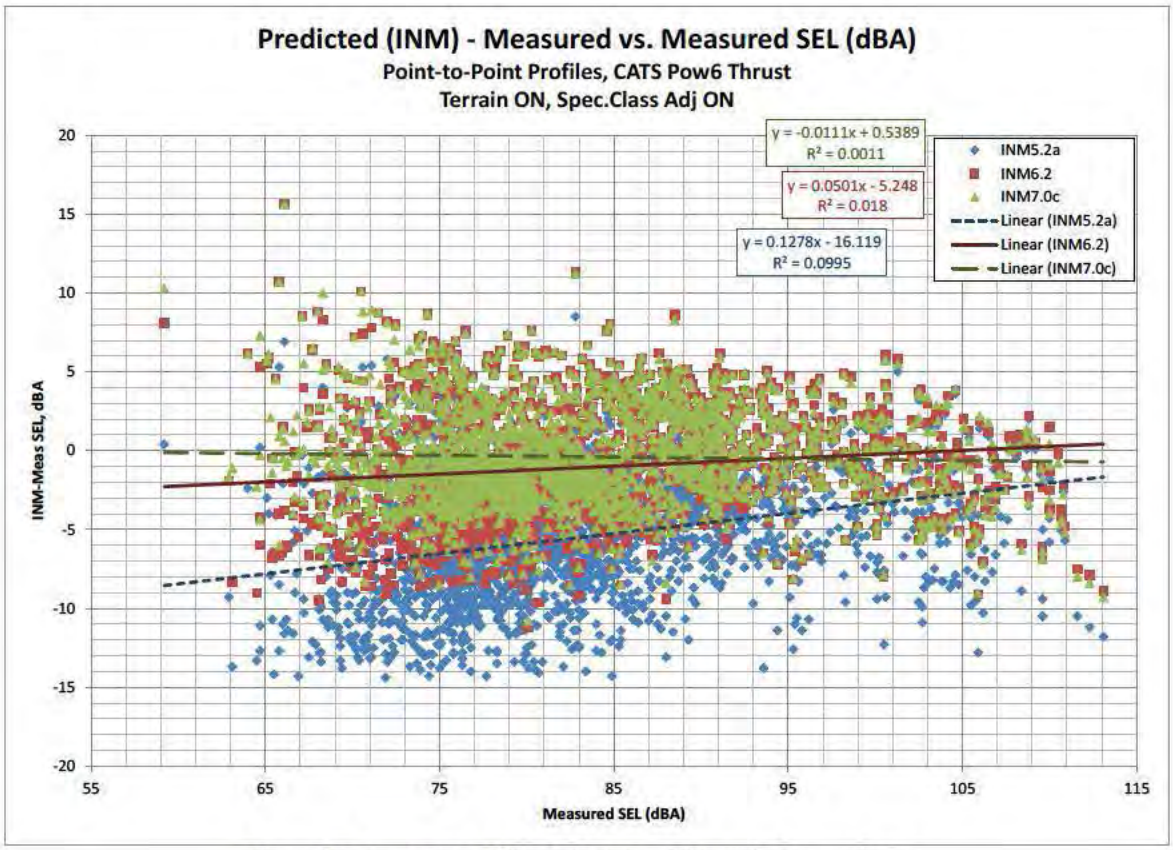

Figure 2-1. Comparison of INM 5.2a, 6.2 and 7.0c with Measured Data. Profiles modeled using the CaTS Assumed Temp Methodology (Power Mode 6).

2.1.1 Denver Measurement Program Overview

Noise monitoring was conducted at Denver International Airport for operations from May 13, 1997 through June 13, 1997.[2-1] Noise monitoring stations included the 31 permanently installed monitors operated by the DIA noise abatement office, as well as 19 additional temporary noise monitors installed by Wyle Laboratories (Figure 2-2). Additional details about the monitoring-site selection process, the equipment used to gather data, and other procedural details are presented in "Validation of Aircraft Noise Prediction Models at Low Levels of Exposure."[2-1]

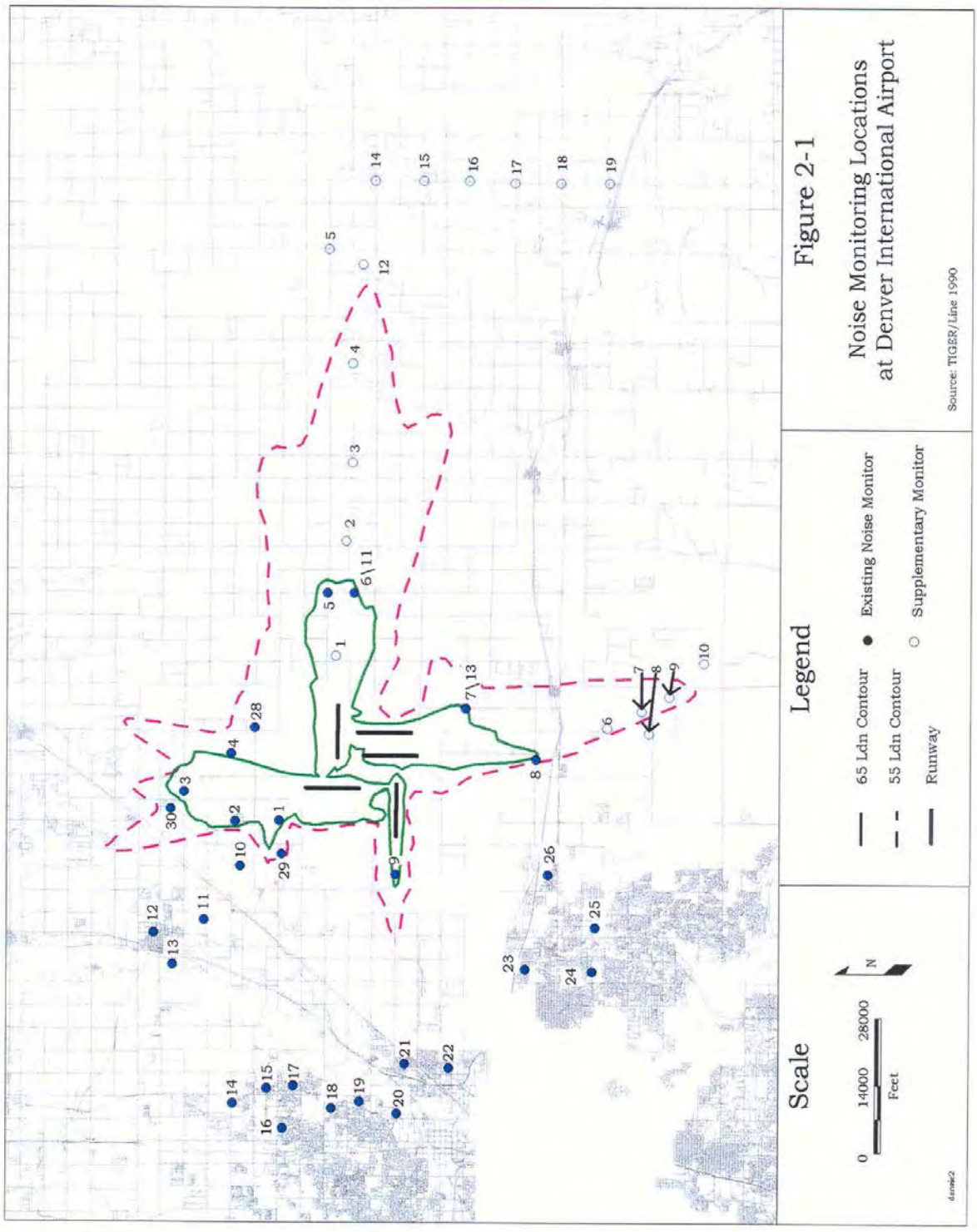

Figure 2-2. 1997 DIA Airport Noise Monitoring Locations.

During this monitoring time period, supporting operational flight and atmospheric information was gathered. Takeoff gross-weight data was obtained from United and Delta Airlines. Exact equipment usage including vehicle nose number, and hence airframe model and engine model, was provided by United Airlines. Hourly surface airport weather data was obtained from the local airport weather station. Upper air and atmospheric profile information was recorded twice daily by the NOAA operating at the Denver-Stapleton Airport facility.

Departure operations considered in the prior study and again in this study are plotted in Figure 2-3 and include a variety of aircraft types as documented in Table 2-1. The flight ground tracks were derived from radar data obtained from DIA. The flight profiles were input and match the radar data (altitude and speed) with thrust computed using the Climb and Throttle Scheduler (CaTS) code developed for the original 1997 DIA study. [2-1] The profiles and thrust values computed in 1997 were imported to INM6 and INM7 for the current analysis (Table 2-2).

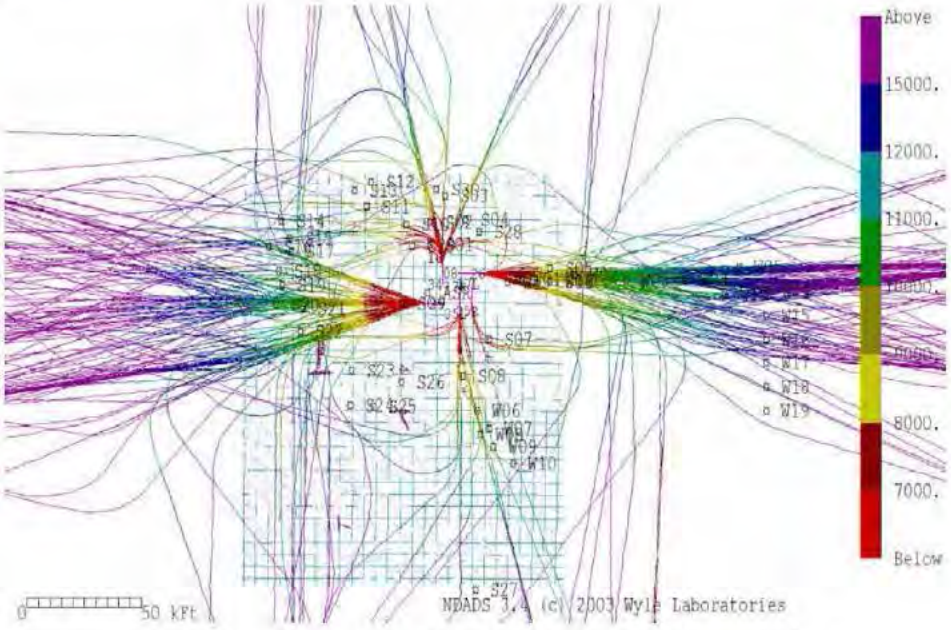

Figure 2-3. Departure Operations Modeled in the Current Analysis.

Table 2-1. Aircraft Types Modeled in INM5, 6 and 7

Type	Description	Noise ID
B727	B727-200/JT8D-15	3JT8D
B73J	B737-300/CFM56-3B-1	CFM563
	B737-500/CFM56-3B-1	CFM563
B73S	B737-300/CFM56-3B-2	CFM563
B757	B757-200/PW2037	PW2037

Table 2-2. Unique Data Points and Flight Tracks Modeled in INM5, 6 and 7

Unique Data points - Flight-MDD-NoiseMon		
All	Used	Tossed
2298	2171	127
Unique Flight Tracks: Flight-MDD		
All	Used	Tossed
634	620	99

Note: "Tossed" flights were removed from the noise comparison to reflect the% of operations which did not utilize a reduced thrust operation at the pilots' discretion even though the weight, performance and temperature data indicated it was feasible. This is consistent with the prior analysis. [2-1]

2.1.2 INM Profile Point Modeling

INM versions 6.2 and 7.0c were run using the Noise-Power-Distance curves provided with the standard INM installation package. Note that there were changes to the NPD data between some INM versions. Terrain was enabled using the 3DS files required by INM. Each specific event included the airport pressure, temperature and humidity from the surface weather observations interpolated to the time of the departure. The "Modify NPD curves" option was selected ON in the INM GUI to permit computation of absorption changes due to humidity.

Noise predictions from INM6 and 7 were compared with INM 5.2a predictions as executed in 1998 based on "Power Mode 6". Power Mode 6 utilized an assumed temperature method to compute the reduced thrust based on airline provided detailed aircraft performance data, known takeoff gross weight information, exact equipment usage and current surface meteorological conditions. The aircraft operating state (N1 or EPR) is computed for takeoff through first and second segment climb. The INM required net corrected installed thrust (Fn/delta, lbs) is then computed based on local atmospheric conditions interpolated to the flight time and flight Mach number for smoothed and thinned radar points. A full description of the radar analysis procedures and the assumed temperature method may be found in References 2-1 and 2-2. This study used the identical flight profiles and flight tracks as were developed in the 1997-1998 timeframe, importing them directly into INM6 and INM7 for the analysis described here. The other power mode computational procedures were not considered since Power Mode 6 was the only methodology capable of modeling reduced thrust operations from a high altitude airport. [2-1]

A comparison of INM 5 and 6 profiles is provided in Figure 2-4 for a single operation of a B737 (UA1029 on 5/22). The sub-segmentation algorithms within INM have been modified to include a small transition segment which can be seen as the closely spaced points in Figure 2-4 and Tables 2-3 and 2-4. Note the alternating small segment, large segment in the segment length column in Table 2-4 (i.e. 4048.2, 38.4, 1532.4, 36.4, 1528.4, 40.4, 1481.9). INM profiles were obtained by exporting them from the GUI to the flight path file.

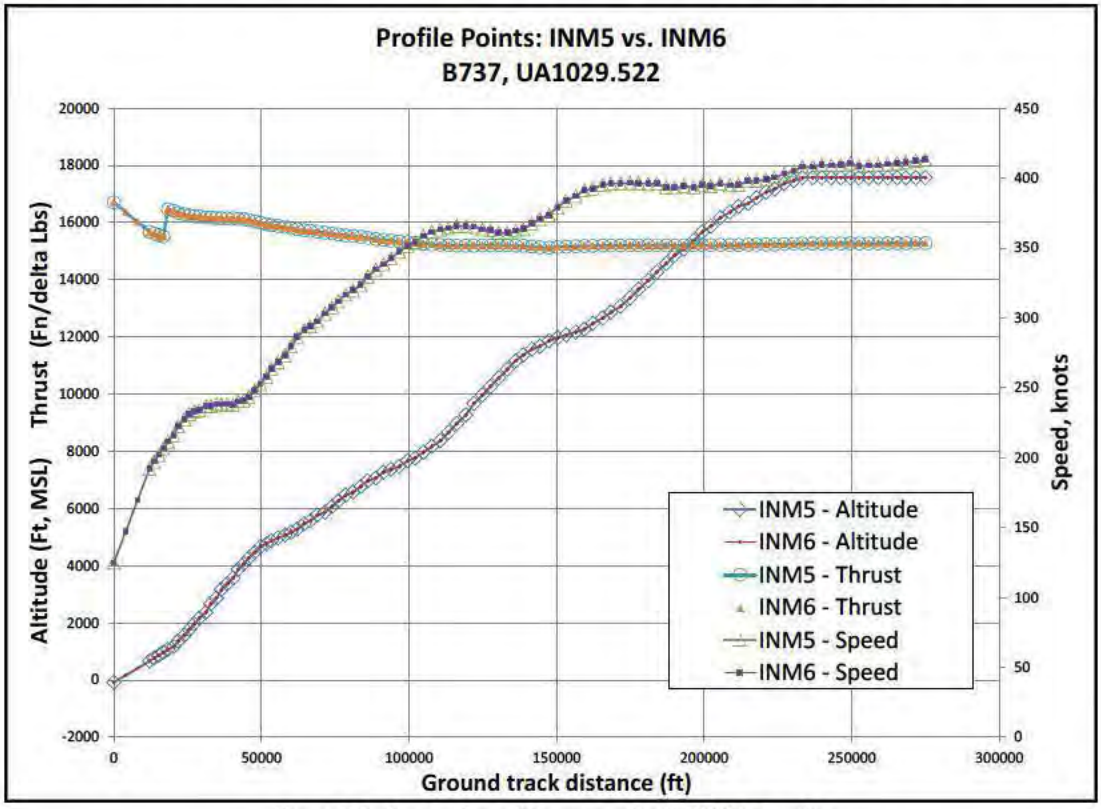

Figure 2-4. Comparison of Segmentation in INM5, 6 and 7.

Table 2-3. Segmentation Comparison, INM5

DISTANCE	ALTITUDE	SPEED	THR_SET	OP_MODE
0	-79.2	125	16705	D
12121.6	669	192.2	15678	D
13689.2	769	197.2	15610	D
15250.8	869	201.9	15560	D
16769.8	969	206.6	15511	D
18337.4	1069	211.4	16467	D
20275.6	1169	216	16415	D
21837.1	1369	222.5	16341	D
23884.8	1569	227.2	16289	D
25586	1769	231.2	16244	D
27281.2	1969	233	16223	D
28982.5	2169	233.8	16212	D
31194.2	2369	236.9	16177	D

Note: Case 01_UA1029: B737-300/CFM56-3B-2

Table 2-4. Segmentation Comparison, INM6

Calc Dist.	seg	start x	start y	start z	unit x	unit y	unit z	length	speed	d.spd	thrust	d.thr	op
0	0	9650.7	-5218.2	-79.2	-0.9978	0.0237	0.0616	4048.2	125	22.4	16705	-342.3	D
4040.543	1	5611.3	-5122.1	170.2	-0.9978	0.0237	0.0616	4048.2	147.4	22.4	16362.7	-342.3	D
8081.086	2	1571.9	-5026	419.6	-0.9978	0.0237	0.0616	4048.2	169.8	22.4	16020.3	-342.3	D
12121.63	3	-2467.5	-4929.9	669	-0.9977	0.0237	0.0637	38.4	192.2	0.1	15678	-1.7	D
12159.94	4	-2505.8	-4928.9	671.4	-0.9966	-0.0531	0.0637	1532.4	192.3	4.9	15676.3	-66.3	D
13689.21	5	-4032.9	-5010.3	769	-0.9965	-0.0531	0.0639	36.4	197.2	0.1	15610	-1.2	D
13725.56	6	-4069.2	-5012.2	771.3	-0.9966	-0.0527	0.0639	1528.4	197.3	4.6	15608.8	-48.8	D
15250.79	7	-5592.3	-5092.7	869	-0.9964	-0.0527	0.0657	40.4	201.9	0.1	15560	-1.3	D
15291.14	8	-5632.6	-5094.8	871.7	-0.9795	0.1904	0.0657	1481.9	202	4.6	15558.7	-47.7	D
16769.8	9	-7084.1	-4812.7	969	-0.9796	0.1904	0.0637	40.4	206.6	0.1	15511	24.6	D
16810.04	10	-7123.6	-4805	971.6	-0.9966	-0.053	0.0637	1530.4	206.7	4.7	15535.6	931.4	D
18337.4	11	-8648.8	-4886.2	1069	-0.9973	-0.0531	0.0515	38.9	211.4	0.1	16467	-1	D
18376.25	12	-8687.6	-4888.2	1071	-0.9987	-0.0053	0.0515	1901.8	211.5	4.5	16466	-51	D
20275.58	13	-10586.9	-4898.4	1169	-0.9919	-0.0053	0.127	37.5	216	0.2	16415	-1.8	D
20312.78	14	-10624.1	-4898.6	1173.8	-0.9905	-0.0524	0.127	1536.8	216.2	6.3	16413.2	-72.2	D
21837.1	15	-12146.3	-4979	1369	-0.9939	-0.0525	0.0972	41.4	222.5	0.1	16341	-1	D
21878.36	16	-12187.5	-4981.2	1373	-0.9776	-0.1866	0.0972	2016	222.6	4.6	16340	-51	D
23884.85	17	-14158.4	-5357.4	1569	-0.9755	-0.1862	0.1168	38.8	227.2	0.1	16289	-1	D
23923.33	18	-14196.2	-5364.6	1573.5	-0.9567	-0.2665	0.1168	1674.1	227.3	3.9	16288	-44	D
25585.99	19	-15797.9	-5810.7	1769	-0.9567	-0.2664	0.1172	36.2	231.2	0	16244	-0.4	D
25621.9	20	-15832.5	-5820.3	1773.2	-0.9567	-0.2665	0.1172	1670.8	231.2	1.8	16243.6	-20.6	D
27281.16	21	-17430.9	-6265.6	1969	-0.9567	-0.2665	0.1168	39	233	0	16223	-0.3	D
27319.89	22	-17468.2	-6276	1973.6	-0.9567	-0.2665	0.1168	1674	233	0.8	16222.8	-10.8	D
28982.48	23	-19069.8	-6722.2	2169	-0.9594	-0.2673	0.0901	35.5	233.8	0	16212	-0.6	D

Calc Dist.	seg	start-x	start-y	start-z	unit-x	unit-y	unit-z	length	speed	d.spd	thrust	d.thr	op
29017.88	24	-19103.9	-6731.7	2172.2	-0.9361	-0.34	0.0901	2185.2	233.8	3.1	16211.4	-34.4	D
31194.24	25	-21149.5	-7474.7	2369	-0.9256	-0.3362	0.1737	38.4	236.9	0	16177	0	D

A total of 635 unique flight operations were modeled for this INM validation assessment (Table 2-2). These operations were correlated with 2298 measured noise events at the monitoring locations. The analysis included B727, B737 and B757 operations of the specific variants listed in Table 2-5. The Type column in Table 2-5 is the ARTS system descriptor. The exact equipment usage was known based on airline provided historical equipment usage data and tail number / equipment tables. The specific airframe and engine type was utilized in the assumed temperature thrust prediction in the CaTS code.

Tables 2-2 and 2-5 itemize the numbers of aircraft types and unique operations in the statistical analysis. The "Tossed" flights were removed from the noise comparison to reflect the percent of operations which did not utilize a reduced thrust operation at the pilots' discretion even though the weight, performance and temperature data indicated it was feasible. This is consistent with the prior analysis.[2-1] The flights were sorted by Predicted-Measured from the INM 5.2a results, and those with the worst underpredicted values were eliminated from the statistical analysis on the grounds that the largest difference in noise exposure is likely due to improper assignment of the reduced thrust. In the case of this study, those 127 unique events with underpredictions greater than 14.5 dBA SEL were eliminated. This is the identical logic applied in Reference 2-1.

Table 2-5. Operations modeled in INM5, 6 and 7

Totals	Type	Description
980	B727	B727-200/JT8D-15
346	B73J	B737-300/CFM56-3B-1
		B737-500/CFM56-3B-1
826	B73S	B737-300/CFM56-3B-2
146	B757	B757-200/PW2037
2298	**All**	
968	B727	B727-200/JT8D-15
305	B73J	B737-300/CFM56-3B-1
		B737-500/CFM56-3B-1
767	B73S	B737-300/CFM56-3B-2
131	B757	B757-200/PW2037
2171	**Used**	
12	B727	B727-200/JT8D-15
41	B73J	B737-300/CFM56-3B-1
		B737-500/CFM56-3B-1
59	B73S	B737-300/CFM56-3B-2
15	B757	B757-200/PW2037
127	**Tossed**	

Note1: ARTS B73J includes -300 and -500. CaTS differentiated between them based on tail number and documented equipment usage from United Airlines.

Note2: "Tossed" flights were removed from the noise comparison to reflect the% of operations which did not utilize a reduced thrust operation at the pilots' discretion even though the weight, performance and temperature data indicated it was feasible. This is consistent with the prior analysis.[1]

2.1.3 Comparisons with Independent Parameters

Figure 2-1 demonstrates the improvements in the INM predictions with the later versions of the software and associated databases. Table 2-6 contains statistical results corresponding to the data in Figure 2-1 based on the 2171 unique noise events with the underpredictions greater than 14.5 SEL dBA removed.

Table 2-6. INM Prediction – Measurement Statistics

INM Predictions – Measurements, SEL, dBA			
	INM5.2a	INM6.2	INM7.0c
Mean	-5.47738	-1.07347	-0.384431
St.Deviation	3.779845	3.482068	3.114751
Count	2171	2171	2171

Comparisons with slant range (based on the radar point of closest approach, PCA, to the noise monitor) are provided in Figure 2-5 and indicate significant improvement in the INM predictions across all ranges. Figure 2-6 also shows an improvement with flight speed (radar based) at the PCA. The later versions of INM have also eliminated the underprediction bias in the predictions at the higher fight speeds.

Prediction of noise from high altitude airports is a particular challenge not only because of the difficulty of modeling aircraft performance, hence thrust, but also because of possible changes in the source noise emission at higher altitudes. Figure 2-7 contains the INM-measured results as a function of the aircraft flight altitude at the PCA. While improvements have been made, there still exists a trend of underprediction with increasing flight altitudes. INM was developed for the terminal area and provides good results, within 2 dB, when the operations are modeled below 15kft. For high altitude airports such as DIA, and for regions increasingly distant from the airport, however, this could be a concern and should be investigated further. These results suggest that a high-altitude NPD dataset be considered for these situations and for enroute noise prediction.

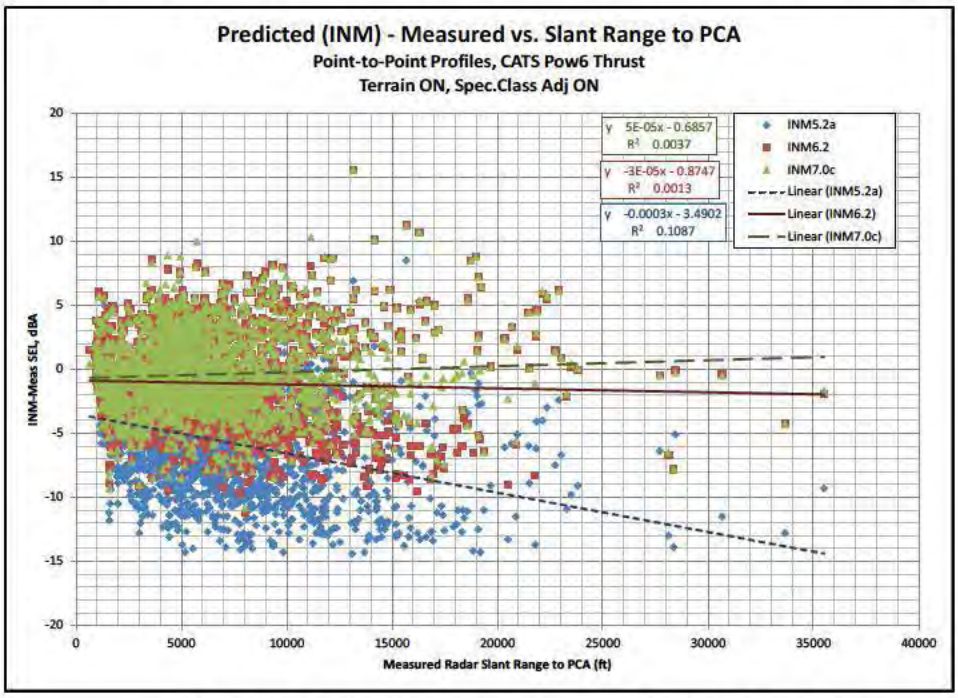

Figure 2-5. INM Prediction – Measurement as a function of Slant Range.

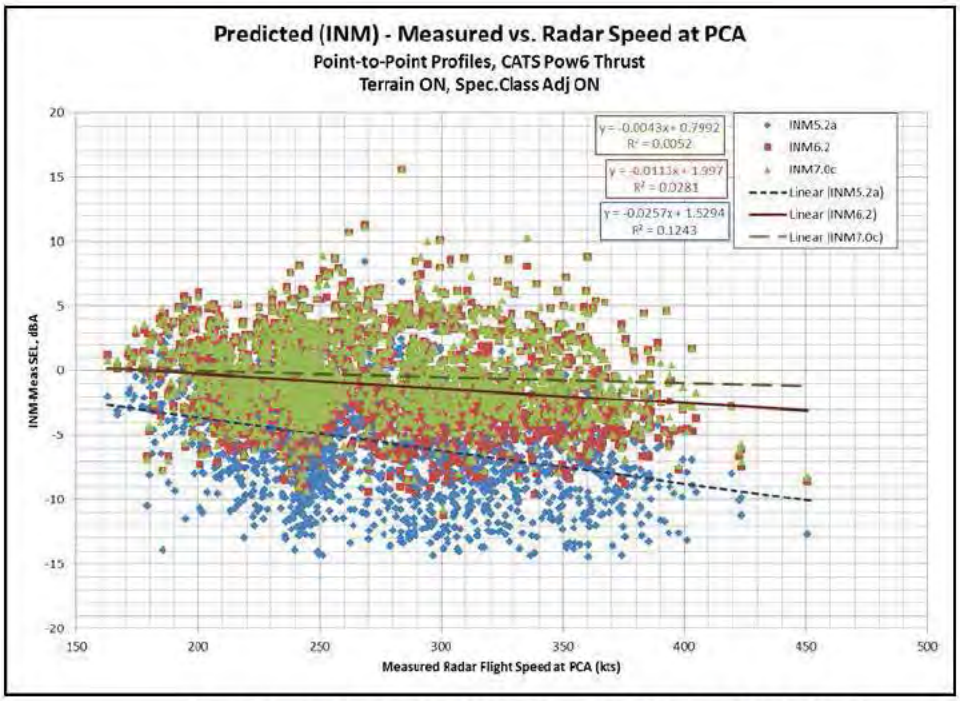

Figure 2-6. INM Prediction – Measurement as a function of Flight Speed.

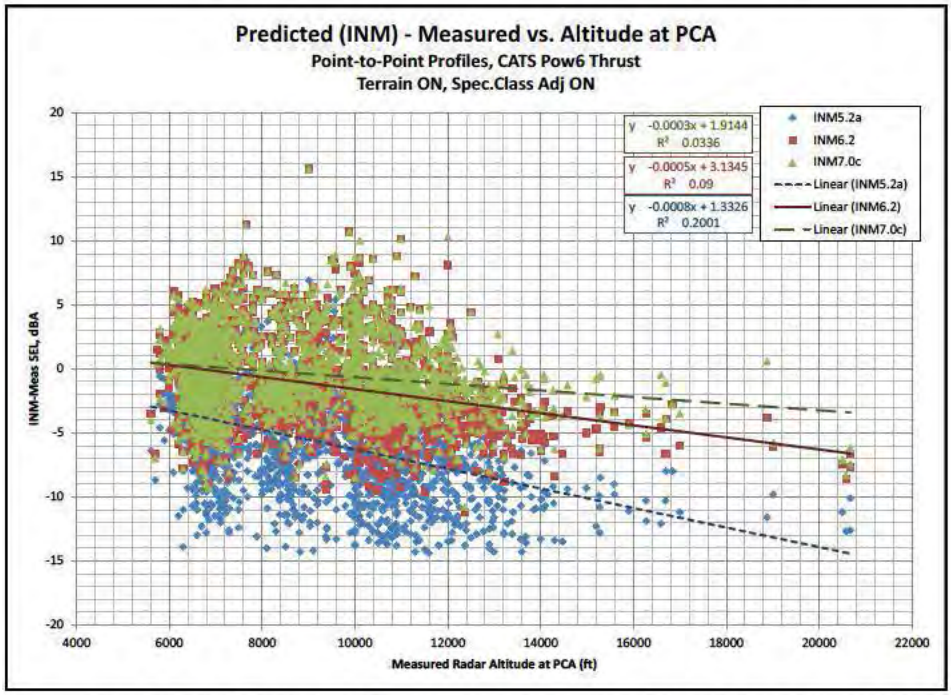

Figure 2-7. INM Prediction – Measurement as a function of Aircraft Flight Altitude (MSL, ft.).

INM 7 predictions with respect to ground track distance show less than 1 dBA SEL sensitivity (Figure 2-8). The slope of the predictions (SEL, dBA) with respect to elevation angle (deg) have increased with INM versions 6 and 7 (-.0073, -.0281 and -.0219), likely due to changes in source directivity, as modeled by the new lateral attenuation algorithms[2-6] (Figure 2-9).

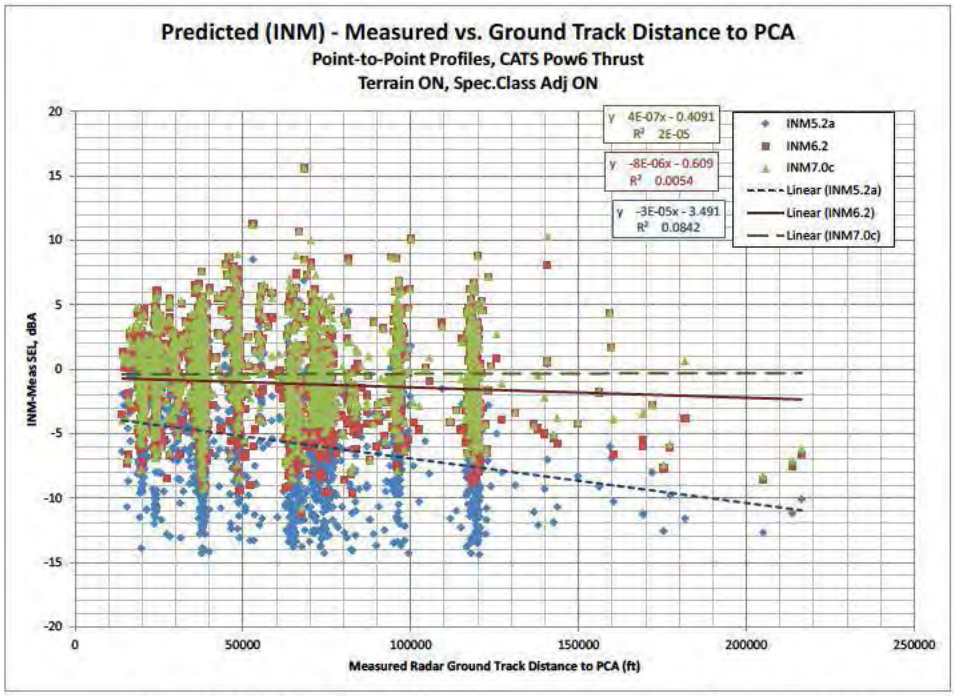

Figure 2-8. INM Prediction – Measurement as a function of Ground Track Distance.

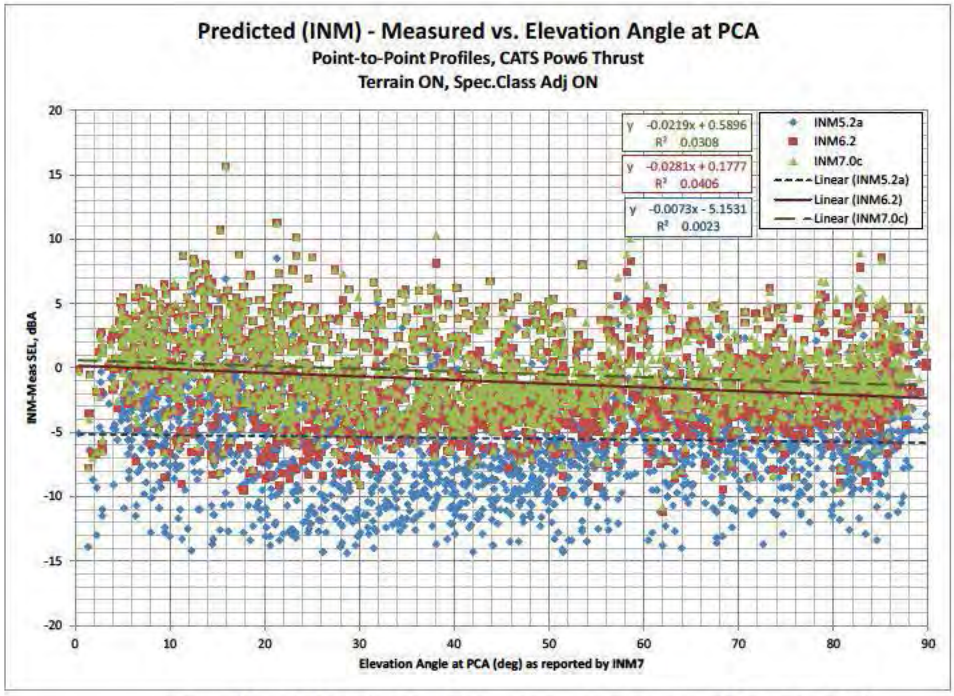

Figure 2-9. INM Prediction – Measurement as a function of Elevation Angle.

The Assumed Temperature method was used to determine the thrust. The differential (Assumed Temp - Outside Air Temp at PCA, °F) was used as an independent parameter to see if there was a bias for those operations with larger derated takeoffs. Figure 2-10 indicates a very slight tendency towards overprediction under conditions where greater thrust reductions are possible. It should be noted that this is likely due to

limitations of the CaTS Power Mode 6 prediction methodology, and not a reflection of the INM modeling itself.

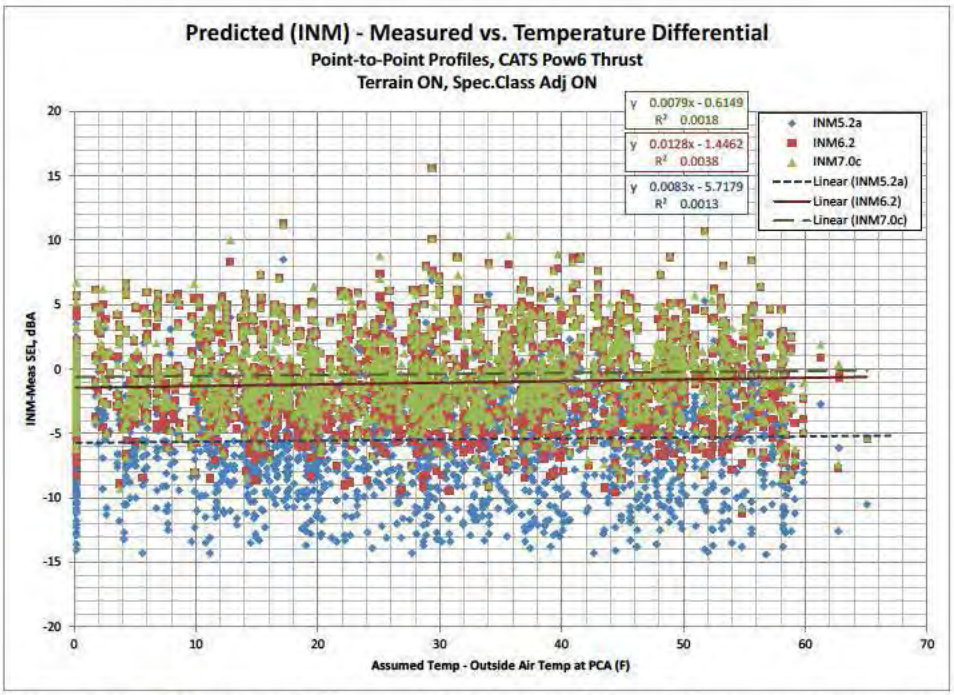

Figure 2-10. INM Prediction – Measurement as a function of Assumed Temperature Differential.

This indication of possible limitations in the reduced thrust prediction methodology is also suggested in Figure 2-11 by the underpredictions during times with lower air temperatures at the time of the operation (more performance margin for thrust reduction). The DIA measurements were conducted in May and June 1997 when the outside air temperature ranged from 41 to 75 °F. It would be interesting to see if this trend continues in the midst of winter and summer when the surface air temperatures at DIA can be more extreme.

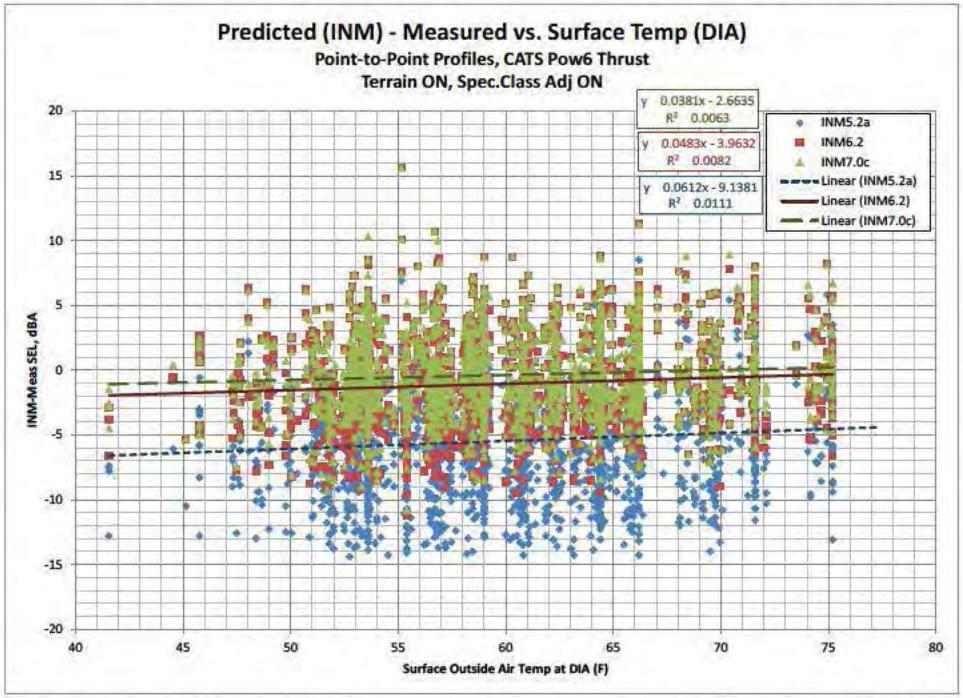

Figure 2-11. INM Prediction – Measurement as a function of Surface Air Temperature (deg F).

Another indication of the limitations of the assumed temperature methodology is the comparison with weight margin (Figure 2-12). Weight Margin is defined as the (Max Allowable – Actual weight)/Actual airline reported weight. The greater the difference between MATOGW and actual TOGW the more opportunity for thrust reduction.

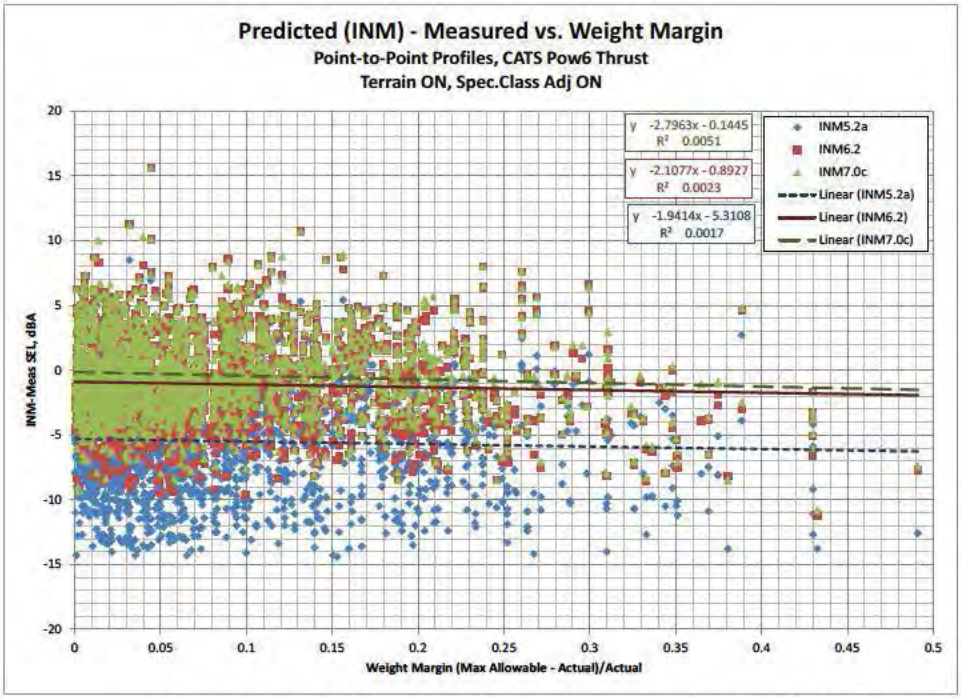

Figure 2-12. INM Prediction – Measurement as a function of Weight Margin

Comparing the sensitivity of prediction accuracy with temperature (Figures 2-10 and 2-11) and weight (Figure 2-12), it would appear that the weight margin might be a stronger driver of the underpredictions. This suggests that perhaps the uncertainty is due to pilot discretion and perhaps updated actual TOGW data beyond that which was made available to Wyle for this study.

Relative Humidity (%) at the PCA was computed by interpolation of the local surface weather and the upper air humidity lapse rates, and was considered as an independent parameter as shown in Figure 2-13. The trends indicate underprediction for higher values of humidity. Since the humidity was not, however, directly measured at the time of the flight there are limits to the validity of this observation. The computations were made with the Spectral Class adjustment option enabled and the humidity entered for each individual operation allowing the most accurate absorption adjustment possible within the algorithm limitations of INM.

A dependency in the accuracy is shown with winds aloft (Figure 2-14). Winds were not considered in the performance modeling in the CaTS code, even though they could affect both the computation of the airspeed, Mach number and the required thrust to match the measured radar airspeed. Winds aloft were based on interpolation of the upper air data (twice daily balloons) with adjustment based on hourly reported surface winds. Further investigation would require a new dataset with more frequent upper air data.

Sensitivity to predictions with interpolated field elevation pressures from hourly surface observations were also computed (Figure 2-15).

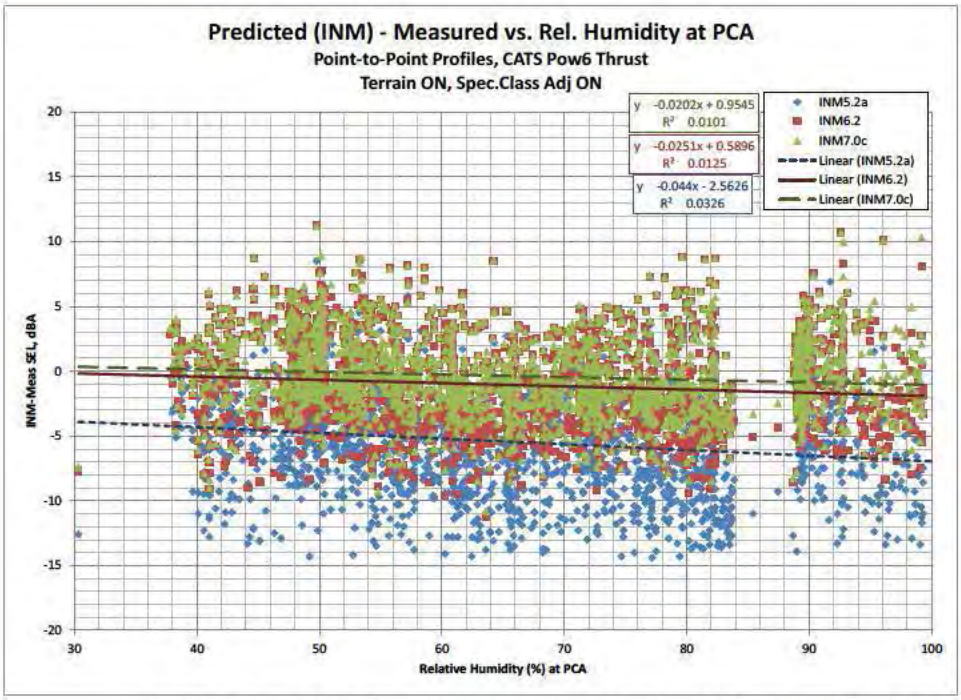

Figure 2-13. INM Prediction – Measurement as a function of Relative Humidity (%).

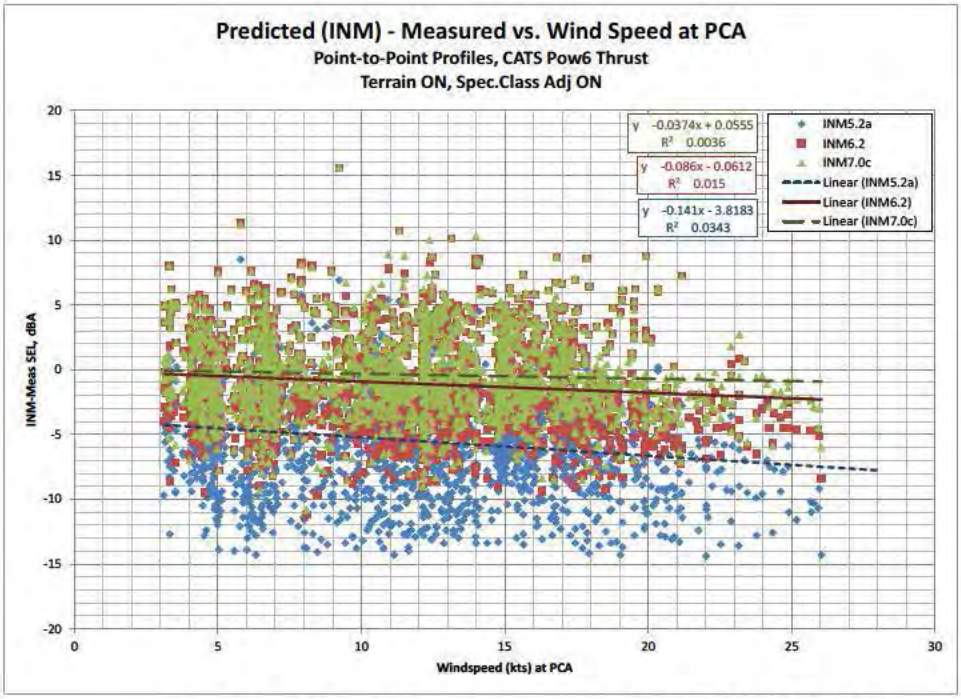

Figure 2-14. INM Prediction – Measurement as a function of Winds aloft (kts).

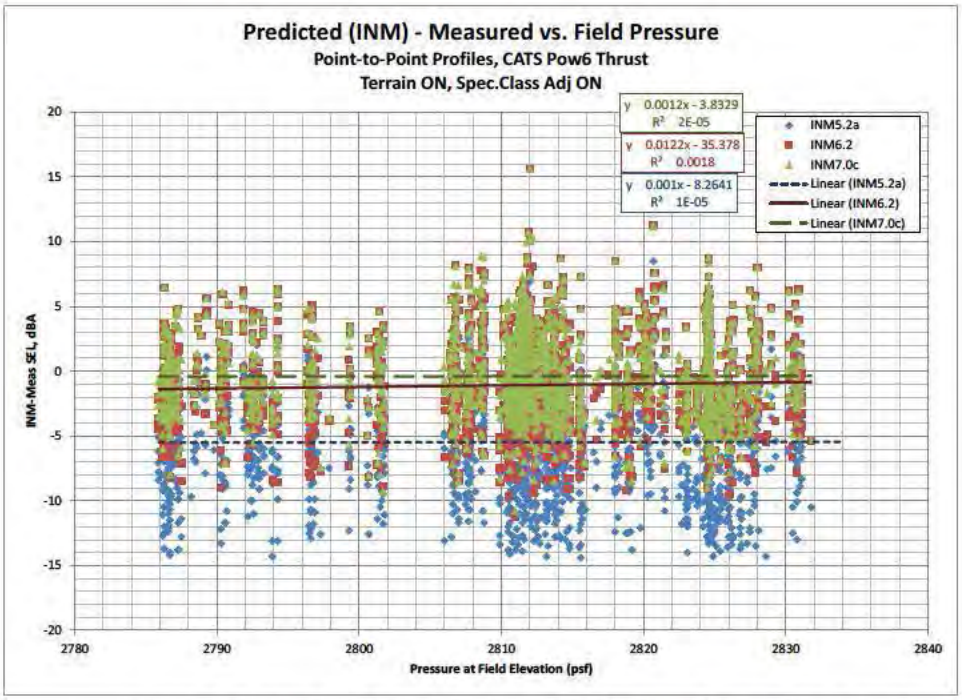

Figure 2-15. INM Prediction – Measurement as a function of Atmospheric Pressure.

2.1.4 Findings and Recommendations Based on INM Profile Point Analysis

INM prediction of noise from high altitude operations has improved considerably since 1998 for physics based modeling (profile point input) of reduced thrust operations. Both the absolute SEL levels (dBA) and the standard deviations of INM minus measured data comparisons have improved. An assessment of prediction accuracy for various independent parameters suggests that source noise modeling for higher altitudes, (above 15,000 ft MSL) be investigated further, both for noise prediction at larger distances from high altitude airports and for enroute noise computation. Tendencies for overprediction with conditions suggesting increase reduced thrust performance margin warrants further investigation into the assumed temperature prediction methodology (CaTS code). No other strong sensitivities with independent parameters were noted.

Analysis of the data included operations on May 21 – 30, 1997. The May 31 CaTS data was not available. Additional data for the first week of June 1997 has been recorded but was not processed during the initial DIA study and was not included here. It could be analyzed in the future if funds are available. Additionally approach data was never processed nor utilized from any of the prior DIA studies. This could provide additional insight into the accuracy of INM in approach flight modes.

2.2 *INM6 and INM7 Analysis of Procedure Step Modeled DIA B737 Departure Operations*

This section documents INM acoustic predictions of high altitude reduced thrust departure operations modeled using procedure-steps in INM versions 6 and 7 and compares them with noise measurement data. A 1998 study[2-1] examined this same dataset with INM 5.2a using profile point analysiswhile a 2005 study[2-2] utilized INM 6.1 batch procedure step analysis. This section compares the prior procedure step results from the batch version of INM 6.1[2-4] with procedure step analyses using INM 7.0c[2-5] for a variety of B737 configurations. The analyses show improvement in the comparison of procedure step predicted and measured acoustic data at the noise monitoring locations with the later versions of INM (Figure 2-16) though it is not possible to discern how much is due to propagation and source modeling improvements, and how much is due to changes in the modeled aircraft profile and operating state. The results from the Procedure Step analysis are

not as good as those obtained by using the Profile Point INM analysis based on the CATs code thrust predictions.[2-6]

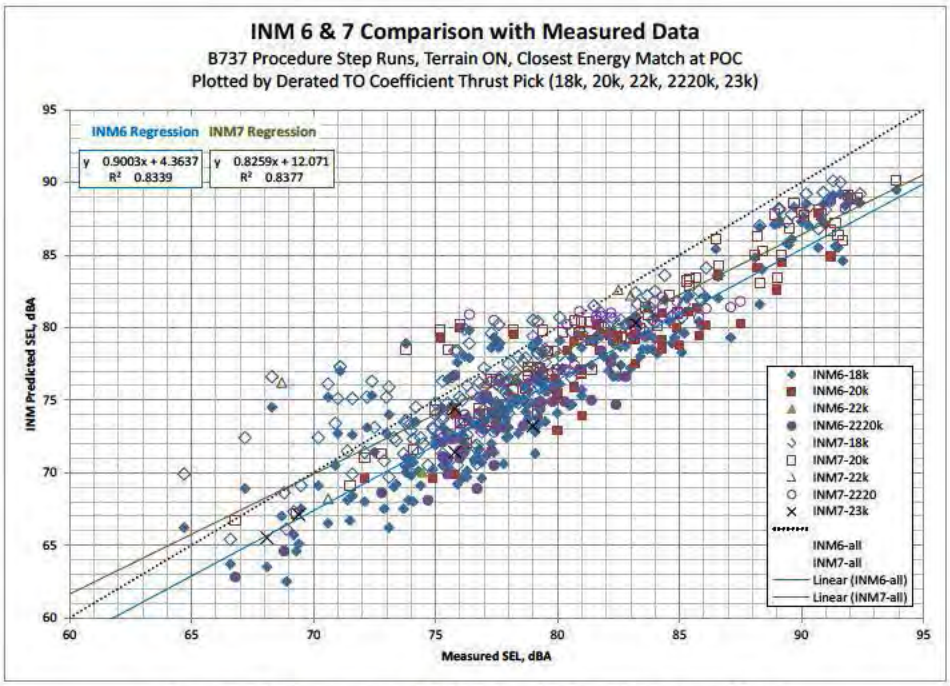

Figure 2-16. Comparison of INM 6.1 and 7.0c with Measured Data.
Profiles modeled using optimized Procedure Steps with Derated Thrust Jet Coefficients.

2.2.1 Denver Measurement Program Overview

As described in Section 2.1, noise monitoring was conducted at Denver International Airport for operations from May 13, 1997 through June 13, 1997. Departure operations considered in the prior studies[2-1, 2-2]and again in this study are plotted in Figure 2-3 and include several variants of the B737 (Table 2-7). The flight ground tracks were derived from radar data obtained from DIA. The flight profiles were modeled in INM using procedure steps with customized, reduced thrust jet coefficients. A total of 5 different reduced thrust profiles were attempted for each operation, and the "best" one selected for the noise assessment based on the closest energy match to the radar data (altitude and speed) at the point of closest approach.

The specific procedure step sequences for each unique flight operation (and for all 5 levels of derated thrust) were developed in the prior study[2-2] using an automated processor which ran the INM6 batch code, modeled sequential profile segments, iteratively adjusting the procedure step parameters to best match the measured radar profile. Full details of the automated procedure step processor are documented in Reference 2-2.

The procedure steps generated for INM6 (for all 5 levels of thrust derate) were then imported into INM7 in order to update the acoustic predictions at the noise monitoring locations. Unfortunately differences between the "auto-fixup" in the INM6 batch and the INM7 GUI versions necessitated that changes be made to the procedure step sequences. The Procedure Step Modeling section of this Memo describes this process in greater detail.

Table 2-7. Aircraft Types And Unique Data Points (Noise Events) modeled in the current INM Procedure Step Analysis

Description	Noise ID	Unique Data Points
B737-300/CFM56-3B-1	CFM563	81
B737-300/CFM56-3B-2	CFM563	149
B737-500/CFM56-3B-1	CFM563	77
	Total:	**307**

The specific procedure step sequences for each unique flight operation (and for all 5 levels of derated thrust) were developed in the prior study[2] using an automated processor which ran the INM6 batch code, modeled sequential profile segments, iteratively adjusting the procedure step parameters to best match the measured radar profile. Full details of the automated procedure step processor are documented in Reference 2-2.

The procedure steps generated for INM6 (for all 5 levels of thrust derate) were then imported into INM7 in order to update the acoustic predictions at the noise monitoring locations. Unfortunately differences between the "auto-fixup" in the INM6 batch and the INM7 GUI versions necessitated that changes be made to the procedure step sequences. The Procedure Step Modeling section of this Memo describes this process in greater detail.

2.2.2 Procedure Step Modeling

As described in Reference 2-2, the batch version of INM6 (originally developed for the Magenta Program) was utilized with an automated procedure step generator program which would iteratively determine a sequence of specific profile steps, starting with takeoff roll and initial climb, flap cleanup and continuing on to the second segment climb which most closely matched the target radar profile trajectory. The procedure step generator builds DBF files which are then run in the batch version of INM. Once the INM flight profile portions of the calulations are run, the INM calculated flight path is exported and compared with the recorded input radar flight trajectory. The parameters of the Procedure Steps are then modified appropriately and the batch version of INM run again until the difference between the INM and radar trajectories (altitude and speed) are minimized. Minimization was based on a potential and kinetic energy optimization scheme (referred to as M2 in Reference 2-2). This process was developed and executed in 2005 to match measured radar B737 departure operations from DIA.

These "final" procedure step sequences (up to five for each flight trajectory) which were based on INM6 batch were then utilized in this current research by importing them into INM7. For some operations, the specific procedure step input sequences had to be modified to run. The batch version of INM6 has additional auto-fixup processes which do not exist in INM7 and can cause the profile steps to fail and INM7 execution to halt. Edits to the procedure steps were necessarry. Some examples of these modifications are provided in Table 2-8. INM7 still encountered some situations which generated warnings, a few of which are provided in Table 2-9. In these cases INM7 performed auto-corrections to the input procedure step profile and continued execution.

Table 2-8. Modifications made to the Optimized Procedure Steps for INM7 Analysis

Elimination of procedure steps calling for reductions in speed PARAM2 for procedure steps of type A if lower than the highest speed the profile had specified thus far.
Sequential re-numbering of DBF procedure steps when steps were removed.
Insertion of procedure step records into INM dbf file template to ensure proper field parameters (i.e. numeric 10.2 vs. numeric 5.2)

Table 2-9. Examples of remaining INM7 Procedure Step Warnings

PROFILE WARNING: 737500 D 449B_521 1 Accelerate step 27: accelerate to speed 286.4 changed to 287.0 kt
PROFILE WARNING: 737500-D-449B_521-1 Accelerate step 31: climb rate 2618 fpm reset to 2603 fpm
PROFILE WARNING: 737500-D-449B_521-1 Climb step 50: climb-to altitude 10000.0 ft reset to 12943.7 ft

There are potential implications to these modifications and to not rigorously optimizing the procedure steps anew. First, the kinetic and potential energy minimization scheme which optimizes the individual procedure

steps is not uniformly applied to each procedure step since the original batch optimizer did not take into account dropped or modified segments. This could result in poorer matches to the radar profile or could artifically bias the profiles to utilize higher thrust settings, thereby increasing predicted noise. (This point will be revisited later). Second, differences in the "auto-fix-up" in the INM Flight module might account for some of the acoustic predictions of INM due to changes in thrust modeling and flying the aircraft along a different trajectory with different speeds. No attempts were made to quantify the impact of these changes between INM6 and INM7, indicated by warning messages such as those shown in Table 2-9.

Comparisons of INM 6 (original) and 7 (after modification / cleaning) procedure step profiles are provided in Figure 2-17 for three different operations for the 18k thrust (maximum derate): UA200-523 (B737-3B2), UA573-523 (B737-3B2) and UA1146-523 (B737-3B1). Figures 2-17 and 2-18 show two adjacent portions of the altitude profile, Figures 2-19 and 2-20 the thrust profile, and Figures 2-21 and 2-22 the speed profile. The particular profiles were selected to provide a range of modifications: Flight 200 was the least modified, retaining 64.4% of the procedure steps intact. Flight 1146 was intermediate with 55.1% retained intact. Flight 573 had more extensive modifications with only 38% of the original INM6 procedure steps unmodified. In Figures 2-17 the original INM procedure step profiles (as computed with INM6 batch) are shown as open symbols, and the modified INM7 procedure step profiles are illustrated with solid symbols and lines.

There were five different levels of reduced thrust considered, corresponding to five derated static takeoff thrust levels. (The CATs code applied in the prior analysis[2-6] permits a variable/performance driven takeoff thrust value rather than only having a discrete number of possible derated thrust levels to choose from.) INM was then run with each of the optimized procedure steps for each of the five derated thrust profiles and the parameters at the point of closest approach are compared with the radar data. The best energy match profile of the five is then picked and used for comparison with measured noise data at that particular microphone location. The reduced thrust / derated thrust departure levels were modeled by using cusomized Thrust-Jet coefficients in INM. These were developed jointly by Wyle and Boeing under the prior study.[2-2] Four of them (18k, 20k, 22k, 23k) represent simple reductions in thrust for both segment 1 and segment 2 climb. A blended set of coefficients (2220k) was also created which permits a 22k (rated static thrust) for segment 1 with a 20k (rated static thrust) for segment 2 climb. As noted before, this portion of the profile modeling analysis was conducted in 2005 and the resultant (optimized) INM 6 procedure steps were reused for this analysis.

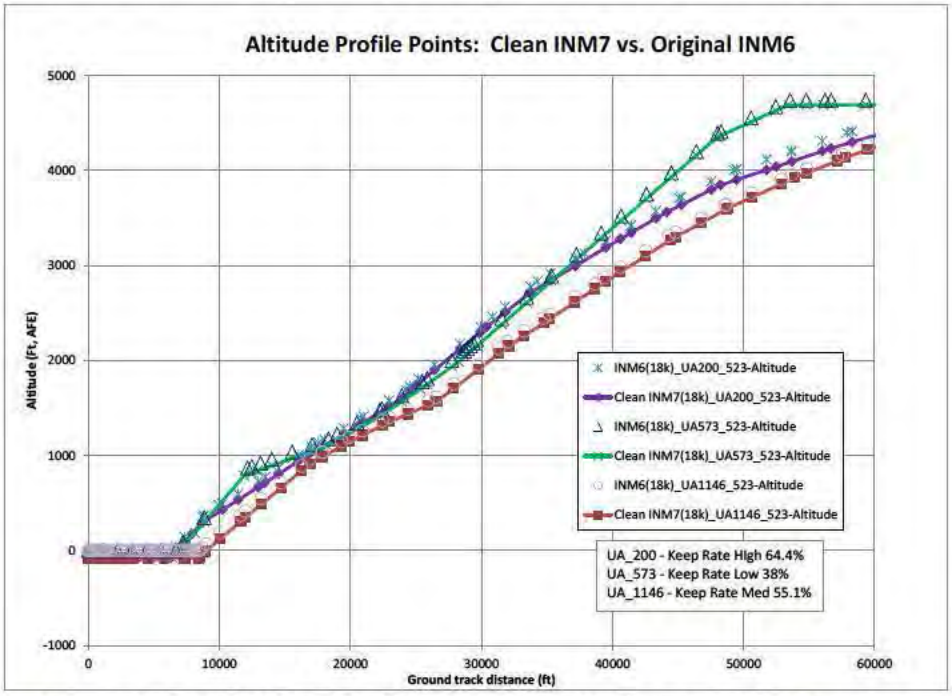

Figure 2-17. Original INM6 and Modified INM7 Climb Profiles (first portion) for 3 Operations.

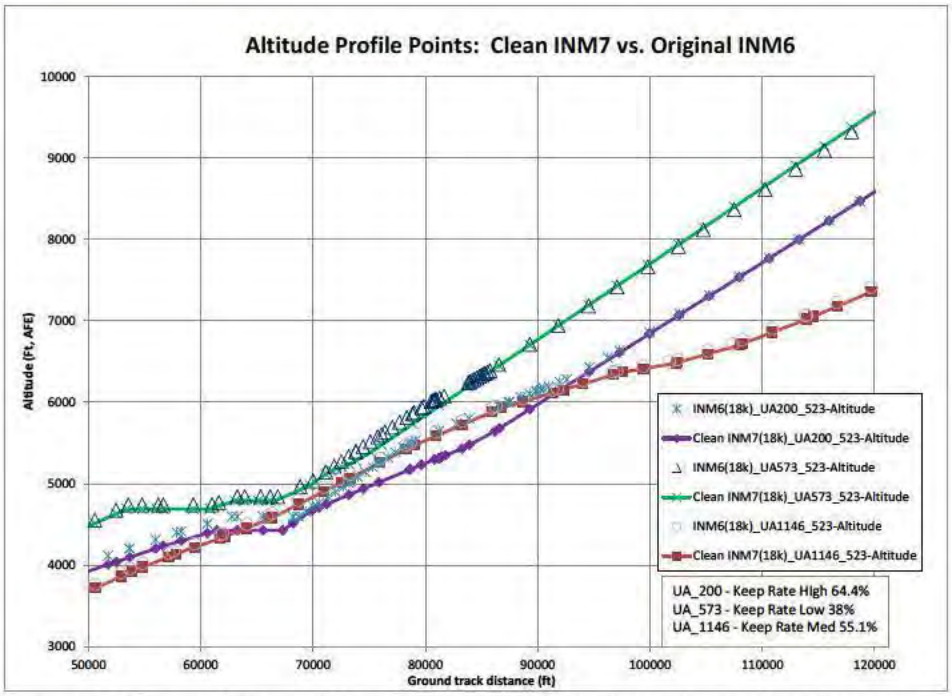

Figure 2-18. Original INM6 and Modified INM7 Climb Profiles (second portion) for 3 Operations.

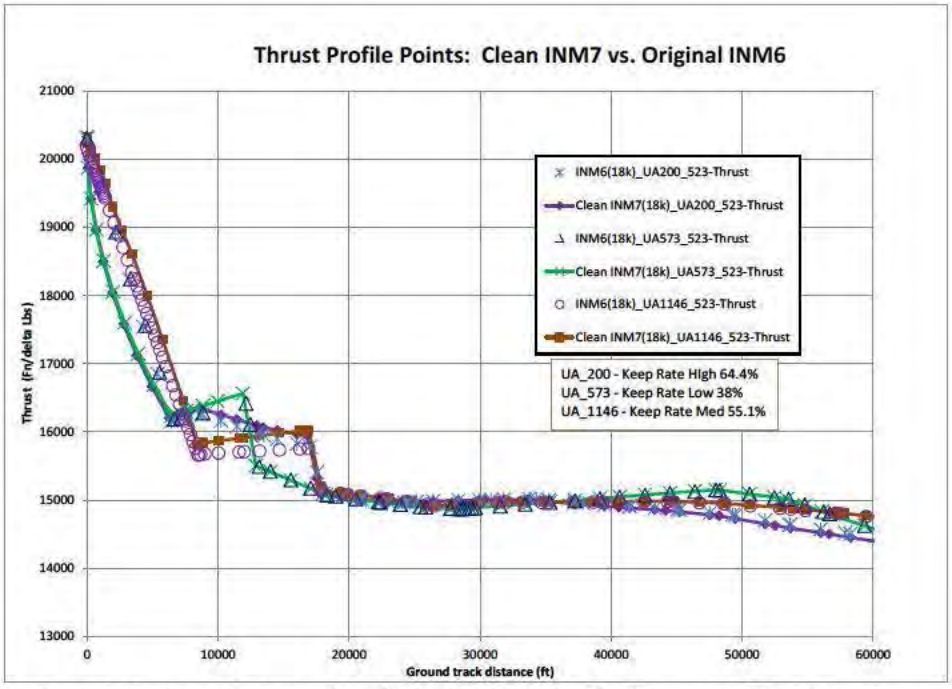

Figure 2-19. Original INM6 and Modified INM7 Thrust Profiles (first portion) for 3 Operations.

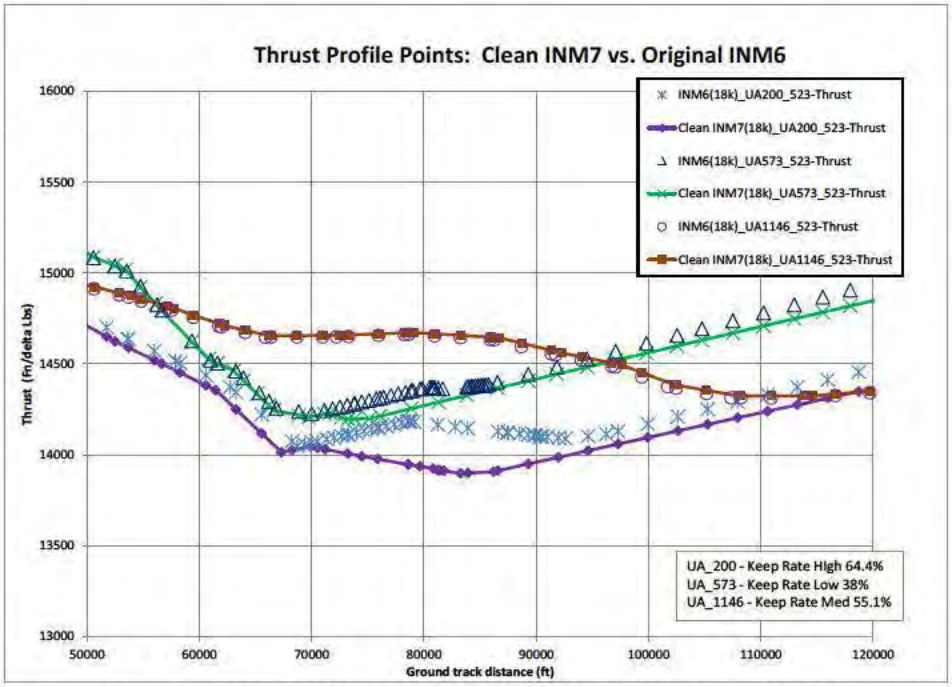

Figure 2-20. Original INM6 and Modified INM7 Thrust Profiles (second portion) for 3 Operations.

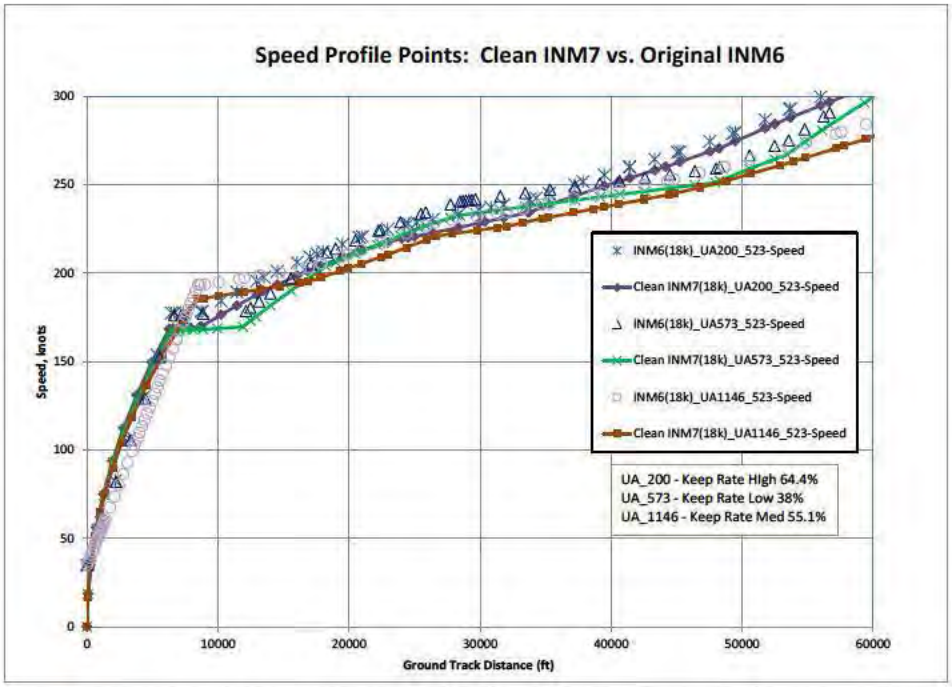

Figure 2-21. Original INM6 and Modified INM7 Velocity Profiles (first portion) for 3 Operations.

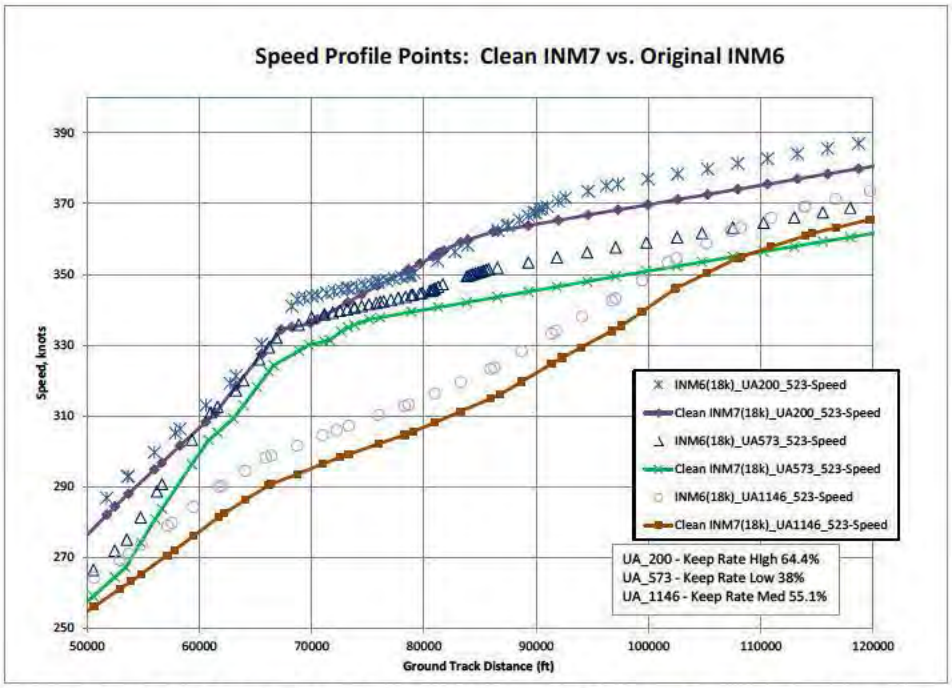

Figure 2-22. Original INM6 and Modified INM7 Velocity Profiles (second portion) for 3 Operations.

2.2.3 INM Modeling

INM Batch version 6.1 was originally run in 2005 with the updated Noise-Power-Distance curves provided by Boeing for the study documented in Reference 2-2. These prediction results were used in the study documented here. INM 7.0c was run using the Noise-Power-Distance curves provided with the standard INM installation package. The NPD values for both these versions of INM are the same. INM Batch 6.1 did not have the updated NPD included, but they eventually were issued with the INM 7.0c software. Terrain was enabled using the 3DS files required by INM. Each specific event included the airport pressure, temperature and humidity from the surface weather observations interpolated to the time of the departure. The "Modify NPD curves" option was selected ON in the INM GUI to permit computation of absorption changes due to humidity.

As described in the profile modeling section, for each flight operation five possible reduced thrust profiles (as described using procedure steps with customized jet-thrust coefficients) were (after some modification) run in INM7. The INM parameters at the point of closest approach (altitude and speed), were then compared with the measured radar parameters. The best profile was chosen for that noise event by selecting the minimum energy difference (potential and kinetic) at the point of closest approach. The noise from this "best pick" was then compared with the measured data. This is the process employed in the INM6 2005 study. It was replicated for the INM 7 analysis. Noise predictions from INM7 were compared with INM6 predictions as executed in 2005.

Table 2-10 describes the datasets used in the statistical analysis and the results of the "best pick" process which identified the best profile (and hence the amount of reduced thrust). Note that the labels used for the Thrust/Jet Coefficients represent the sea level static thrust for that nominal reduction in throttle setting. The actual thrust (units of Fn/delta, lbs as required by INM) are quite different (see Figures 2-19 and 2-10) due to a) operations are at DIA, non-standard day and once the aircraft is moving include momentum losses. The label of the reduced thrust is nominally the value of the "E" coefficient.

Table 2-10. Operations modeled in INM 6 and 7

INM 6		INM 7	
Thrust/Jet Coefficients	**Number of Events**	**Thrust/Jet Coefficients**	**Number of Events**
18k	228	18k	173
20k	40	20k	86
22k	3	22k	7
2220k	36	2220k	35
23k	0	23k	6
Total	**307**	**Total**	**307**

A comparison of the INM Predicted – Measured SEL (dBA) with the "best pick" Energy$^{2-2}$ parameter (displayed on a semi-log graph) is provided in Figure 2-23. Even though the linear fit is closer to zero, the increase in scatter and outliers is likely indicative of a more optimal development of the procedure step parameters with the use of INM6 batch. Unfortunately resources did not permit development of an INM7 batch tool or updates to the procedure step optimizer to improve the fit between the modeled and measured flight profiles.

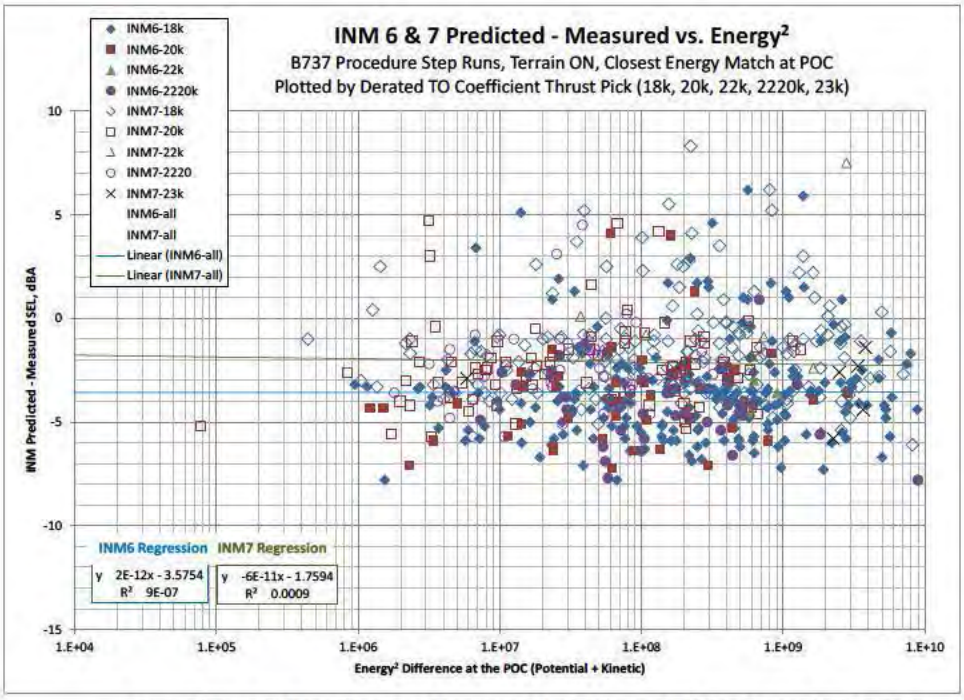

Figure 2-23. INM Prediction – Measurement as a function of Best Energy^2 Fit at POC.

2.2.4 Comparisons with Independent Parameters

Figure 2-16 demonstrates the improvements in the INM predictions from version 6 to version 7 using Procedure Step Modeling. Table 2-11 contains statistical results corresponding to the data in Figure 2-16 based on the 307 unique noise events and the selected best energy match reduced thrust profile modeled using procedure steps. Figures 2-24 to 2-34 display the data comparisons, the linear regression and equation.

Table 2-11. INM Prediction – Measurement Statistics

INM Predictions – Measurements, SEL, dBA		
	INM 6.1 Batch	INM 7.0c
Mean	-3.57	-1.79
St.Deviation	2.36	2.30
Variance	5.59	5.30
Count	307	307

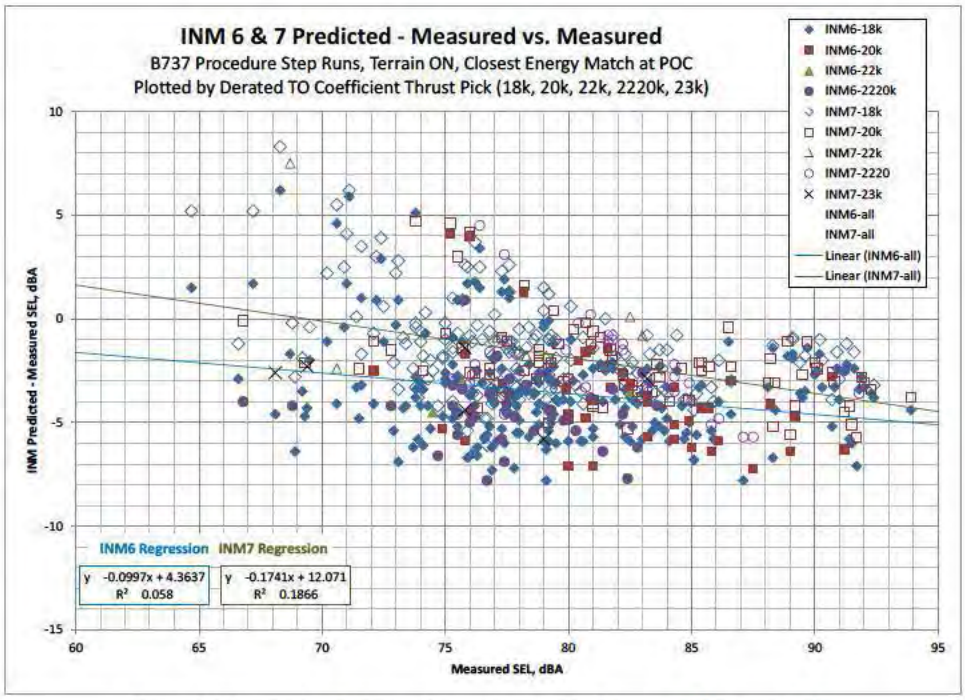

Figure 2-24. INM Prediction – Measurement as a function of Measured SEL.

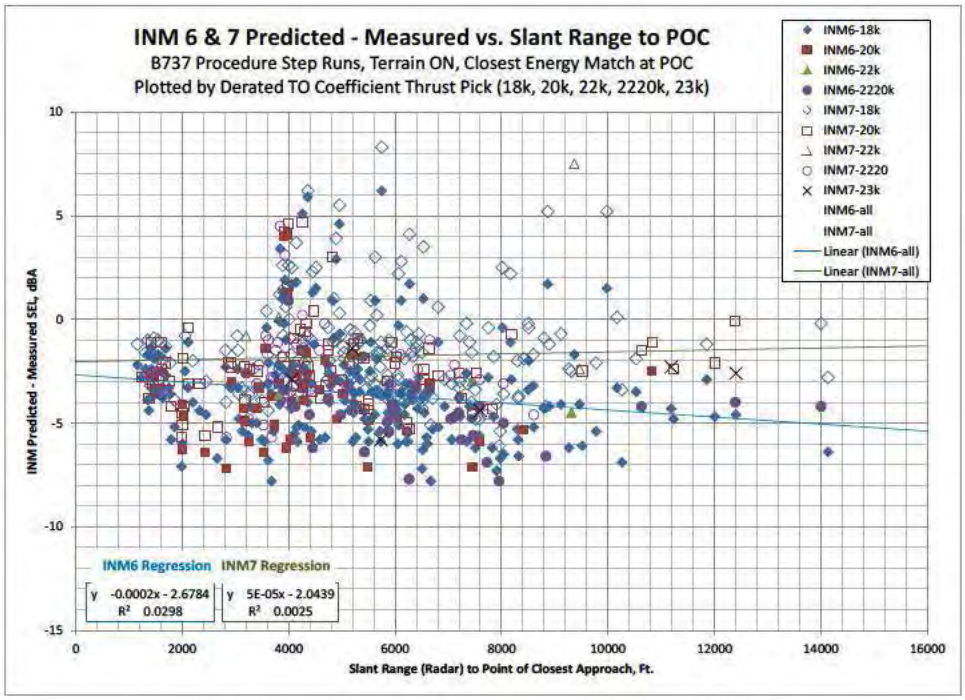

Figure 2-25. INM Prediction – Measurement as a function of Slant Range

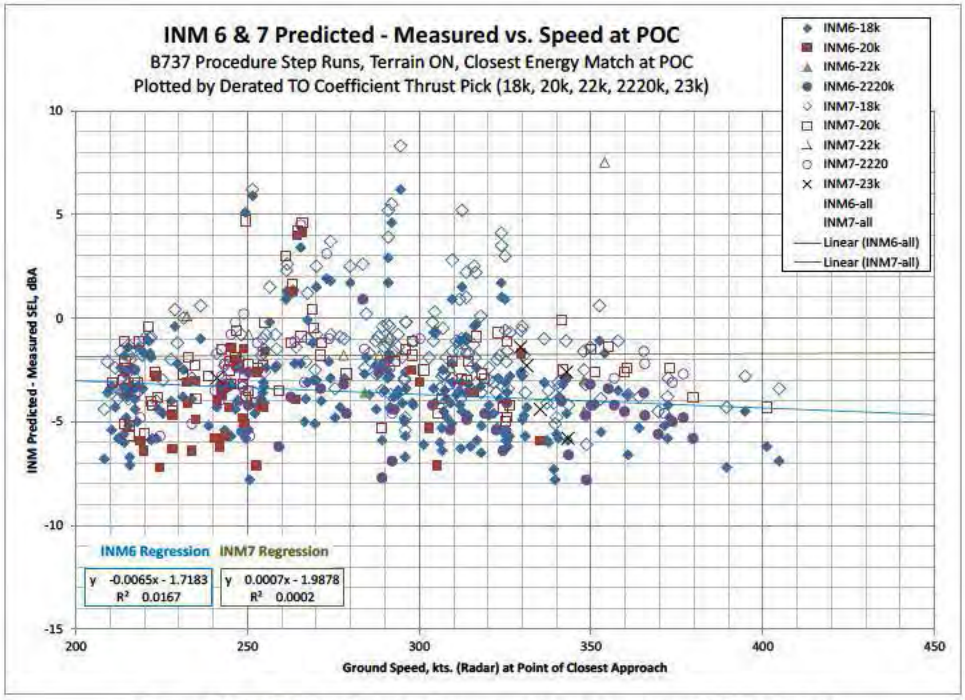

Figure 2-26. INM Prediction – Measurement as a function of Flight Speed

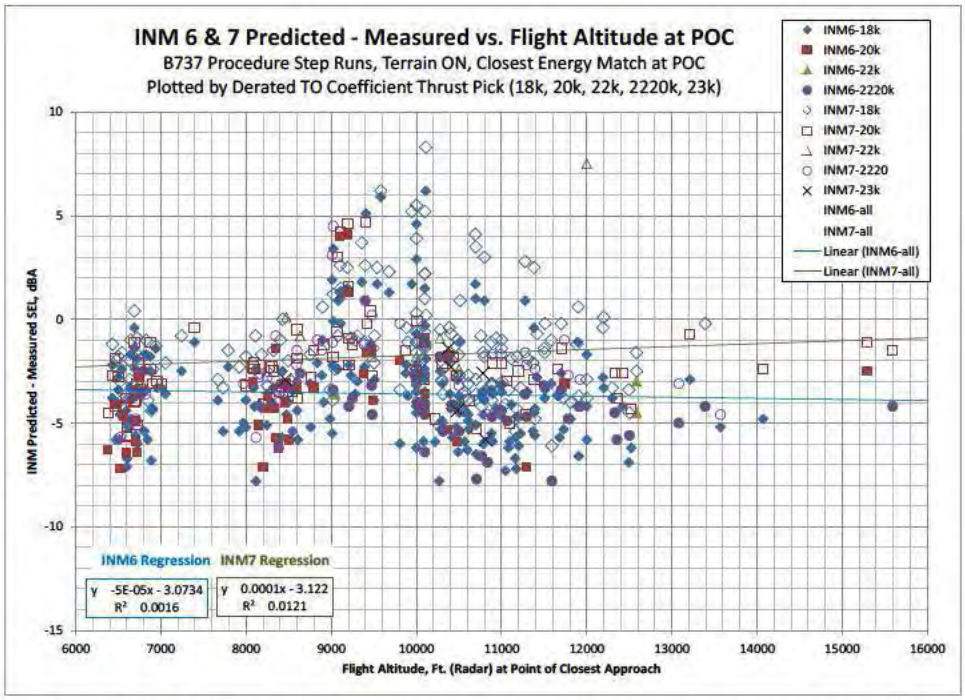

Figure 2-27. INM Prediction – Measurement as a function of Aircraft Flight Altitude (MSL, ft.)

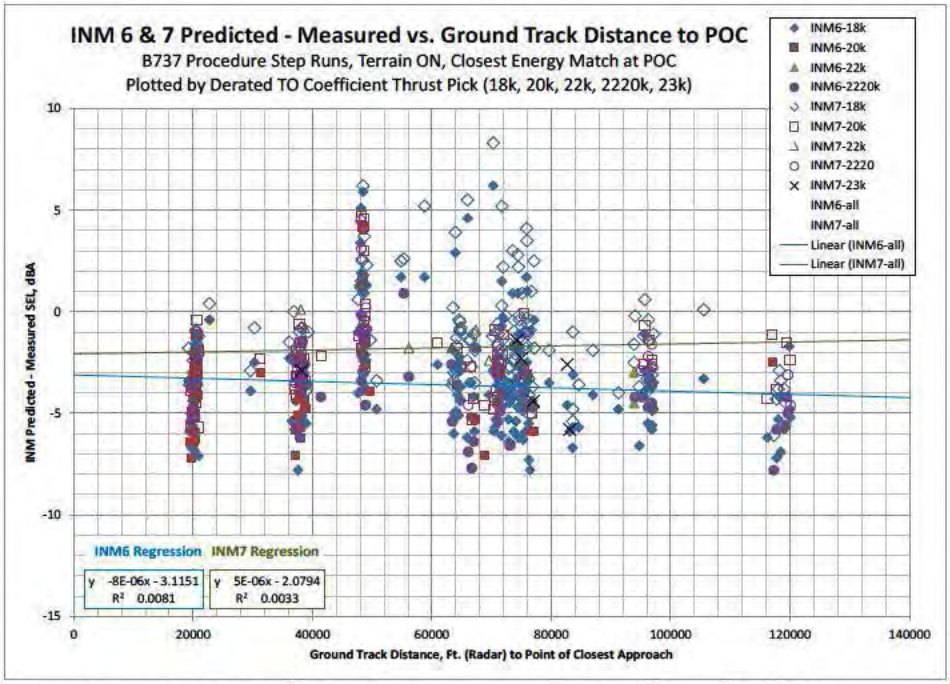

Figure 2-28. INM Prediction – Measurement as a function of Ground Track Distance

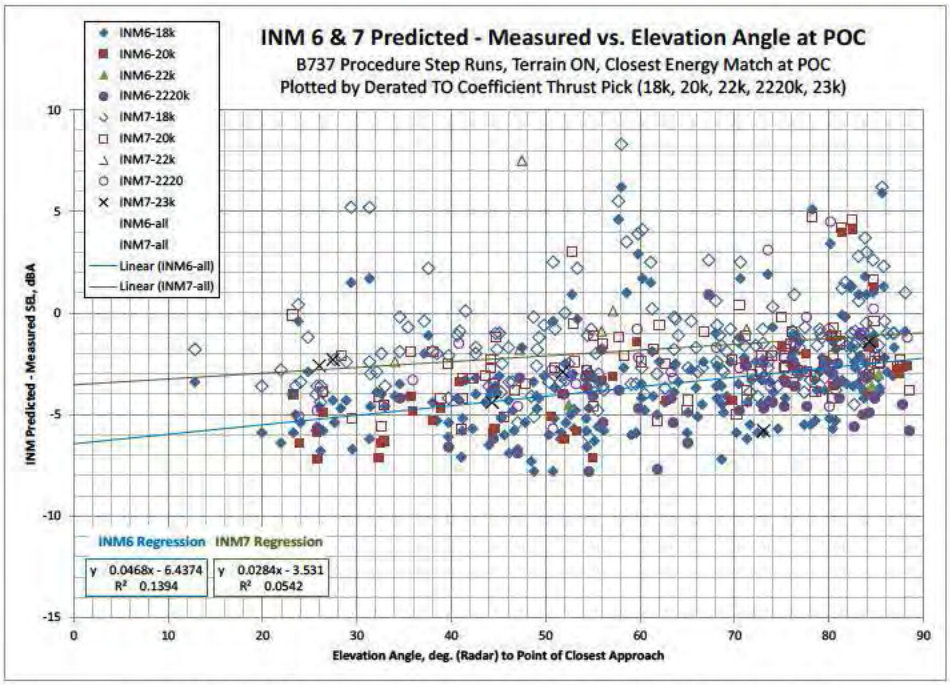

Figure 2-29. INM Prediction – Measurement as a function of Elevation Angle

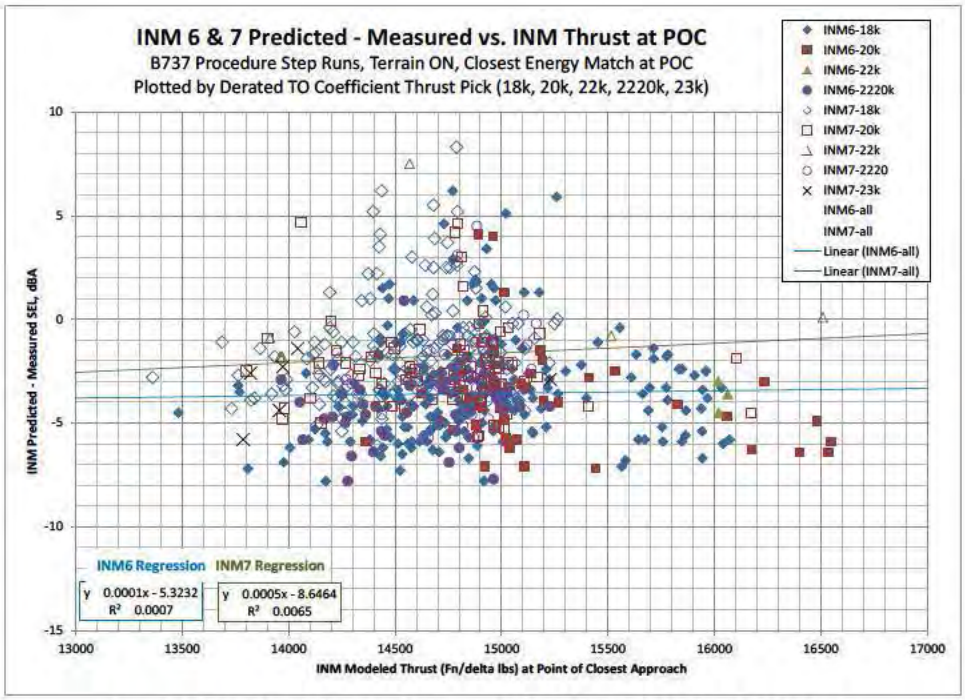

Figure 2-30. INM Prediction – Measurement as a function of Thrust at the PCA.

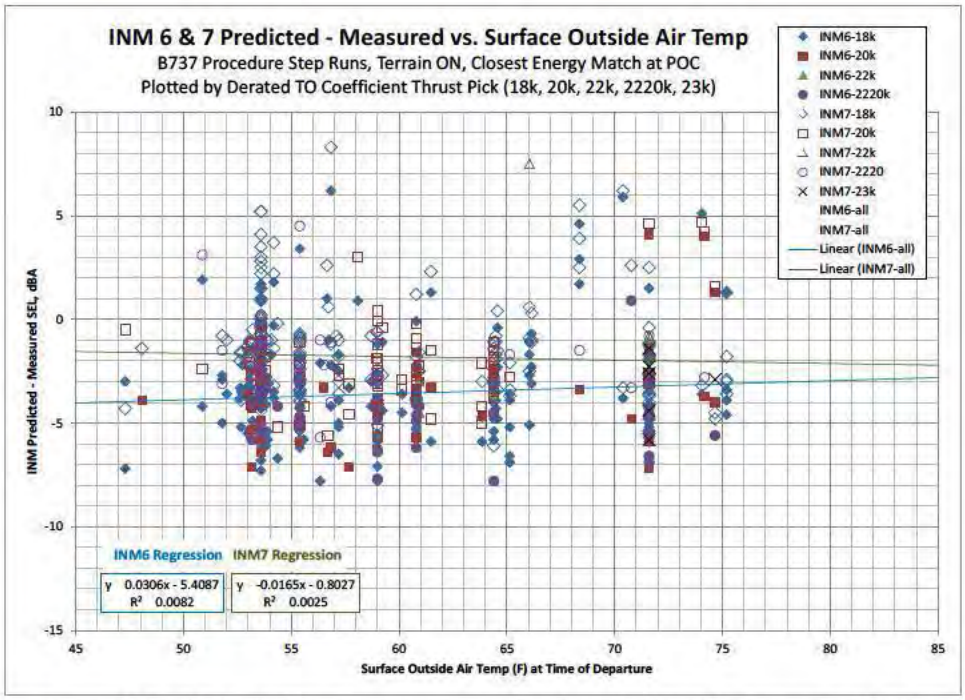

Figure 2-31. INM Prediction – Measurement as a function of Surface Air Temperature (deg F)

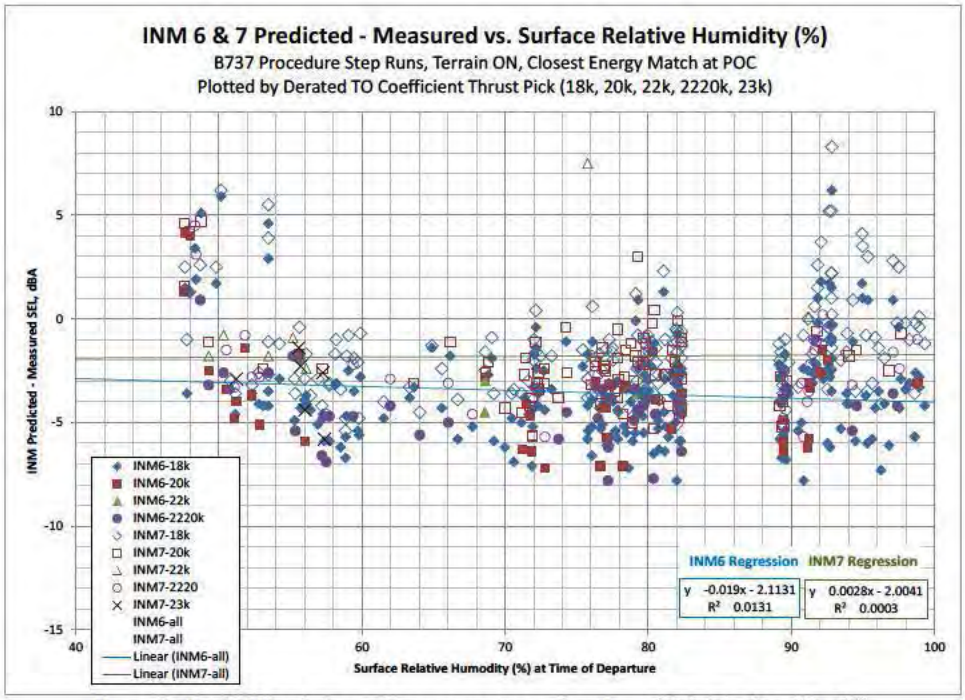

Figure 2-32. INM Prediction – Measurement as a function of Relative Humidity (%).

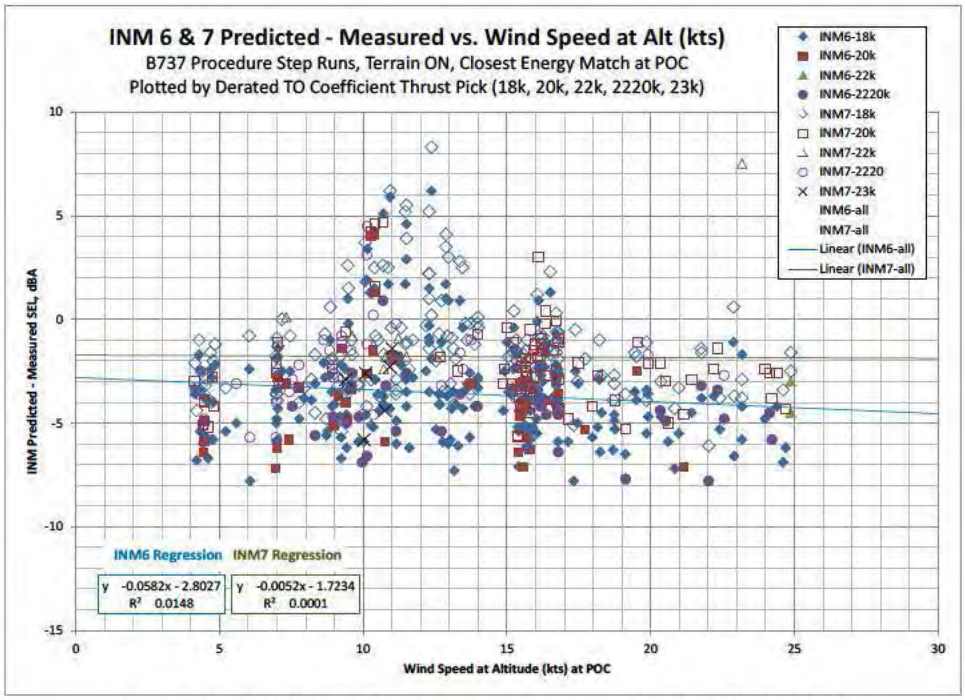

Figure 2-33. INM Prediction – Measurement as a function of Winds aloft (kts).

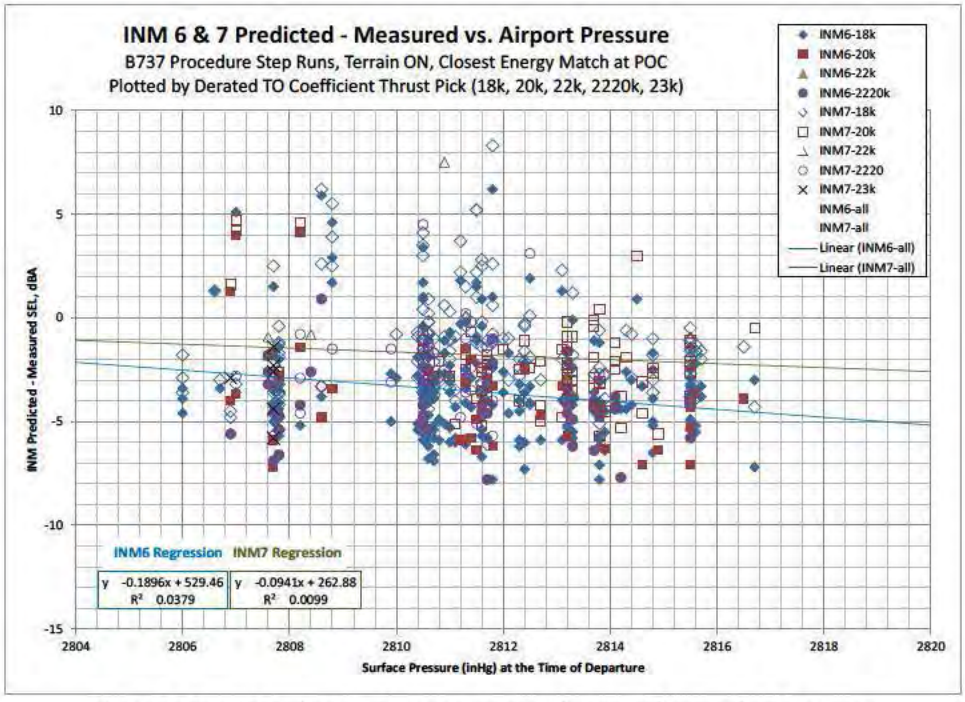

Figure 2-34. INM Prediction – Measurement as a function of Atmospheric Pressure.

2.2.5 Findings and Recommendations Based on INM Procedure Step Analysis

Comparison of INM predicted noise with measurements from high altitude operations for procedure step modeled profiles for three variants of the B737 has reduced the INM underprediction for reduced thrust high altitude departures. However due to an increase in the difference between the modeled and measured aircraft energy state at the point of closest approach, one cannot definitively credit this reduction in the predictions to improvements in the INM acoustic modeling. Differences in modeled thrust, speed and aircraft location are playing a role as well. The analysis described in Section 2.1utilized profile point trajectories, and held the aircraft location, speed and thrust constant, and was therefore able to provide a definitive indication of the INM acoustic propagation and source modeling improvements. Due to multiple variations in modeling parameters, the analysis described in this section was not able to reach a firm conclusion.

A more direct comparison of INM6 and INM7 procedure step modeling could be obtained by computing new optimal Procedure Steps for the five possible derated thrust jet coefficients using a batch version of INM, or by developing additional automated procedures which permit optimization. As noted earlier, the scope of the current effort did not permit development of new optimization procedures.

It is recommended that an additional study comparing predictions from AEDT thrust-from-position algorithms (or INM algorithms, if available) with the as-measured radar profiles be considered. An assessment of use of these algorithms with reduced thrust jet coefficients should also be explored.

2.3 A Comparison of INM Profile Point and Procedure Step Modeled DIA Departures Operations

This section compares results presented previously from INM modeling analysis of DIA operations using Profile Points (CATs) methodology (Section 2.1) and the Procedure Step methodology (Section 2.2). Prior studies examined this same dataset with INM 5.2a using profile point analysis[2-3] and procedure step analysis.[2-4] Table 2-12 itemizes the specific INM runs included in the analysis described in this Section.

Table 2-12. INM Versions Used in the DIA Analysis

	INM5	INM 6*	INM 7
Profile Points (CATs)	INM 5.2a	INM 6.2 Default NPDs	INM 7.0c
Procedure Steps	n/a	INM 6.1 batch Modified NPDs	INM 7.0c

**Note: The modified NPDs utilized in INM 6.1 are the same as the default NPDs of INM 6.2.*

A common set of 191 operation-noise measurement events were extracted from the five sets of INM runs identified in Table 2-12. These results include three variants of the Boeing 737 as those were the only aircraft for which procedure step reduced thrust jet coefficients were made available under the 2005 study.[2-2] Denver International Airport departure operations from 21, 22 and 23 May were modeled using both the CATs code (profile points) and INM Procedure Steps and only those which were successfully executed in INM were retained, yielding a total of 191 data points for each INM analysis. The iterative optimization results from the 1998 study[2-1] were utilized directly and re-run for the five possible degrees of reduced thrust (18k, 20k, 22k, 2220k, 23k) with the "best" one selected using the energy fit as described in Reference 2-2. All INM runs were conducted with Terrain enabled and temperature and humidity based on the departure time.

The results of n=191 data points for INM predicted – Measured SEL are characterized in Table 2-13. For comparison, Table 2-14 characterizes the results from the n=2171 Profile Points (CATs) analysis[2-1] and the n=307 Procedure Step analyses.[2-2] A relatively close agreement of the overall predicted – measured SEL mean level accompanied by a reduction in the standard deviation and the variance, indicates that outliers were eliminated in the comparison. This could be due to failures of the INM procedure step modeling to handle

situations which were previously considered in the CATs analysis, and it could also be because resources permitted analysis of only three days of departure operations.

Overall, improvements in the predictions are shown for the original full datasets and those with n=191 with later versions of INM when modeling with either Profile Points (CATs) or Procedure Steps. The standard deviation and variance is relatively consistent between INM 6 and 7 for both profile techniques. Figure 2-35 shows the 191 data points for each analysis mode graphically. Also displayed on Figure 2-35 are linear regressions to the 5 individual datasets.

Table 2-13. Comparative Dataset - Procedure Step vs. Profile Points Results Characterization
INM Predicted – Measured SEL, dBA

	INM5	INM 6	INM 7
Profile Points (CATs) N	191	191	191
Mean	-5.5	-2.0	-0.7
Standard Deviation	2.9	2.5	2.5
Variance	8.2	6.2	6.2
Procedure Steps	n/a	191	191
Mean		-3.5	-1.8
Standard Deviation		2.4	2.4
Variance		5.9	5.7

Table 2-14. Full Dataset - Procedure Step and Profile Points Results Characterization
INM Predicted – Measured SEL, dBA

	INM5	INM 6	INM 7
Profile Points (CATs)	2171	2171	2171
Mean	-5.5	-1.1	-0.4
Standard Deviation	3.8	3.5	3.1
Variance	14.3	12.1	9.7
Procedure Steps	n/a	307	307
Mean		-3.6	-1.8
Standard Deviation		2.4	2.3
Variance		5.6	5.3

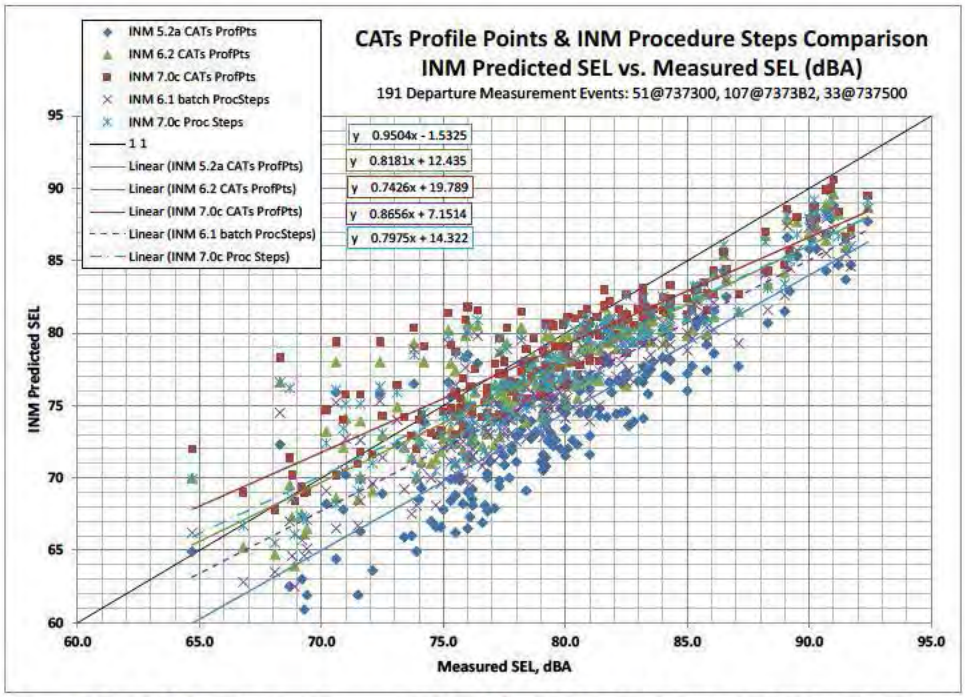

Figure 2-35. INM Predicted vs. Measured SEL (dBA) for CATs Profile Point and INM Procedure Steps.

2.3.1 Comparisons with Independent Parameters

The difference between predicted and measured SEL (dBA) values were compared with several different independent variables to assess sensitivity and perhaps gain insight as to a possible physical mechanism associated with the prediction sensitivity. Figures 2-36 through 2-39 include prediction results with respect to Measured SEL.

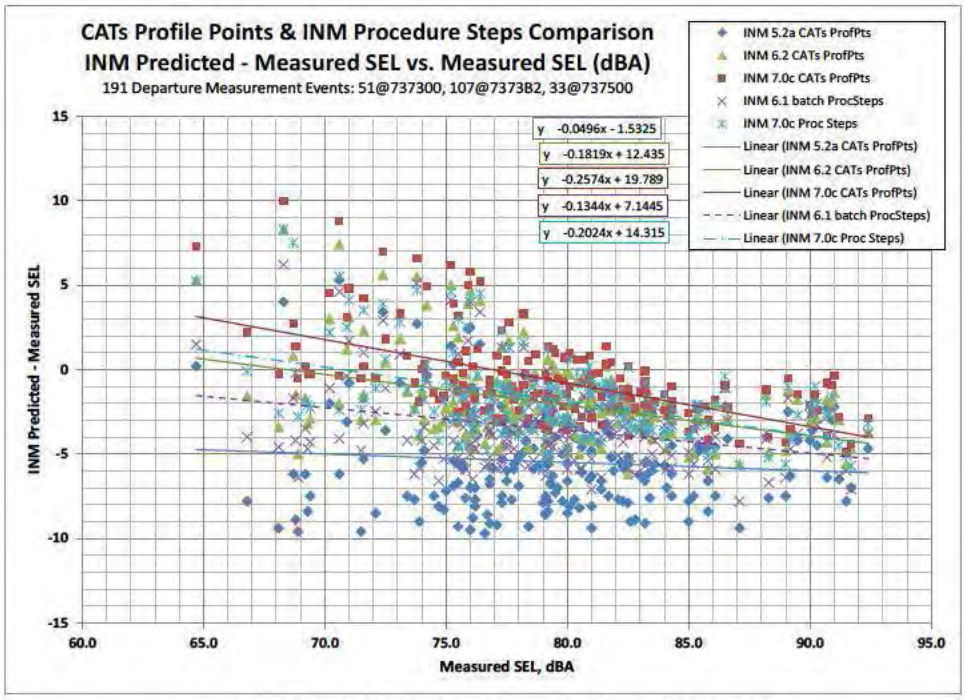

Figure 2-36. INM Prediction Sensitivity to Measured SEL (dBA).

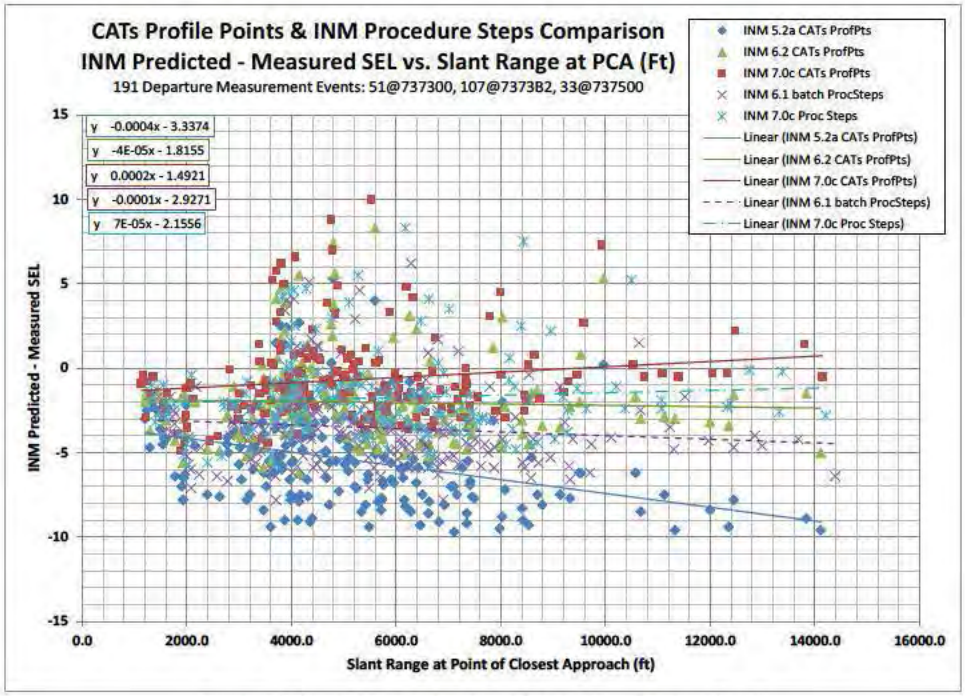

Figure 2-37. INM Prediction Sensitivity to Slant Range (feet).

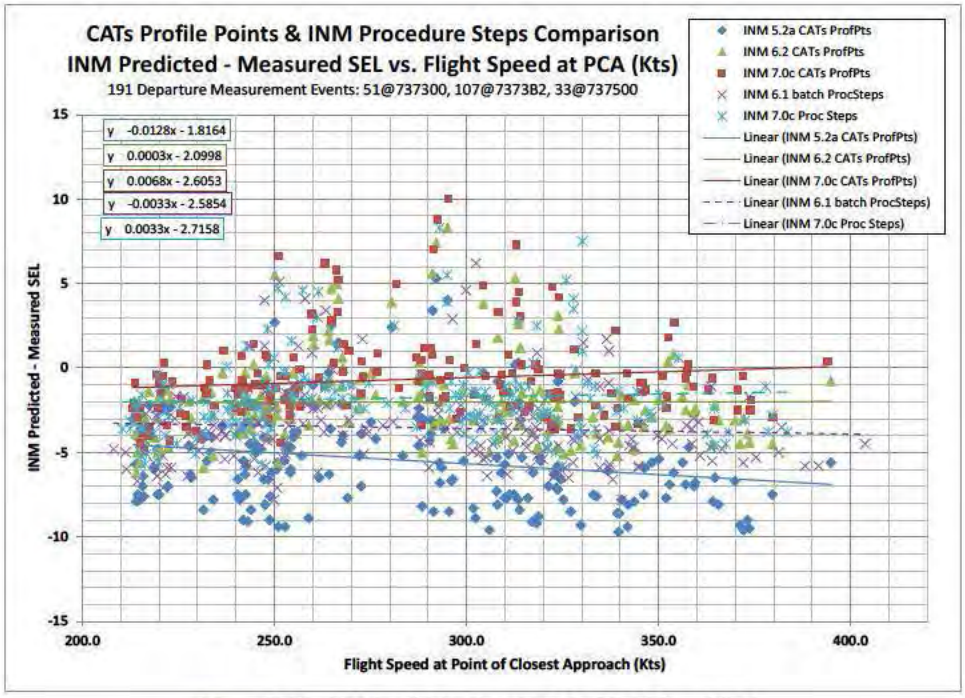

Figure 2-38. INM Prediction Sensitivity to Flight Speed (kts).

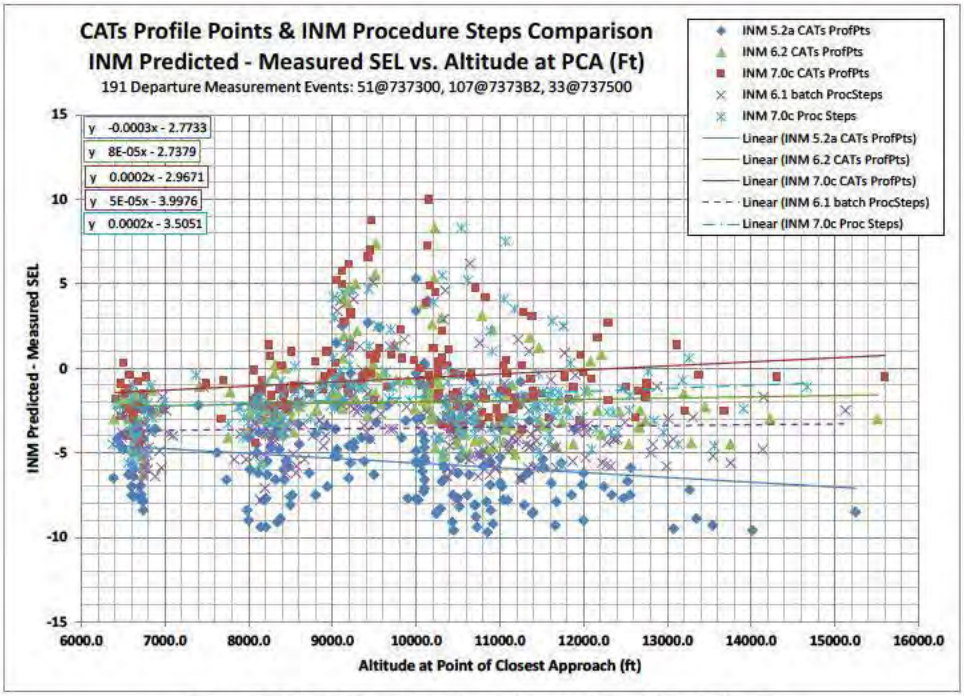

Figure 2-39. INM Prediction Sensitivity to Flight Altitude (feet).

2.3.2 Comparison Between Profile Modeling Techniques

A comparison was made of the profile parameters at the point of closest approach for the various modeling techniques. Figures 2-40 through 2-43 are included to provide a visual representation of the differences in aircraft slant range, altitude, speed and thrust at the point of closest approach between the two analysis modes – Profile Points and Procedure Steps. The profile points very nearly match the measured data and the procedure steps exhibit considerably more scatter.

The CATs profile points were based on measured and smoothed radar trajectories, so naturally Figures 2-40 and 3-41 show the Profile Points data closer to measured (radar) data altitude and speed. Within INM, segmentation algorithms take the input procedure steps and divide them into smaller pieces for noise analysis. Segmentation occurs for both profile point and procedure step modeling modes. Figure 2-42 displays the slant range between the point of closest approach and the noise monitor. All versions of INM run with the CATs code are a near perfect match (as expected) to the measured radar data. Considerable differences in the measured slant range values may be seen in the Procedure Step modeling (Figure 2-42).

The original CATs development process was limited to 100 profile points due to INM version 5 modeling restrictions on the number of profile points. Over the course of INM development some changes have likely been made to the segmentation algorithm. These algorithm changes manifest as slightly different values of the altitude and speed at the point of closest approach for the exact same profile point input values and explain some of the differences seen in Figures 2-40 and 2-41 for the Profile Points values. Other reasons for the differences in the altitudes could be due to the lack of fidelity in the radar altitude values, which are only reported as flight levels, in increments of 100 Ft, but which were interpolated during development of the Profile Points.

The INM Procedure Step modeling input was also limited in terms of the number of steps which could be entered. These were developed iteratively by optimizing the particular procedure step type, and step parameters and were reused as exact input in both versions of INM.

When examining the Procedure Step profile parameters (Figures 2-40 through 2-42) at the point of closest approach, one sees considerable variability. The original INM 6.1 batch version, which was used to iteratively optimize the procedure steps themselves, as well as the INM 7.0c analysis of those exact same procedure steps, has more scatter than Profile Points, as is expected. That both INM versions of procedure steps have similar R^2 values suggests that the fit of modeling to measured data is comparable for both versions of INM.

INM was run five times – one for each amount of derated thrust – for each sequence of optimized procedure steps. For each flight trajectory the best derated thrust from the five was selected by minimizing the energy difference (potential and kinetic) at the point of closest approach. Figures 2-40 through 2-43 display only the "best" derated thrust selected profile. Table 2-15 itemizes the number of the final "best" fit derated thrust operations for INM 6 and 7 using Procedure Steps. In general the thrust values from INM 7 were higher than those in INM 6. It is important to note that Table 2-15 reflects the 'selected' best fit operation based on the energy optimization. Note that the optimized procedure steps for an 18k derated thrust are not the same steps as the optimized procedure steps for a 22k derated thrust.

Table 2-15. Number of "best fit" Derated Thrust Operations using Procedure Steps

Thrust/Jet Coefficient	Number of INM 6 Ops	Number of INM 7 Ops
18	126	96
20	35	59
22	3	6
2220	27	24
23	0	6

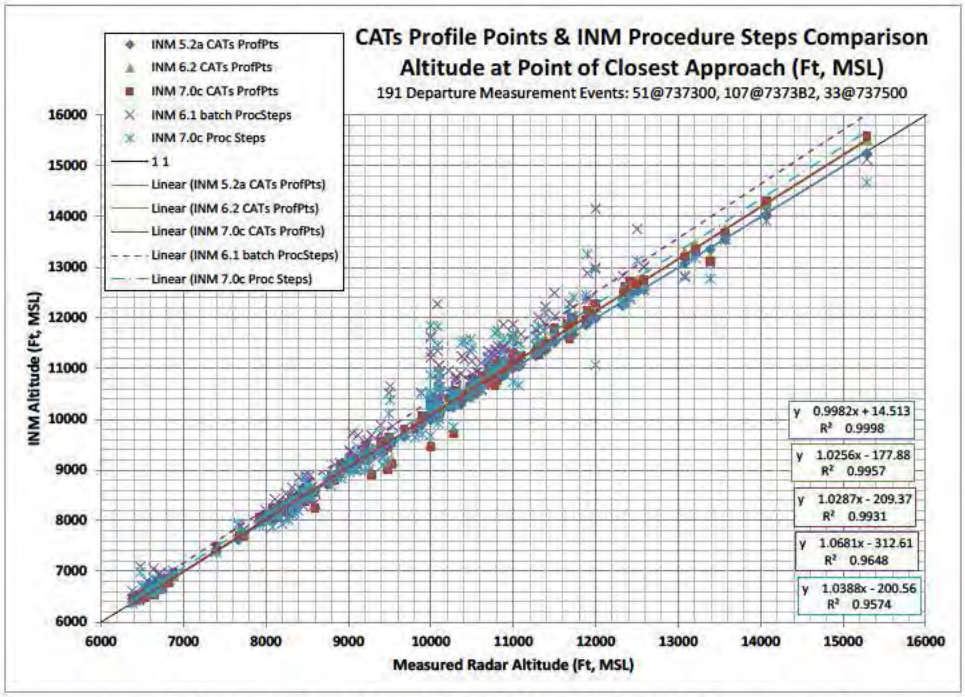

Figure 2-40. Comparison of Profile Altitude (Ft) at the Point of Closest Approach.

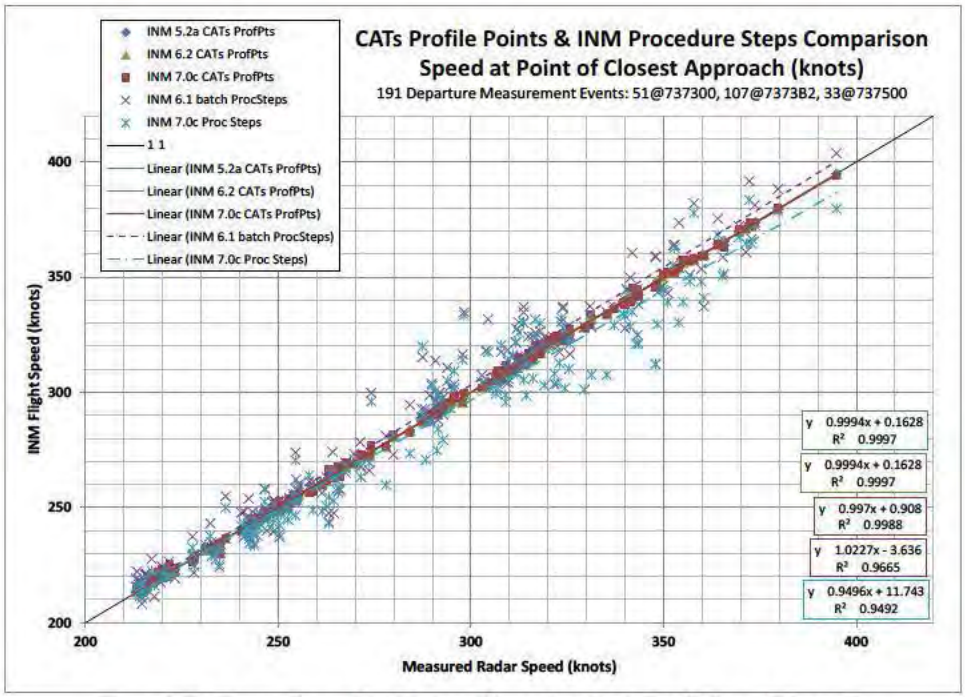

Figure 2-41. Comparison of Profile Speed (knots) at the Point of Closest Approach.

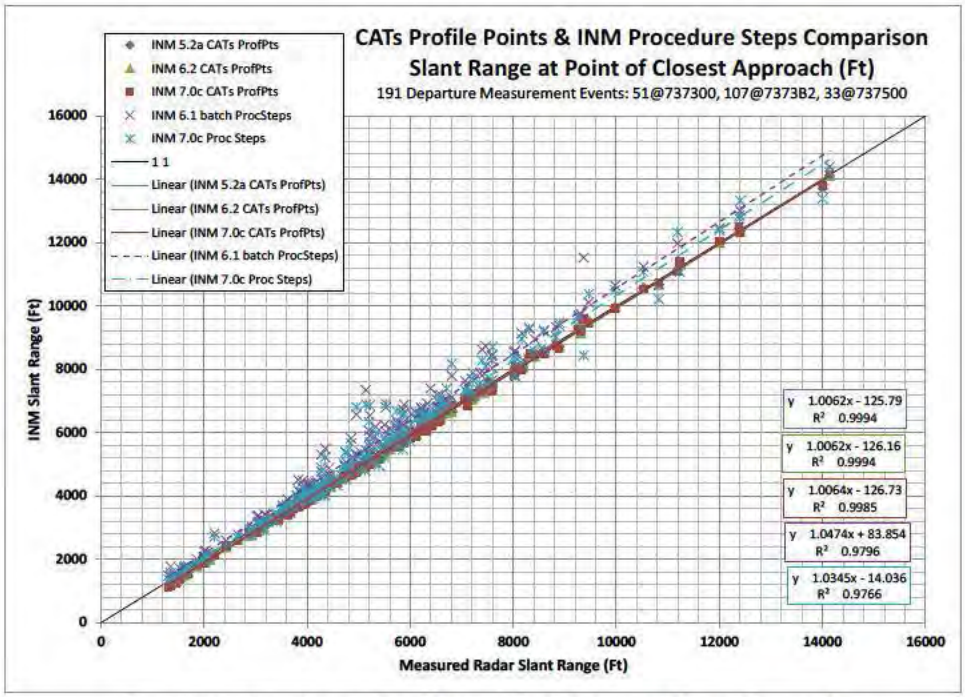

Figure 2-42. Comparison of Slant Range (ft) at the Point of Closest Approach.

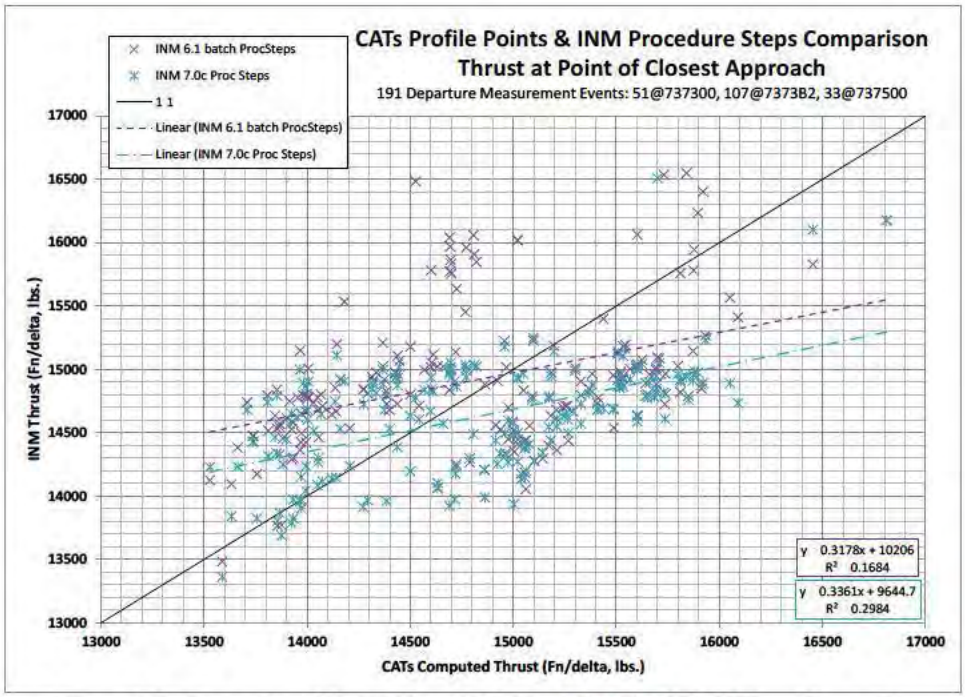

Figure 2-43. Comparison of Profile Thrust (Fn/delta, lbs) at the Point of Closest Approach.

2.3.3 Findings and Recommendations Based on INM Profile Point and Procedure Step Comparisons

Modeling in this study using profile points more closely matches the measured radar data and provides better agreement with acoustic measurement data than the iterative procedure step modeling process. There were considerable differences between the altitude and speed prediction of thrust based on the Assumed Temperature modeling method (CATs) and the INM prediction of thrust using modified reduced thrust jet-thrust modeling coefficients and the energy match at the point of closest approach. These differences cannot be exclusively attributed to the acoustic propagation or noise source database improvements. There are considerable differences in the location of the point of closest approach and the aircraft operating state at that location between the two classes of profile modeling techniques.

Additional research is needed to ascertain how much of the acoustic differences are due to profile modeling effects and how much is due to INM improvements. It is recommended that the procedure step modeling process be revisited using a newer version of INM. This will likely require a batch version of INM7. The procedure step process relied on five discreet amounts of thrust reduction, however better fits to the measured radar profile might be obtained by utilizing more datasets with higher fidelity.

References

2-1. Page, J.A., Hobbs, C.M., Plotkin, K.J., and Stusnick, E. 2000. "Validation of Aircraft Noise Prediction Models at Low Levels of Exposure", NASA CR 2000-21012, April.

2-2. Forsyth, D.W., and Follet, J.I. 2006. "Improved Airport Noise Modeling for High Altitudes and Flexible Flight Operations", Appendix B, Page, J.A. and Usdrowski, S., "Reduced Thrust Departures

from a High Altitude Airport Using Procedure Steps with the Integrated Noise Model", NASA CR 2006-214511, October.

2-3. "Integrated Noise Model (INM) Version 5.1 Technical Manual". 1997. FAA-AEE-97-04, December.

2-4. "Integrated Noise Model (INM) Version 6.0 Technical Manual". 2002. FAA-AEE-02-01, January.

2-5. "Integrated Noise Model (INM) Version 7.0 Technical Manual". 2008. FAA-AEE-08-01, January.

2-6. Juliet A. Page. 2012. "Technical Memorandum: INM 5, INM6 and INM7 Analysis of Profile Point Modeled DIA Departure Operations", Delivered to Volpe, 31 December.

2-7. SAE AIR 5662-2006. 2006. "Method for Predicting Lateral Attenuation of Airplane Noise," Society of Automotive Engineers, Warrendale, PA.

2-8. Page, J.A. 2012. "Technical Memorandum: INM 5, INM6 and INM7 Analysis of Profile Point Modeled DIA Departure Operations", 31 December.

2-9. Page, J.A. 2013. "Technical Memorandum: INM6 and INM7 Analysis of Procedure Step Modeled DIA B737 Departure Operations", 31 January.

2-10. Page, J.A., Hobbs, C.M., Plotkin, K.J., and Stusnick, E. 2000. "Validation of Aircraft Noise Prediction Models at Low Levels of Exposure", NASA CR 2000-21012, April.

2-11. Forsyth, D.W., and Follet, J.I. 2006. "Improved Airport Noise Modeling for High Altitudes and Flexible Flight Operations", Appendix B, Page, J.A. and Usdrowski, S., "Reduced Thrust Departures from a High Altitude Airport Using Procedure Steps with the Integrated Noise Model", NASA CR 2006-214511, October.

3.0 Simulation Noise Modeling of Selected Flights at KDEN

In Section 2 noise measured at Denver International Airport[3-1] was compared to predictions from INM Versions 5, 6 and 7. As part of the original KDEN study, INM 5 predictions were made using profile point analysis. In a follow-up study[3-2] INM 6 predictions were made using procedure step profiles. A subset of 90 eastbound departures was further analyzed[3-3] using the NMSim simulation model.[3-4] The conclusions at the time were that simulation provided better agreement with measurements, and that atmospheric absorption played a key role in the results. That analysis has been revisited using the current INM predictions and simulation via the Advanced Acoustic Model (AAM).[3-5]

3.1 Data Set and Original Comparisons

Figure 3-1 shows the layout of Denver International Airport and the noise monitoring sites. The subset considered here consisted of departures from Runway 8 and noise recorded at the sites circled in red. A criterion for selecting the subset was that noise from each operation was recorded on at least two sites. There are 264 points in the data set, so there was an average of just under three per flight. Aircraft types were Boeing 727, 737 and 757, for which United Airlines provided takeoff weight and power/configuration data.

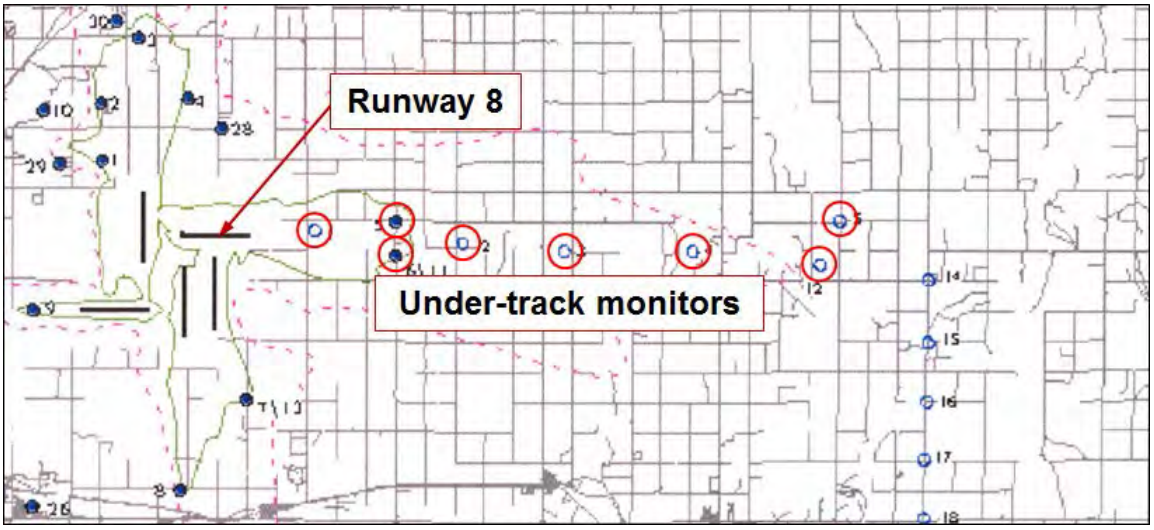

Figure 3-1. KDEN runways and monitoring sites

Figure 3-2 shows the original comparison between INM 5 predictions and measurements. Individual data points are marked in color according to the three aircraft types considered. There are 57 data points for B727, 194 for B737, and 13 for B757. The B727 data points are at higher levels because that older aircraft type is noisier and was also generally at lower altitude (as seen in Figure 3-3) because of its lesser climb performance compared to the other two types. The total number of points in the plot and the correlation coefficient R of a linear fit are indicated. There is a 45 degree dashed line that represents perfect agreement. Lines of "y(x)" and "x(y)" fits that form R are included in the plot. A table in the lower right corner of the plot shows the average and rms deviation from perfect agreement for the whole data set and for each aircraft type.

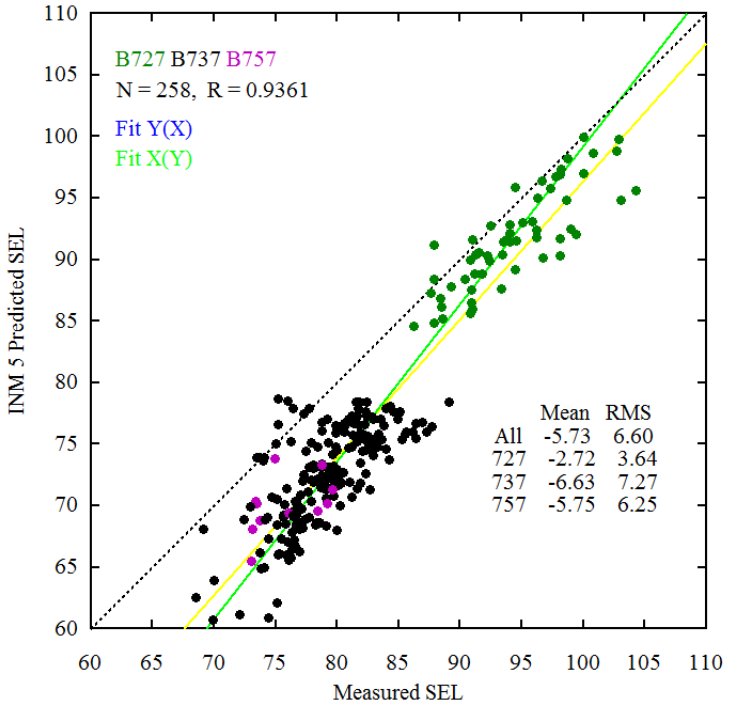

Figure 3-2. Comparison between Measured SEL and INM5 Predicted SEL.

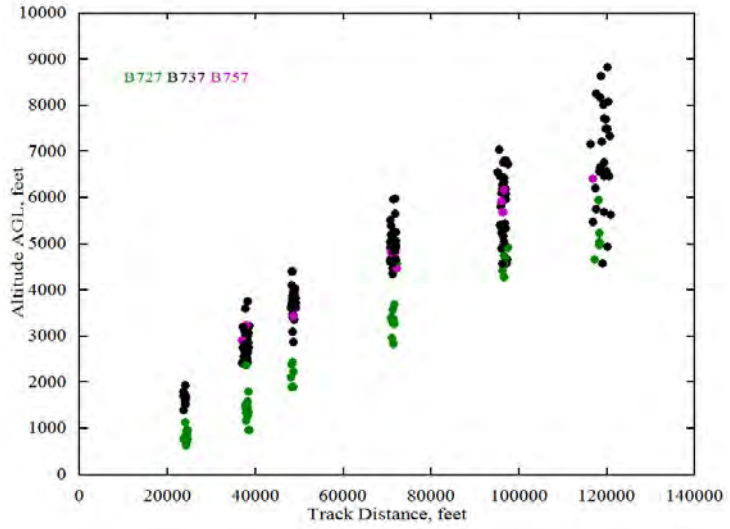

Figure 3-3. Altitude versus Track Distance for the Three Aircraft Types.

The differences seen in Figure 3-2 were thought to be associated with propagation and air absorption. The NPD tables in INM are for reference temperature and humidity (59° F, 70% RH), and at the time INM 5 did not adjust for local absorption conditions. Figure 3-4 shows the temperature and humidity for each data point, together with the reference condition. (Humidity is represented by mole fraction, which is physically more meaningful than relative humidity. For reference, relative humidity ranged from 41% to 99%) The hypothesis that absorption was a major factor was supported by the differences seen in Figure 3-4 and the better agreement for 727s, which were at lower altitude and hence less subject to absorption effects. Simulation modeling offered the opportunity to use actual temperature and humidity, either surface data or layered profiles.

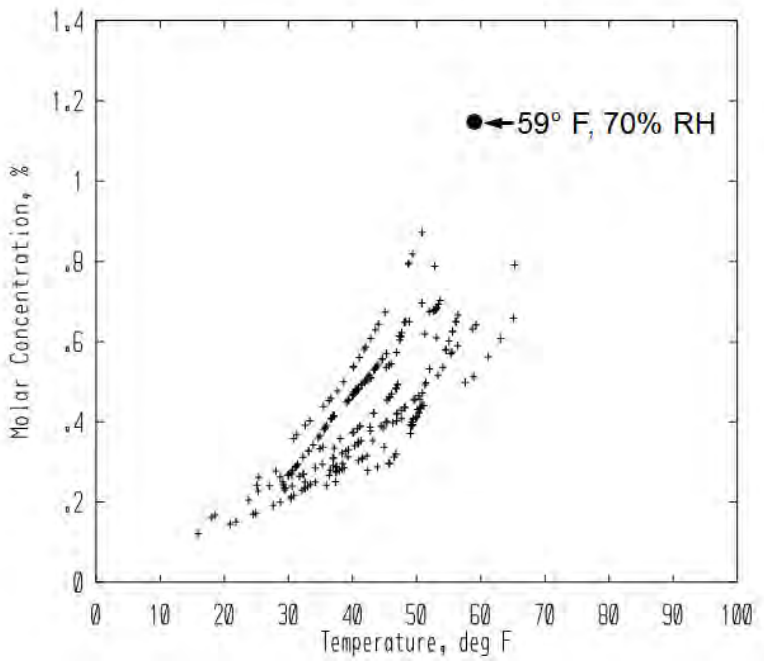

Figure 3-4. Surface Temperature and Humidity for Time of Flight, compared with Reference Temperature and Humidity.

Figure 3-5 shows a comparison[3-3] between simulation modeling via NMSim[3-4] and the measured SEL.[3-1] The flight paths and power profiles are the same as used in the INM analysis; their derivation is described in Reference 3-1. The noise source spheres were derived from INM NPD in the following way:

- Directivity was taken to be omnidirectional in the forward quadrants, and INM start-of-takeoff-roll in the aft quadrants.
- Spectra were taken to be INM spectral class. Departure spectrum was used for maximum power, approach spectrum for minimum power, and linearly interpolated for intermediate powers.
- An offset was applied so that SEL would match NPD at 1000 feet.

Atmospheric absorption was computed using the current ANSI standard.[3-5] Layered absorption, based on upper air profiles, was used. The agreement between measured and simulation-predicted SEL is substantially better than the INM 5 results shown in Figure 3-2. INM 6 predictions (Figure 3-6) fared better than INM 5, but it is not clear whether the improvement was from updated absorption modeling or from updates to trajectory modeling. It was concluded that absorption was a major factor in the differences between INM predictions and measured noise levels. Reference 3-3 contains further analysis of the sensitivity of aircraft noise modeling to atmospheric conditions.

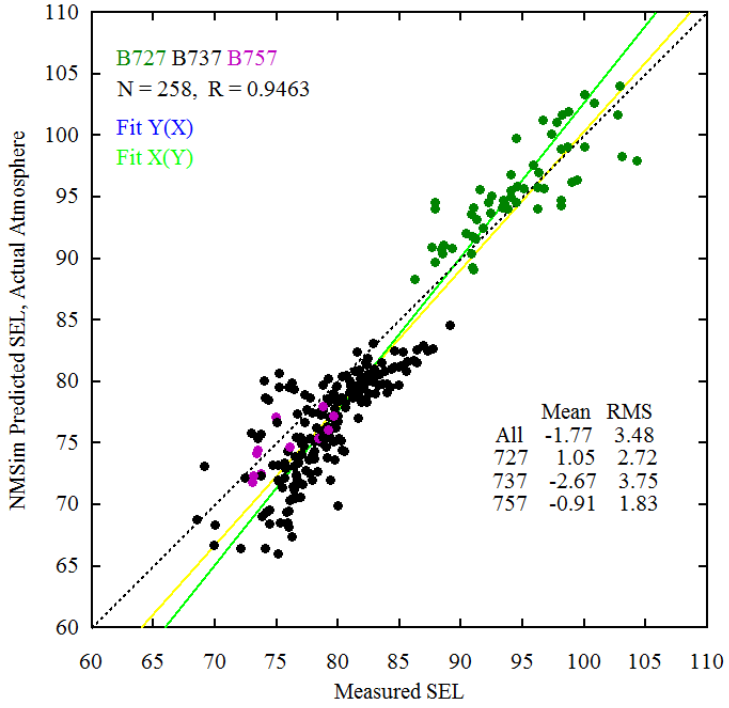

Figure 3-5. Comparison between Measured SEL and NMSim simulation predicted SEL.

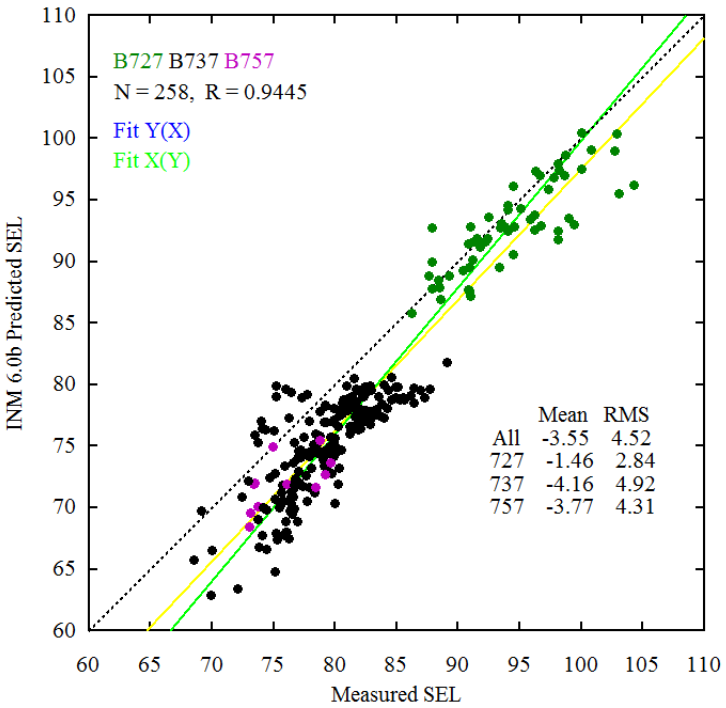

Figure 3-6. Comparison Between INM 6 Predictions and Measured Noise, from Reference 3-4.

3.2 Comparisons with INM 6, INM 7 and AAM

Under Task D-2 of the current effort, the INM 5 analysis of Reference 3-1 was repeated for INM 6 and INM 7. The analysis focused on aircraft analyzed in both Reference 3-1 and Reference 3-2. Reference 3-2 addressed only B737 aircraft, and included profile modeling via the profile point trajectories developed in Reference 3-1 and new procedure step modeling. The INM runs in Task D-2 did, however, include the 727 and 737 in the Reference 3-3 subset. For the current analysis, only profile point results are examined, so as to concentrate on propagation without confounding by trajectory modeling. The profile point trajectories are based on actual aircraft position from radar data, with power based on aircraft weight and balanced runway departure procedure data provided by the airline.

Figures 3-7, 3-8 and 3-9 show comparisons of INM 6, INM 7 and AAM with measured noise levels. All three, including INM 6 using the same profile point trajectory, show very good agreement with the measurements. They are also consistent with each other. Figures 3-10, 3-11, and 3-12 are cross plots between INM 6, INM 7 and NMSim versus AAM. Data in the cross plots are all very close to the 45 degree perfect agreement line.

Figures 3-13 and 3-14 show AAM predictions for two alternate cases: 59° F 70% RH reference condition, and SAE 1845[7] absorption. The scatter is somewhat different from that of the actual condition calculations presented in Figures 3-5, 3-7, 3-8 and 3-9, but none show the significant offset seen in Figure 3-2 for the initial INM 5 predictions. Table 3-1 summarizes the differences for the various cases. INM 6 and 7 perform substantially better than INM 5, with INM 7 showing the best agreement with measurements. The two simulation models, NMSim and AAM, also performed better than the initial INM 5 predictions. The improvement from NMSim to AAM is most likely due to the revised source models, which are based on the current INM database and updated algorithms for converting NPD data to spheres.

In addition to the analysis shown, calculations were run with alternate layering algorithms, including just surface conditions. Very little difference was found in the details. This is probably because humidity for all cases was above 40%, well out of the dry range where absorption is high, and propagation distances were generally less than 10,000 feet. The sensitivities to high absorption conditions and long propagation distances, as presented in Reference 3-3, can still occur over wider ranges of conditions.

Two alternate absorption conditions were modeled: the reference condition of 59° F and 70% RH, and the absorption coefficients specified in SAE 1845. These results are shown in Figures 3-13 and 3-14, respectively. Standard conditions yielded results with greater offset and scatter than the as-flown conditions, but still less than for the original INM 5 results. The SAE 1845 results compare very favorably with INM 6 and 7 and AAM results, further supporting the conclusion in Reference 3-3 that if a single standard absorption table is to be used the 1845 table is a good choice. It also does not appear that the use in INM of the obsolescent SAE 866A[8] absorption standard has adverse practical effects.

Table 3-1 summarizes the variations noted in the figures for all of the comparisons between predicted and measured SEL.

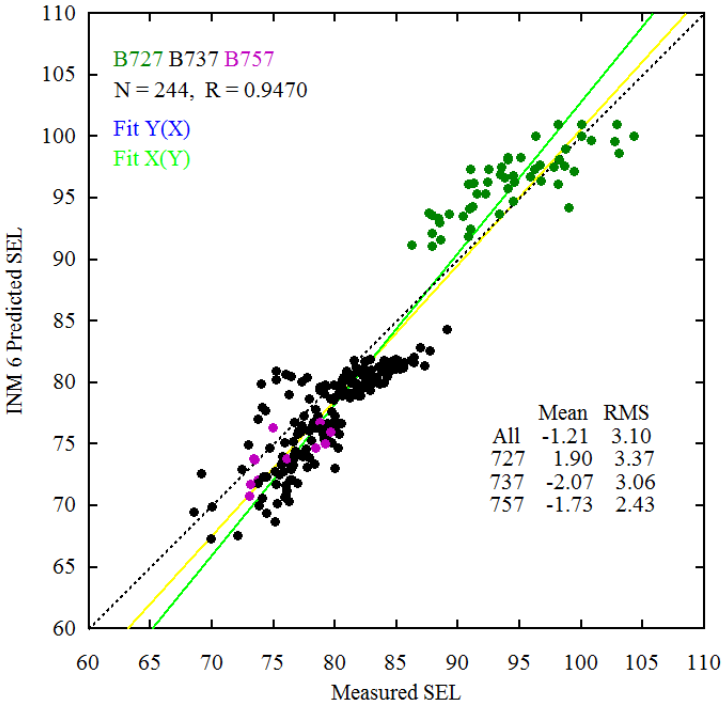

Figure 3-7. Comparison Between Current INM 6 Predictions and Measured Noise.

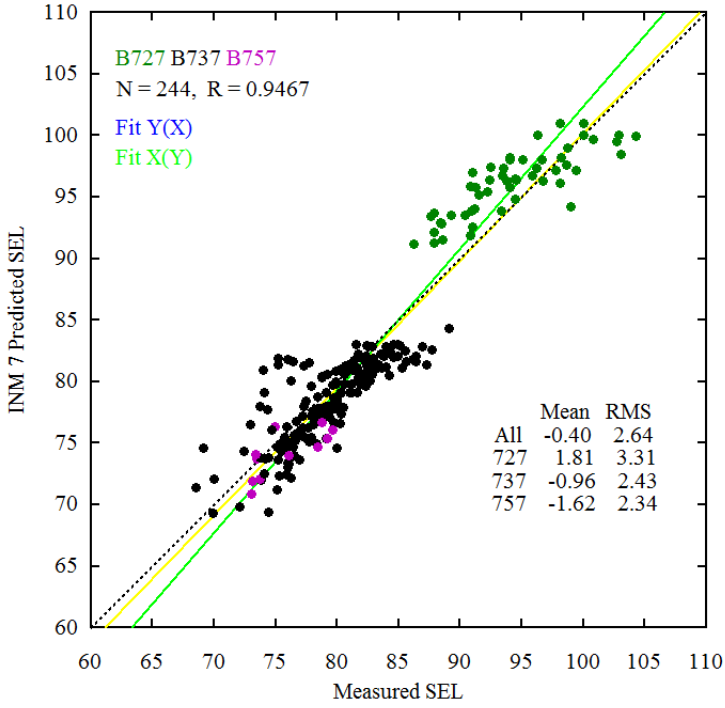

Figure 3-8. Comparison Between INM 7 Predictions and Measured Noise.

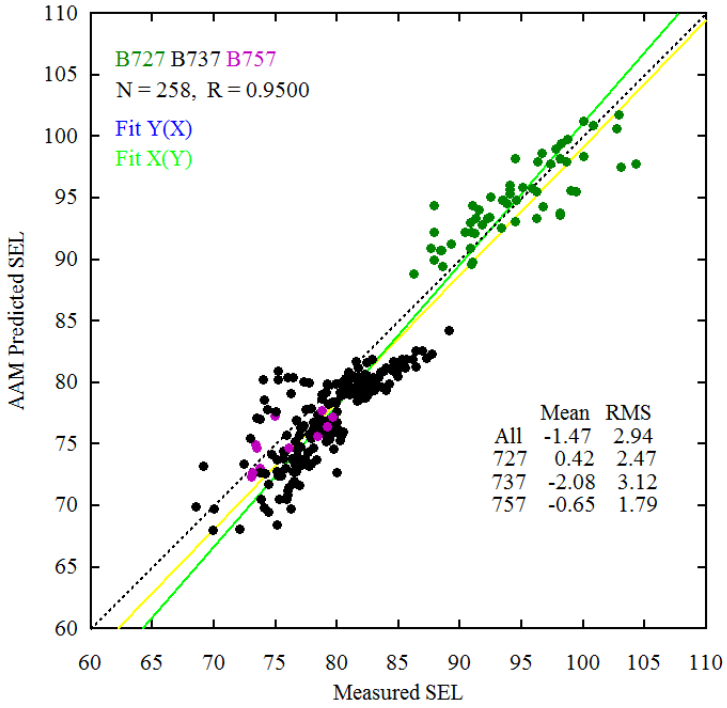

Figure 3-9. Comparison Between AAM Predictions and Measured Noise.

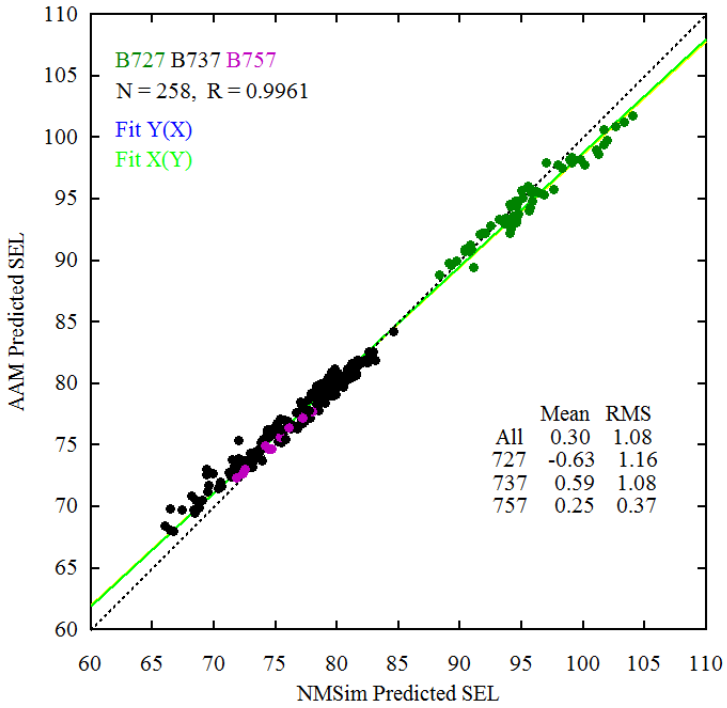

Figure 3-10. AAM versus NMSim Predictions.

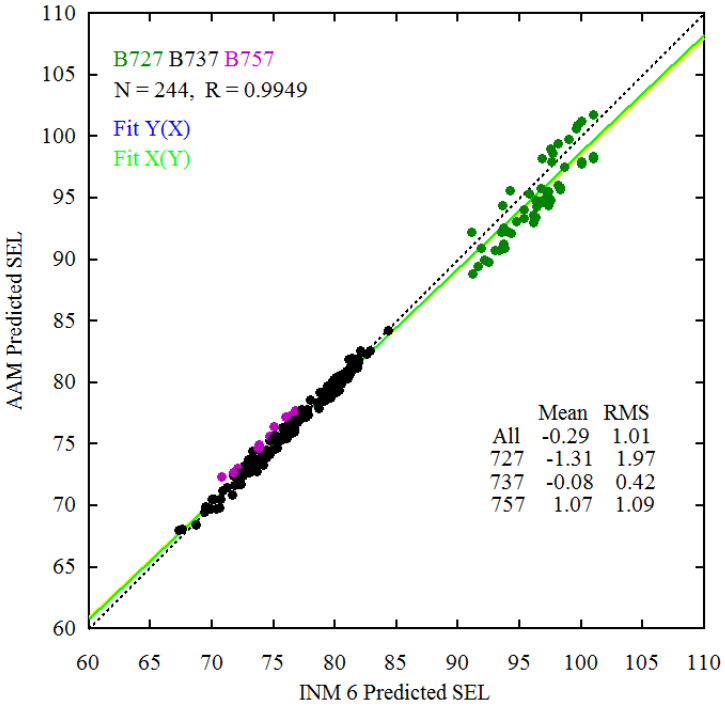

Figure 3-11. AAM versus INM 6 Predictions.

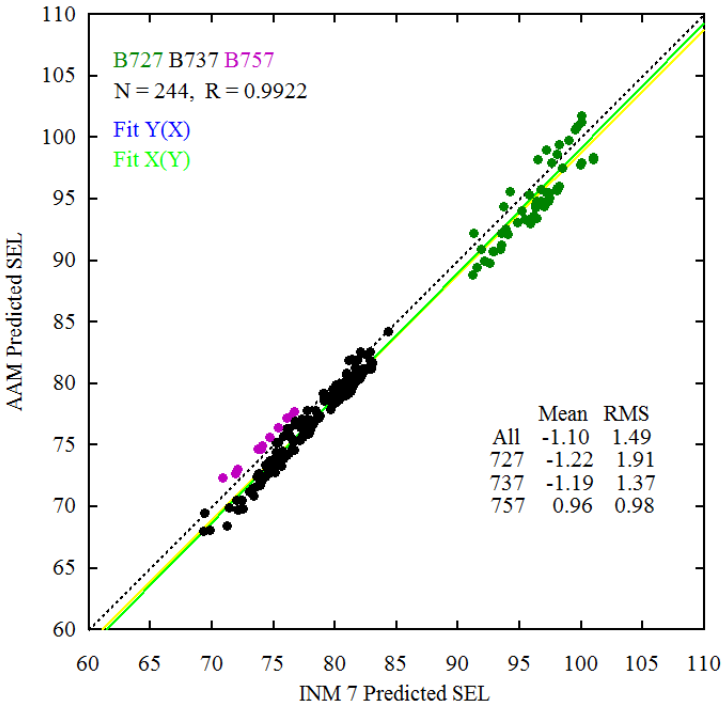

Figure 3-12. AAM versus INM 7 Predictions.

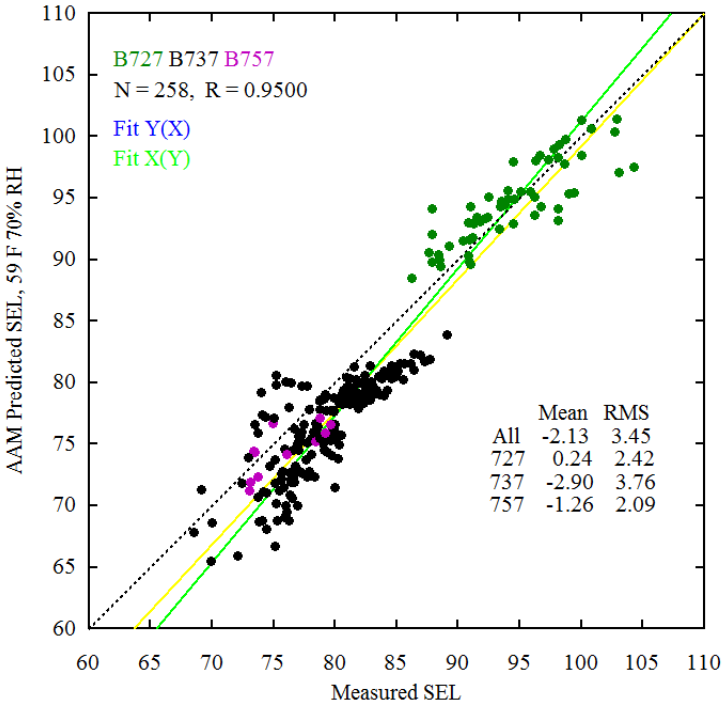

Figure 3-13. AAM Predictions using Reference Conditions 59° F and 70% RH.

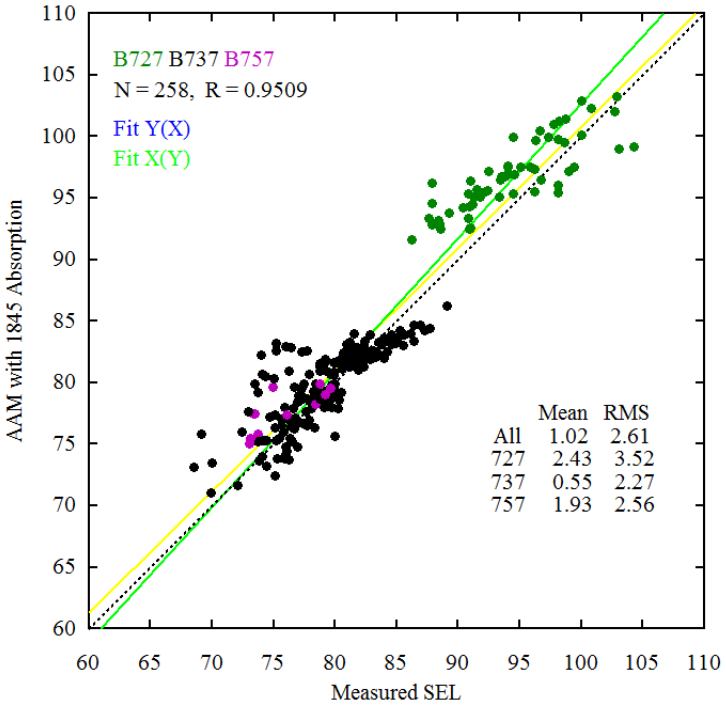

Figure 3-14. AAM Predictions using SAE 1845 Absorption.

Table 3-1. Summary of Deviations of Predictions from Measurements

Model	Average Difference, dB*	RMS Difference, dB
INM 5	-5.73	6.60
INM 6	-1.21	3.10
INM 7	-0.40	2.64
NMSim	-1.77	3.48
AAM	-1.47	2.94
AAM, 59° 70%	-2.13	3.45
AAM, SAE 1845	1.02	2.61

** Positive = overpredicted.*

3.3 Conclusions

A subset of operations from the 1997 KDEN measurements has been analyzed with three versions of INM and with simulation modeling. The 90 selected operations were departures to the east, generally straight out. INM 6 and 7 and simulation results were comparable to each other, with INM 7 performing best for this data set. The original NMSim results were comparable to newer AAM results. AAM results were slightly better, probably because of updates in the INM database and recent refinements in the sphere making process.

The results were found to be not sensitive to details of layering. Use of narrow band absorption at one third octave band center frequencies was adequate. The current data set, with humidity of 40% and above, is in a relatively low absorption regime and did not exhibit the kind of sensitivity that would occur under dry high absorption conditions. The absorption table specified in SAE 1845 worked well for this data set, comparable to the modern INM and simulation analyses with actual absorption.

Given the very good agreement between the current INM and simulation for this data set, it does not appear that INM's use of SAE 866A absorption[3-8] instead of the current recognized ANSI standard[3-6] has practical adverse effects, but it would be appropriate to use the current standard in future versions.

References

3-1. Page, J.A., Hobbs, C.M., Plotkin, K.J., and Stusnick, E. 2000. "Validation of Aircraft Noise Exposure at Low Levels of Exposure," NASA CR-2000-210112, April.

3-2. Forsyth, D.W., and Follet, J.I. 2006. "Improved Airport Noise Modeling for High Altitudes and Flexible Flight Operations", Appendix B, Page, J.A. and Usdrowski, S., "Reduced Thrust Departures from a High Altitude Airport Using Procedure Steps with the Integrated Noise Model", NASA CR 2006-214511, October.

3-3. Plotkin, K.J., "Analysis of Acoustic Modeling and Sound Propagation in Aircraft Noise Prediction". 2001. Wyle Report WR 01-24, November.

3-4. Plotkin, K.J. 2001. "The Role of Aircraft Noise Simulation Models," Inter-Noise 2001 Proceedings, August.

3-5. Page, J.A., Wilmer, C., Schultz, T.D., Plotkin, K.J., and Czech, J.J. 2012. "Advanced Acoustic Model Technical Reference and User Manual," Wyle Report WR 08-12, Revised February.

3-6. "Method for the Calculation of Absorption of Sound by the Atmosphere". 2004. ANSI S1.26-1995 (R1999) (Subsequently reaffirmed 2004).

3-7. Society of Automotive Engineers, Committee A-21, Aircraft Noise. 1986. "Procedure for the Computation of Airplane Noise in the Vicinity of Airports," Aerospace Information Report No. 1845, Warrendale, PA: Society of Automotive Engineers, Inc., March.

3-8. Society of Automotive Engineers, Committee A-21, Aircraft Noise. 1975. "Standard Values of Atmospheric Absorption as a Function of Temperature and Humidity," Aerospace Research Report No. 866A, Warrendale, PA: Society of Automotive Engineers, Inc., March.

Intentionally left blank

4.0 Detailed Weather Modeling in FAA Tools

4.1 Introduction

FAA's noise modeling tools (INM,[4-1] AEDT[4-2]) are integrated models. They are based on a noise-power-distance (NPD) database of SEL for straight infinite flybys. Actual flight paths are divided into segments. The noise contribution of each segment is based on scaling the NPD values according to a noise fraction.

NPD data are based on flyover measurements at a distance on the order of 1000 feet. Adjustments to standard conditions and other distances are based on the SAE AIR 1845[4-3] full spectral method, which is mathematically equivalent to a simulation model, and accounts for point-to-point air absorption effects and spectral directivity in the original flyover data. The contribution from a segment is scaled from NPD by the noise fraction, which is computed on the basis of a simple power law representation of air absorption. The effect of finite ground impedance is based on empirical measurements of line source flight data,[4-4] without accounting for spectral content. The atmosphere is assumed to be homogeneous and still.

Atmospheric gradients are known to affect sound propagation, and can have an effect on individual noise footprints[4-5] and long term noise contours.[4-6] The FAA has recently invested in two propagation models that account for atmospheric gradients: "Hybrid Propagation Model" (HPM)[4-7] and "Advanced En-Route NOise Model" (AERNOM).[4-8] HPM is a combination of PE and FFP methods, which can address atmospheric gradients and uneven terrain. AERNOM is a ray tracing model that accounts for atmospheric gradients during propagation of noise from flight at high altitudes. Both are physical models that account for propagation from a point source to a receiver. An approach is needed for practical application of these models to FAA's integrated, NPD-based models.

4.2 Background and Approach

Complex propagation associated with weather has been handled by simulation,[5,6] and complex propagation associated with terrain has been handled by both simulation and integrated models. Application to a simulation model is straightforward, since simulation is implicitly point-to-point.[4-9] The primary issue is computation time. Application to integrated models can take two approaches.

The first approach is to divide the flight path into small segments. This essentially simulates a simulation model, but does not account for source directivity. When applied as a simulation model for single event prediction in NORTIM with one second segments,[4-10] results were variable, with a tendency to underpredict. When applied to INM for prediction of cumulative metrics (time audible and DNL) over complex terrain[4-11,4-12] results were very good, closely matching full simulation predictions and (in Reference 4-11) measurements. The only drawback was computation time. In Reference 4-12 the short segment INM method benchmarked slower than the NMSim[4-10] simulation, although it is likely that INM's performance was adversely affected by over-aggressive segmentation.

The second approach is to adjust segment contributions by point-to-point propagation from a few selected points. This is the approach taken for DoD's NOISEMAP,[4-13] where terrain effects from three points (both ends and point of closest approach) are aggregated. Arntzen et al[4-14] and Heblij et al[4-15] have taken this approach for analysis of weather effects using an integrated noise model. Use of a few points (or even one point) per segment is feasible for weather effects in a horizontally stratified atmosphere or for gently varying terrain. For rugged terrain, as in References 4-11 and 4-12, segmentation must be at a scale consistent with the lateral scale of the terrain, so the prospects of efficient integrated formulation diminish. Around airports, however, terrain tends to be flat or gently varying, while variable weather is a topic of concern.

Taking advantage of the homogeneity of a horizontally stratified atmosphere over flat terrain, the analyses of References 4-5, 4-6, 4-14 and 4-15 pre-compute propagation effects as a function of source elevation and propagation direction/distance. The noise model then interpolates from tabulated pre-computed values, rather than perform the calculations anew for each path.

Figure 4-1 shows typical pre-computed propagation results from RNMwea, the ray tracing component of the Advanced Acoustic Model (AAM),[4-16] a simulation model developed by Wyle for the DoD. Both show propagation levels, relative to a source distance of 1 meter, for propagation from a source 1000 feet above the ground to a receiver at 4 feet above. Temperature and density profiles correspond to the US Standard atmosphere, humidity is taken to be 70%, and the ground is soft. In Figure 4-1a there is no wind. In Figure 4-1b there is a north wind with a linear gradient from 0 at the ground to 10 meters/sec at the source height of 1000 feet. Both footprints are rendered with the same amplitude scale. The attenuation directly under the source is about 47 dB, representing spherical spreading, approximately 3 dB ground doubling, and a small amount of air absorption.

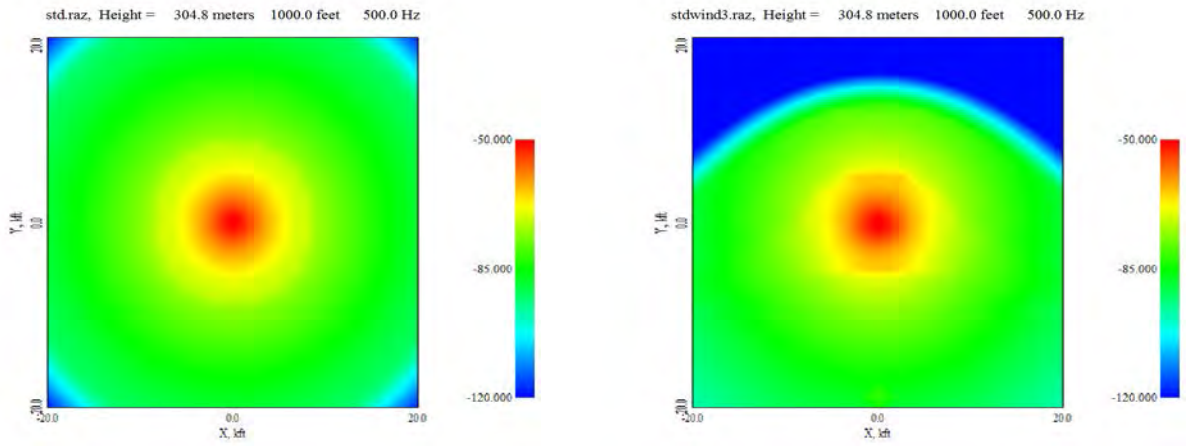

a. b.

Figure 4-1. Propagation footprint at 500 Hz for a source at 1000 feet, without and with wind (a) US Standard Atmosphere, calm; (b) US Standard Atmosphere, North wind

Note that the footprint in the region near the center (under the source) is essentially the same for both cases, while the effect of wind is to give the impression of pushing the outer part of the footprint in the direction of the wind. While there is some displacement of sound rays in the direction of the wind vector, the primary physical mechanism is that the wind-induced change in ray curvature causes significant changes in the ray-ground incidence angle and the geometry associated with ground attenuation. Ray tube area changes – focusing and defocusing – also occur, but (other than local caustic formation) tend to be less significant than the change in ground effect. This was the finding in References 4-5 and 4-6. Figure 4-2 shows a touch and go footprint, under crosswind propagation conditions, from Reference 4-5. Most of the effect is seen to the sideline during the takeoff roll portion; there is no displacement of the footprint during the departure ascent to the right. This is not just a low altitude finding. Figure 4-3 shows en-route footprints, Figure 4-24 of Reference 4-8, with a similar result.

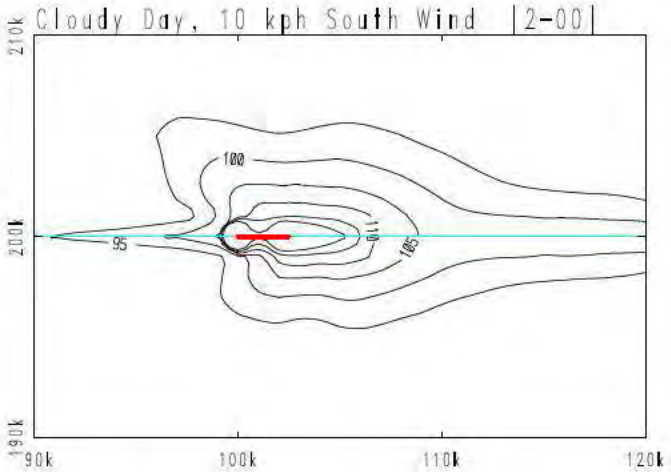

Figure 4-2. Touch and go footprint with crosswind[4-5]

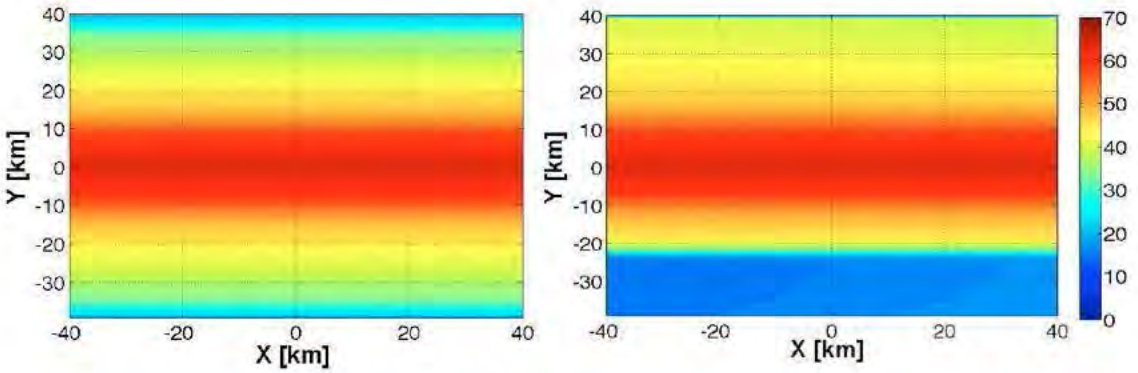

a. b.

Figure 4-3. En-route footprints without and with crosswind[4-5]
(a) Head or tail wind; (b) Crosswind

Air absorption, which varies with temperature and humidity, can play a significant role in propagation. Figure 4-4, taken from Reference 4-17, shows the variation in absorption of A-weighted levels from a B737 during a winter month at Dulles, VA. This variation is typical for a winter month in a temperate region; Reference 4-17 has similar plots for summer and winter in a number of locations in the US. The absorption was computed accounting for layered temperature and humidity. Because absorption is linear, the average absorption coefficient can be pre-computed for a vertical path from source altitude to receiver altitude, then applied to slanted paths by applying this average to the actual distance. While absorption is important, it was shown in Task D-3 that the details of layering in a particular case are not critical. Absorption can be incorporated into a pre-computed propagation analysis, as in the RNMwea file illustrated in Figure 4-1, with no loss of generality. Complex propagation can be computed on an absolute basis, or it can be prepared as the difference between complex propagation and standard or reference conditions. AAM, in fact, uses both methods. The RNMwea files illustrated in Figure 4-1 are used directly, in place of its internal flat earth, straight ray model. AAM also operates with NASA's APET2[4-18] model. APET2 uses a combination of ray tracing and parabolic equation methods to account for atmospheric gradients and terrain. For use with AAM, it prepares a file that is the difference between its calculations and a flat earth, straight ray model. Within AAM APET2

differences are then applied to the internal mode results, rather than switching between modes as is done with RNMwea and AAM's topography algorithms.

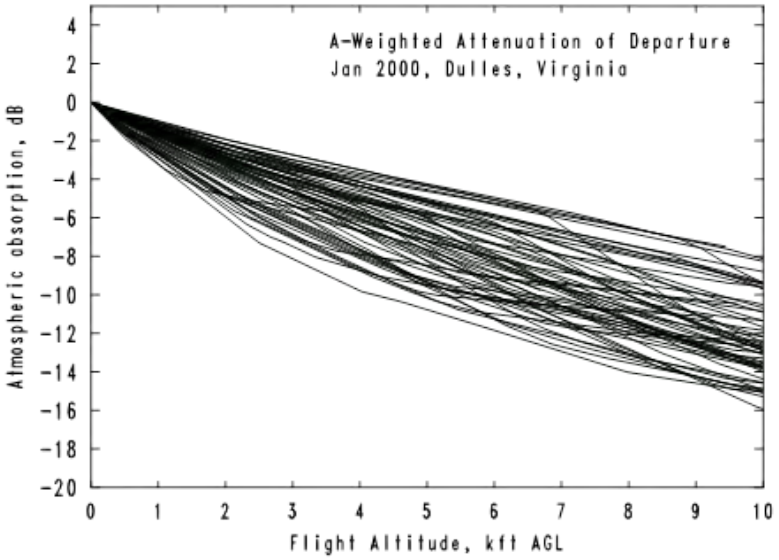

Figure 4-4. Variation in A-Weighted Air Absorption, Winter, Dulles, VA

Complex propagation is readily applied to simulation models. For application to integrated models, the critical element is non-isotropic effects associated with wind gradients and/or irregular terrain. The objective of this task is to identify efficient methods of accomplishing this. It is expected that the second method discussed earlier (apply complex propagation to a few points on each segment) would be appropriate.

A specific goal is to define how HPM[4-7] and AERNOM[4-8] can be incorporated into FAA tools, INM[4-1] and/or AEDT.[4-8] This posed challenges in that, while the documentation for all models was available, only the INM executable (not source) was available for use in this task, and neither source nor executable for HPM and AERNOM were available.

A generic approach to this task has therefore been taken, using AAM. AAM has been run for finite segments, in full propagation mode and with its internal propagation algorithms modified to simulate INM algorithms. The modified runs form a foundation on which simplified application of complex weather can be tested and compared with the full versions.

4.3 Emulation of Integrated Model

AAM is a time simulation model that uses a 3-D directional source based. INM is a simulation model that uses an NPD database prepared from analysis equivalent to simulation modeling, adjusting infinite-segment NPD values to finite segments via a noise fraction based on simple power law attenuation. A B737, as used in Task D-3, was selected for AAM runs to emulate an INM segment and test application of propagation algorithms.

Figure 4-5 is the SEL footprint for the B737, generated by AAM including directivity and using AAM's internal straight ray, soft ground algorithms. The flight segment, from west to east, is 10,000 feet long, altitude 1000 feet, speed 250 kts. Altitude and speed are the reference conditions for that sphere. Segment length was selected as being longer than typical, since the issue is long segments versus points or very short segments. The

simulation was run at 0.5 second intervals, so the trajectory points are slightly over 200 feet apart, with just under 50 points in the segment. Note that there is an asymmetry due to source directivity. The NPD process averages out directivity, so an omnidirectional source is more appropriate than the full noise sphere. An omnidirectional source was generated by replicating, at all Euler angles, the spectra at one point of the directional sphere. Figure 4-6 shows the footprint for the same conditions, using the omnidirectional source. There is still a slight asymmetry, due to accurate treatment of the source motion, but this is a simple footprint suitable as a basis for analysis.

Figures 4-5 and 4-6 each cover an area ±20000 feet relative to the center. The computational grid has s mesh size of 200 feet, and is 201x201 points. Every 10th grid point is marked on the plots. All subsequent footprints in this memorandum are on the same grid, and for the omnidirectional source.

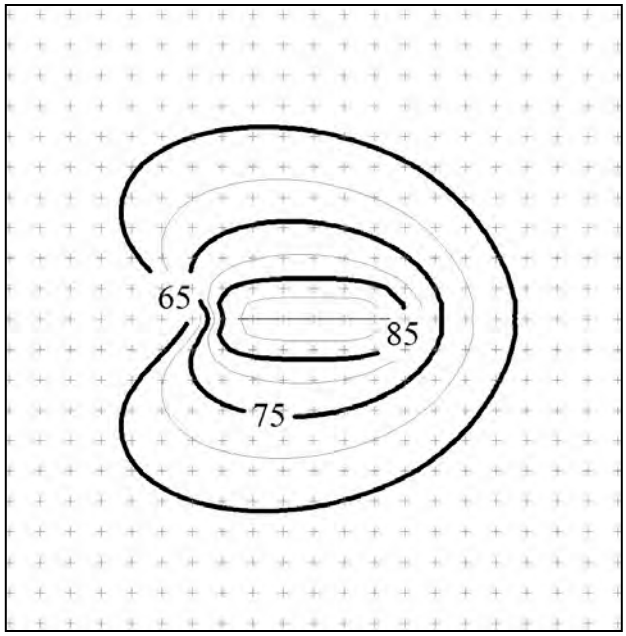

Figure 4-5. SEL footprint for B737, 1 kft, uniform atmosphere

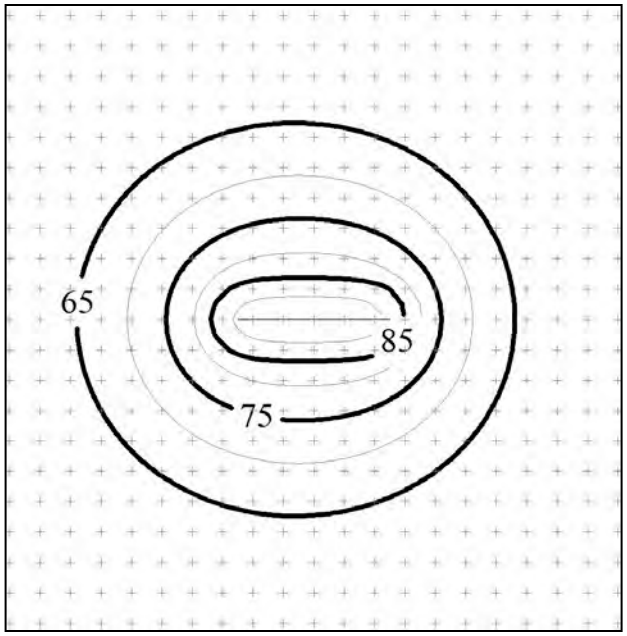

Figure 4-6. SEL footprint for omnidirectional source, 1 kft, uniform atmosphere

Figures 4-7 and 4-8 show footprints for the same track, but in the standard atmosphere (Figure 4-7) and in the standard atmosphere with a north wind (Figure 4-8). The atmospheric profiles correspond to those described earlier for Figures 4-1 and 4-2. Figure 4-9 shows the difference between the standard atmosphere (Figure 4-7) and uniform atmosphere (Figure 4-6) footprints. Note that the scale is ±2 dB. Other than the shadow zones in the corners of the analysis domain, differences are modest. Figure 10 shows the difference between the north wind atmosphere (Figure 4-8) and the quiescent standard atmosphere (Figure 4-7) footprints. There are some local differences at modest distances from the runway. The largest distances are associated with the shift in the shadow zones to the north and south, similar to that seen in the en-route footprint shown in Figure 4-3.

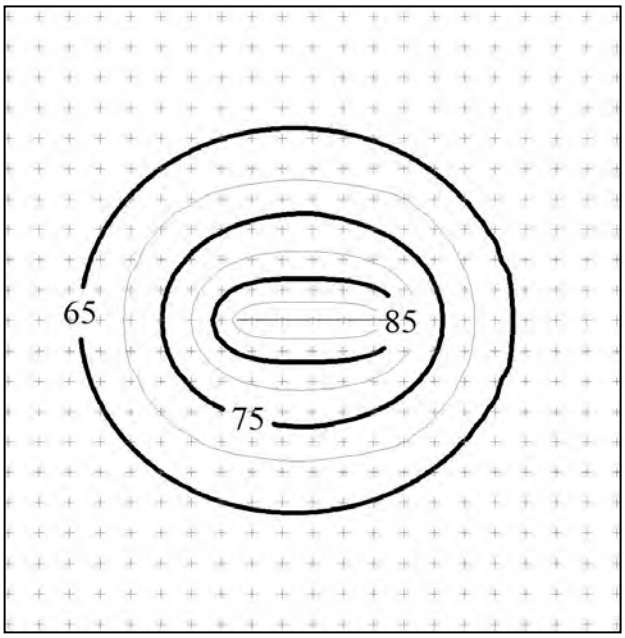

Figure 4-7. Footprint, 1000 ft, standard atmosphere

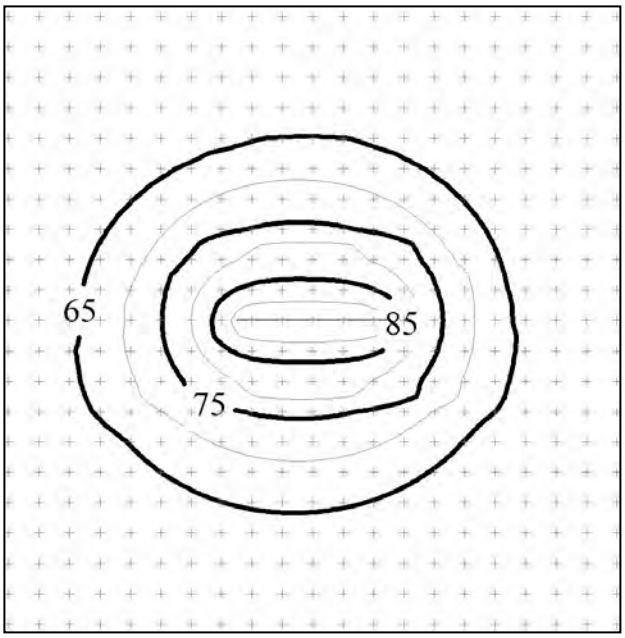

Figure 4-8. Footprint, 1000 ft, north wind

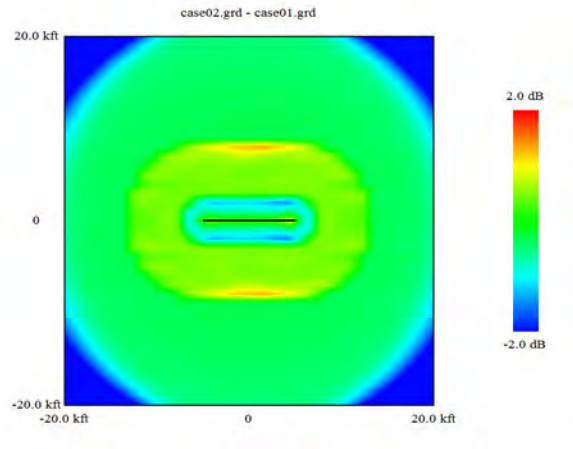

Figure 4-9. Difference between standard atmosphere and uniform atmosphere footprints, 1000 foot altitude

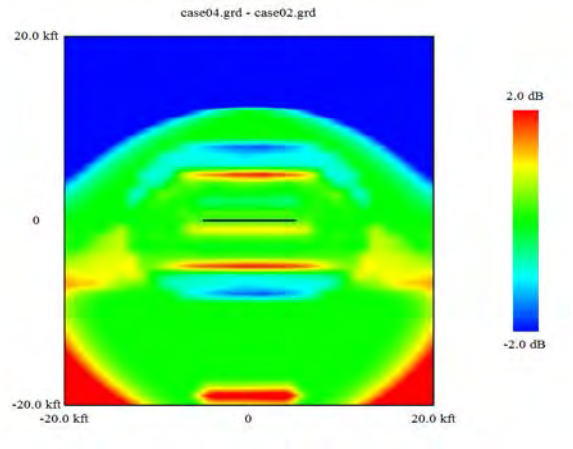

Figure 4-10. Difference between north wind atmosphere and standard atmosphere footprints, 1000 foot altitude

As seen in Figure 4-2, refraction effects are more significant at lower altitudes than higher, Figures 4-11 and 4-12 show footprints for a case similar to Figures 4-7 and 4-8 but for a 200 foot flight altitude. Figures 4-13 and 4-14 show the differences, at ±2 dB and ±40 dB scales. The wind effect is much greater than for the 1000 foot case. Note that the atmospheric gradient is the same for both cases, so the wind speed at flight altitude is 2 meters/second rather than 10.

The 200 foot case has thus been chosen for analysis of anisotropic propagation. Two wind conditions are used: the north wind atmosphere shown so far, and a similar gradient for a northeast wind. Figures 4-15 and 4-16 show the footprint and the difference between the northeast and quiescent footprints. The northeast case is included to avoid bias from alignment between wind direction, flight path and the grid.

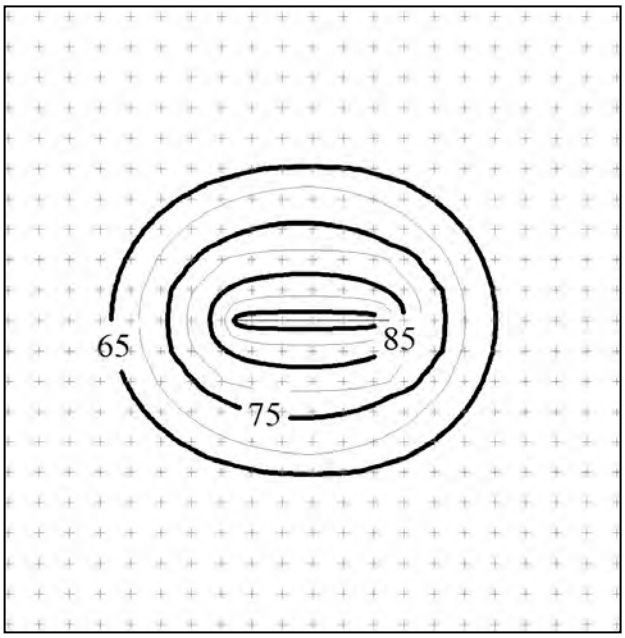

Figure 4-11. Footprint for 200 foot altitude, standard atmosphere

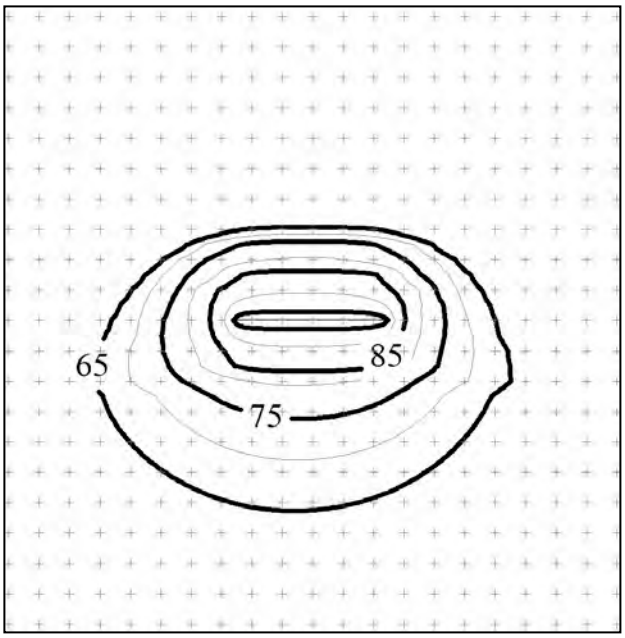

Figure 4-12. Footprint for 200 foot altitude, north wind

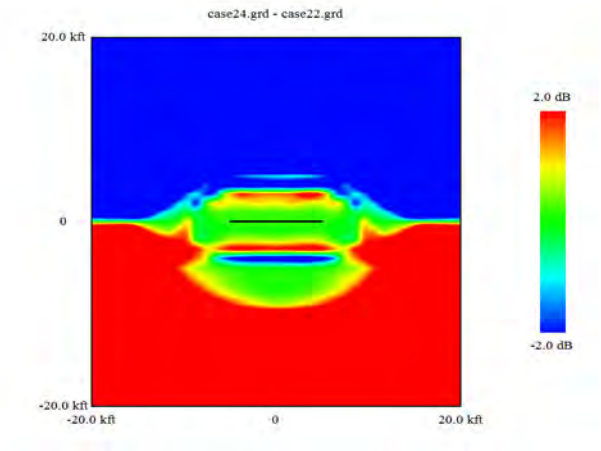

Figure 4-13. Difference between north wind atmosphere and standard atmosphere footprints, 200 foot altitude, ±2 dB scale

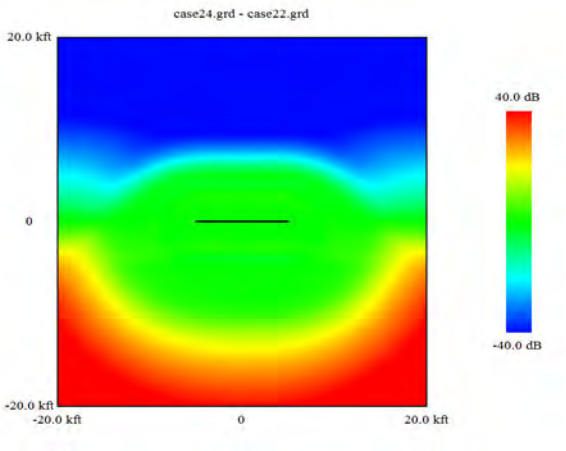

Figure 4-14. Difference between north wind atmosphere and standard atmosphere footprints, 200 foot altitude, ±40 dB scale

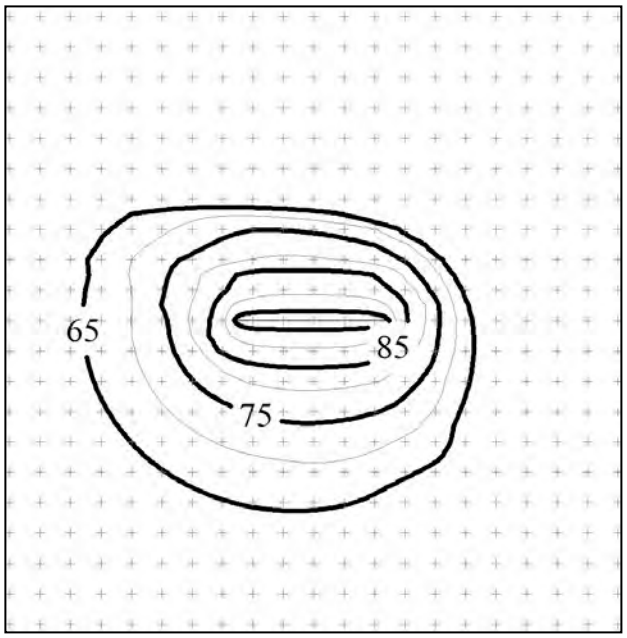

Figure 4-15. Footprint for 200 foot altitude, northeast wind

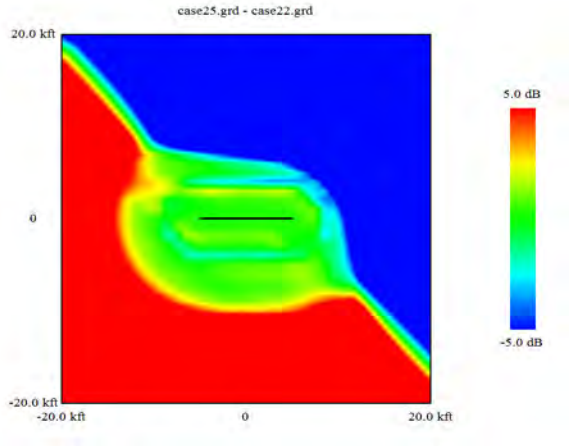

Figure 4-16. Difference between northeast wind atmosphere and standard atmosphere footprints, 200 foot altitude, ±5 dB scale

4.4 Algorithms for Anisotropic Propagation

Tests of application of anisotropic weather propagation algorithms (i.e., refraction in a windy atmosphere) have been run and applied to a simulation of an integrated model segment. The following steps were involved:

1. The basic segment simulation is an AAM run for the omnidirectional source at 200 feet altitude, uniform atmosphere, and soft ground. Propagation elements include spherical spreading, air absorption and ground effect for straight rays.
2. The "exact" solution is the AAM run with RNMwea propagation applied at each time step along the trajectory. Propagation elements include ray tube area (replacing spherical spreading), air absorption (essentially the same as basic), and ground effect for refracted rays.
3. Approximate algorithms are similar to Step 2, except that for each receiver a single value of RNMwea is applied. That value is based on RNMwea propagation from a limited number of points along the segment.

When applying Step 3, the following detailed adjustments are made:

- Straight ray ground effect is removed from the baseline.
- Air absorption is removed from RNMwea, since air absorption is implicit in integrated model NPD
- RNMwea ray tube area effect is normalized by spherical spreading, since spherical spreading is implicit in NPD and noise fraction.

Air absorption, spherical spreading and straight ray ground effect are all available within the AAM routine that applies RNMwea, so the adjustments were straightforward to incorporate. Specific "limited number of points" investigated were one (the center of the segment or the point of closest approach), which is apparently what was done in References 4-14 and 4-15, and a weighted combination of three (point of closest approach and segment ends) which is done in NOISEMAP.[4-13]

4.4.1 Test Cases

The process described above has been applied to four segment lengths (1000 ft, 2000 ft, 5000 ft and 10000 ft) at an altitude of 200 feet, for each of the three atmospheres (standard calm, north wind and northwest wind). The baseline full simulation footprints for the 10000 ft segment were shown in Figures 4-7, 4-8 and 4-15. The crux of the analysis is to identify a suitable method of obtaining the single value required for Step 3. The following methods were tested:

- Single point, center of segment.
- Single point, closest point of approach (CPA).
- Weighted average of CPA and ends, based on energy.
- Weighted average of CPA and ends, based on level (dB weighted average).
- NMAP method: maximum propagation (lowest loss) of CPA and ends.

Calculations were all performed for a flight altitude 200 feet above ground level. Noise values are all A-weighted sound exposure level.

4.4.2 Results and Analysis

Each method was applied to the four segment lengths and each of the three atmospheres. Segment length is an important parameter, since a method is sought that is more efficient than full simulation or short segment. The plots are:

- Figures 4-17 through 4-21 are sets of differences between approximate application and full simulation for the four segment lengths for each method, for the calm standard atmosphere.
- Figures 4-22 and 4-23 show differences for 2000 and 5000 foot segments, for the four propagation methods, calm atmosphere. These are cross sections of plots from Figures 4-17 through 4-21, and clearly show that the dB weighted average method best approximates the full simulation.
- Figures 4-24 and 4-25 show differences for 2000 and 5000 foot segments, four propagation methods, for the north wind and northwest wind atmospheres. These show the relative performance for anisotropic propagation.
- Figure 4-26 shows differences for four segment lengths, dB weighted average method, NE wind. This is the best performing weighting method and worst case atmosphere.
- Figure 4-27 shows the full simulation and dB weighted method footprints for three segment lengths, NE wind.

Each plot in Figures 4-17 through 4-26 is a color gradient chart of the difference between footprints using an approximate propagation method and that using full simulation. All are to the same scale, ±3 dB, which emphasizes differences. Ideally, the approximate method should be within 1 or 2 dB of the full simulation. That is generally the case for the dB weighted average method for segments up to 2000 feet. Results are marginal for the 5000 foot segment, and rather poor for the 10000 foot segment. Results for the other four approximate methods are not satisfactory.

The footprints in Figure 4-27 show that the differences in contours are not as spectacular as they appear in the spatial difference charts. The contour differences between c and d (5000 foot segment) are of a magnitude not uncommon when alternate decisions are made in modeling an airport, but not readily acceptable. The differences between e and f (10000 foot segment) are well beyond acceptable.

4.5 Conclusions

The feasibility of incorporating detailed weather propagation modeling, which are inherently point-to-point, within FAA's integrated noise modeling tools has been examined. Key prior studies that addressed aircraft noise propagation through atmospheric gradients were reviewed. These included full simulation, short segment operation of an integrated model, and simplified application of detailed propagation to integrated models. Short segment modeling is always feasible, but can result in computational times as long as (sometimes longer than) a full simulation model. The goal is to apply a small number of propagation points within segments of practical length. Five approximate methods were used:

- Single point, center of segment.
- Single point, closest point of approach (CPA).
- Weighted average of CPA and ends, based on energy.
- Weighted average of CPA and ends, based on level (dB weighted average).
- NMAP method: maximum propagation (lowest loss) of CPA and ends.

The effectiveness of each was calculated by using a simulation model to emulate an integrated segment. Analysis was performed on four segment lengths, from 1000 to 10000 feet. The dB weighted average method, using three points (CPA and segment ends) performed very well for segments up to 2000 feet, and marginally acceptably for segments of 5000 feet. This represents an order of magnitude reduction in computational effort relative to the simulation model, which required steps about 200 feet apart.

The feasibility of this simplification relies on a laterally homogeneous atmosphere, i.e., horizontally stratified over a flat ground surface. This horizontal homogeneity permits a one-time pre-computation of propagation as a function of source elevation and the distance and bearing to the receiver. Propagation through a 3-D atmosphere would not allow this simplification, and also raises the issue that propagation to different points are not smoothly varying functions of bearing. Similarly, this kind of simplification is not generally amenable to propagation over irregular terrain. Segmentation for propagation over terrain must be on a scale comparable to (or finer than) the lateral scale of the terrain.

Atmospheric absorption was not exercised in this analysis. Because absorption in a layered atmosphere is linear, and has been shown to be somewhat insensitive to details of the layering, absorption adjustments based on three segment points and representative spectra (i.e., spectral classes) would have less stringent requirements.

This task was conducted with modest scope, and also without access to the code for FAA's noise and propagation models. A follow-up effort would be warranted using the actual FAA tools, supported by simulation modeling closely aligned to the FAA tools. That effort should exercise the analysis over a wider range of conditions to develop guidelines for practical and accurate segmentation dimensions.

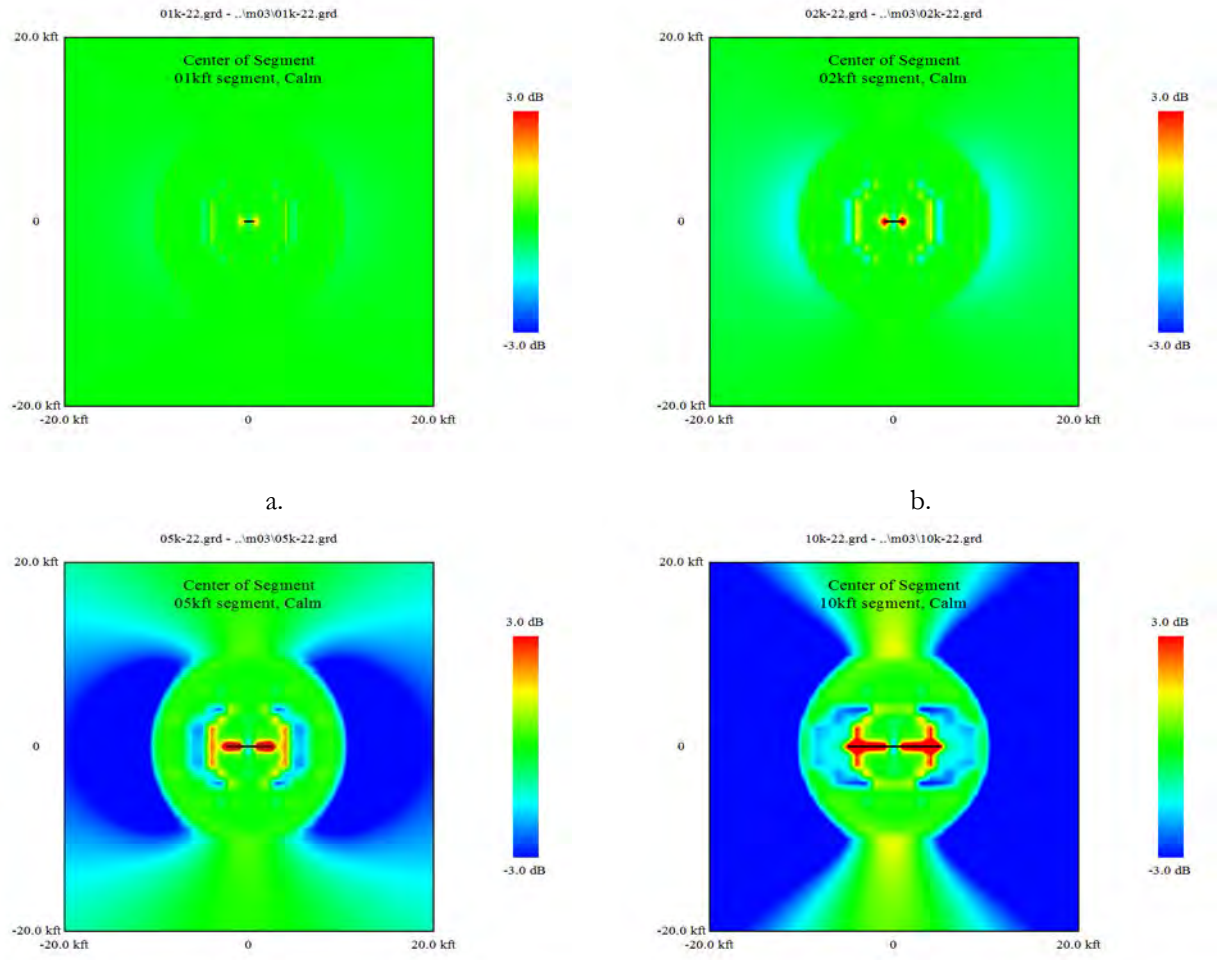

Figure 4-17. Differences, propagation based on center of segment, calm atmosphere
(a) 1000 foot segment; (b) 2000 foot segment; (c) 5000 foot segment; (d) 10000 foot segment

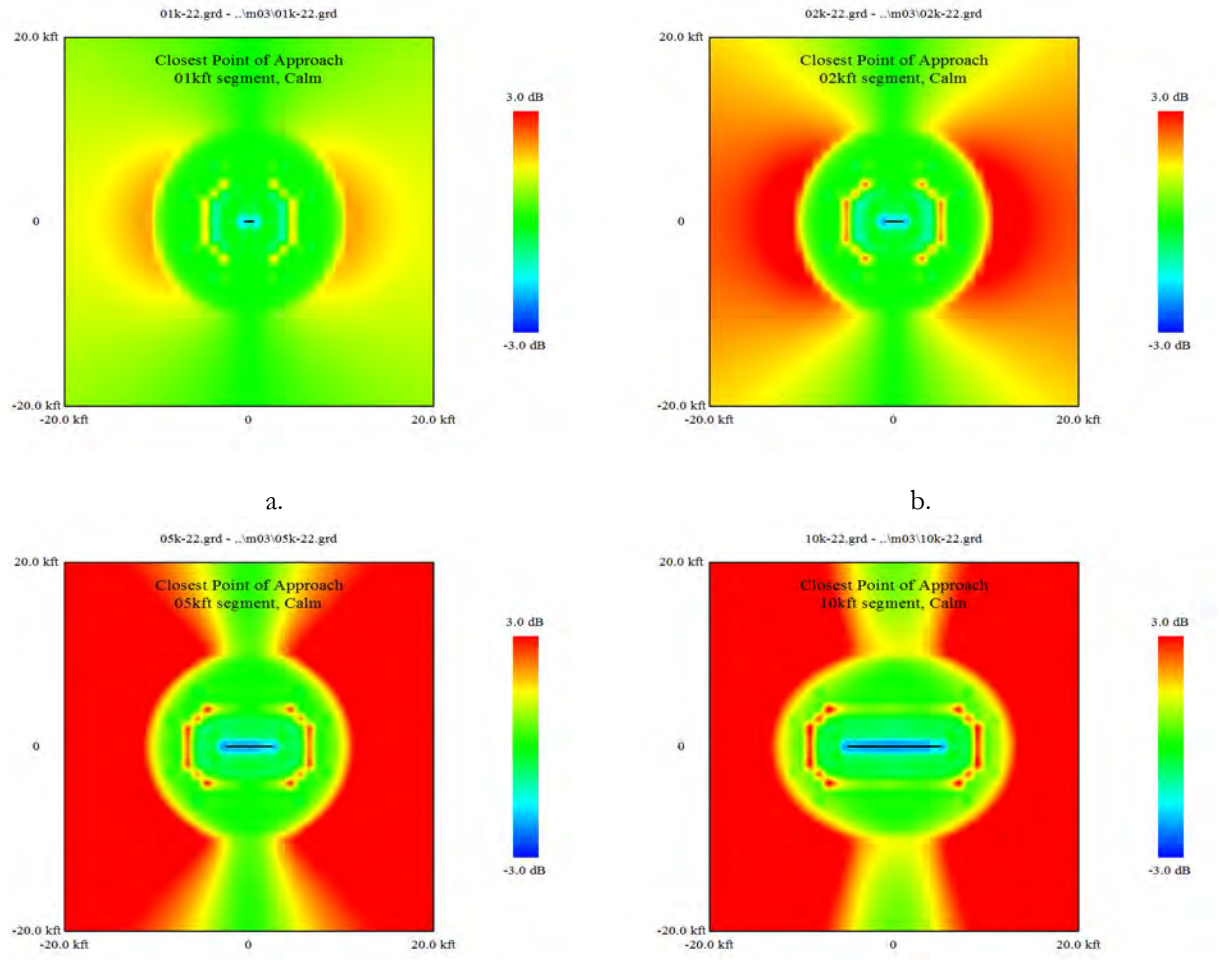

Figure 4-18. Differences, propagation based on CPA, calm atmosphere
(a) 1000 foot segment; (b) 2000 foot segment; (c) 5000 foot segment; (d) 10000 foot segment

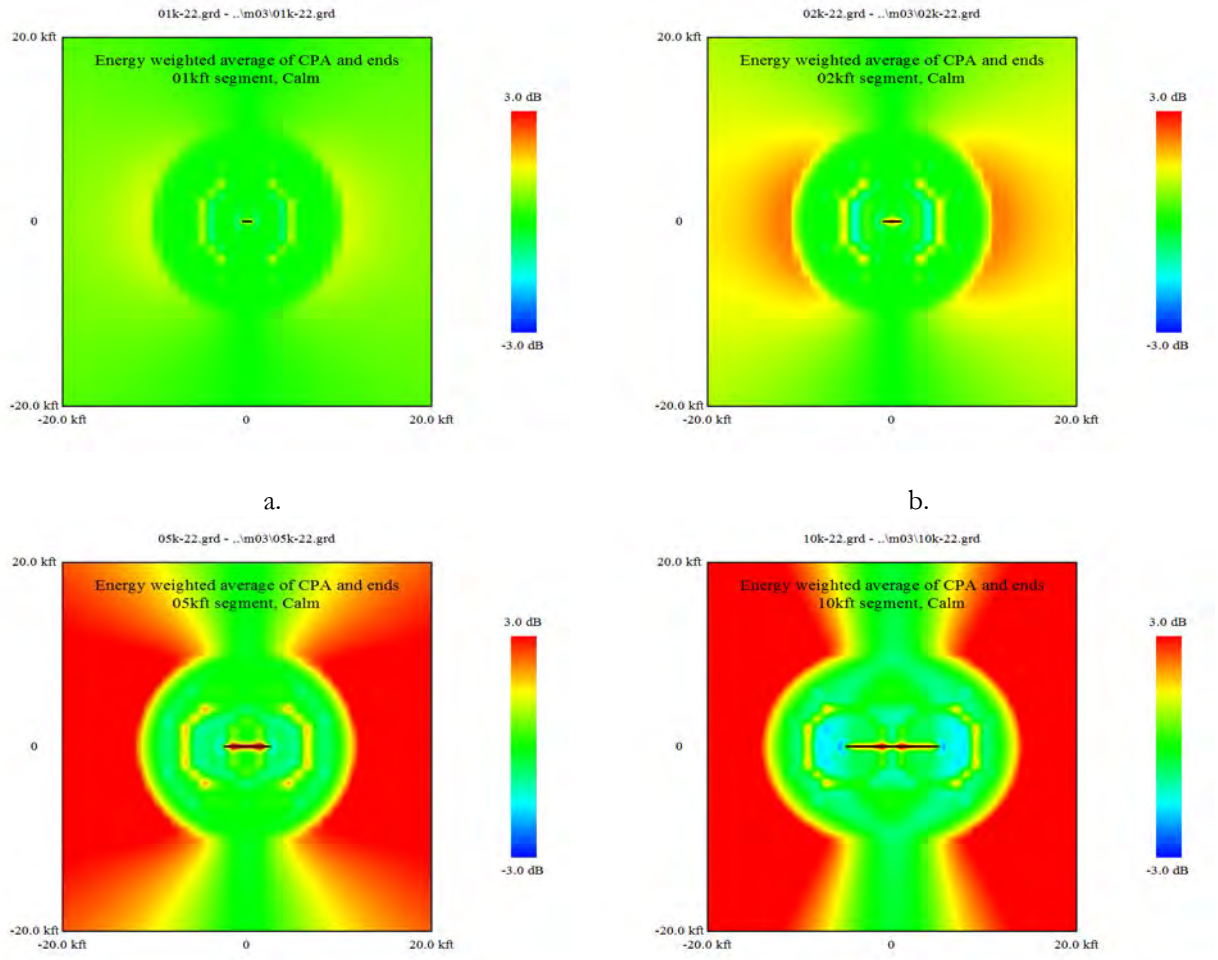

Figure 4-19. Differences, propagation based on energy weighted average, calm atmosphere (a) 1000 foot segment; (b) 2000 foot segment; (c) 5000 foot segment; (d) 10000 foot segment

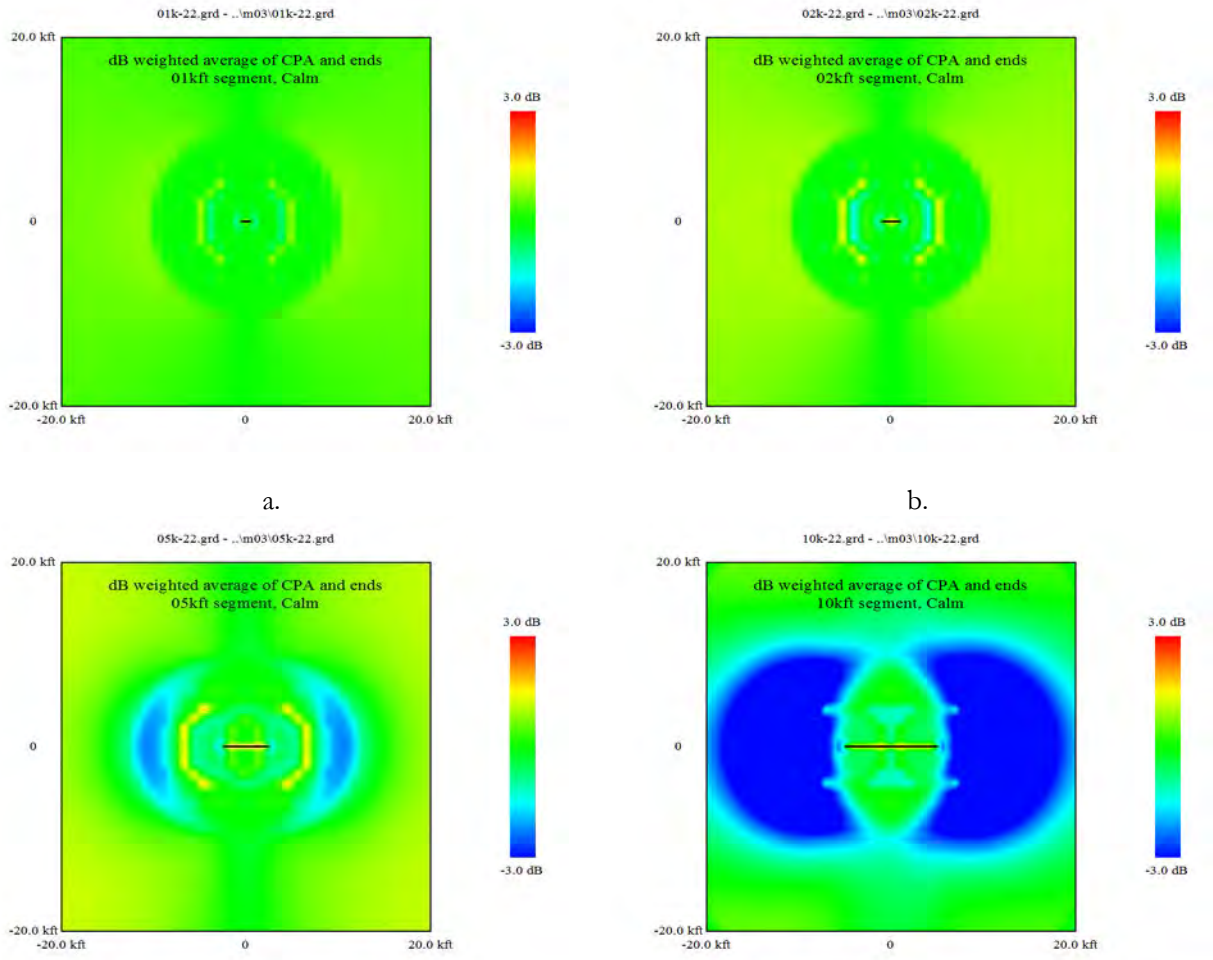

Figure 4-20. Differences, propagation based on dB weighted average, calm atmosphere| (a) 1000 foot segment; (b) 2000 foot segment; (c) 5000 foot segment; (d) 10000 foot segment

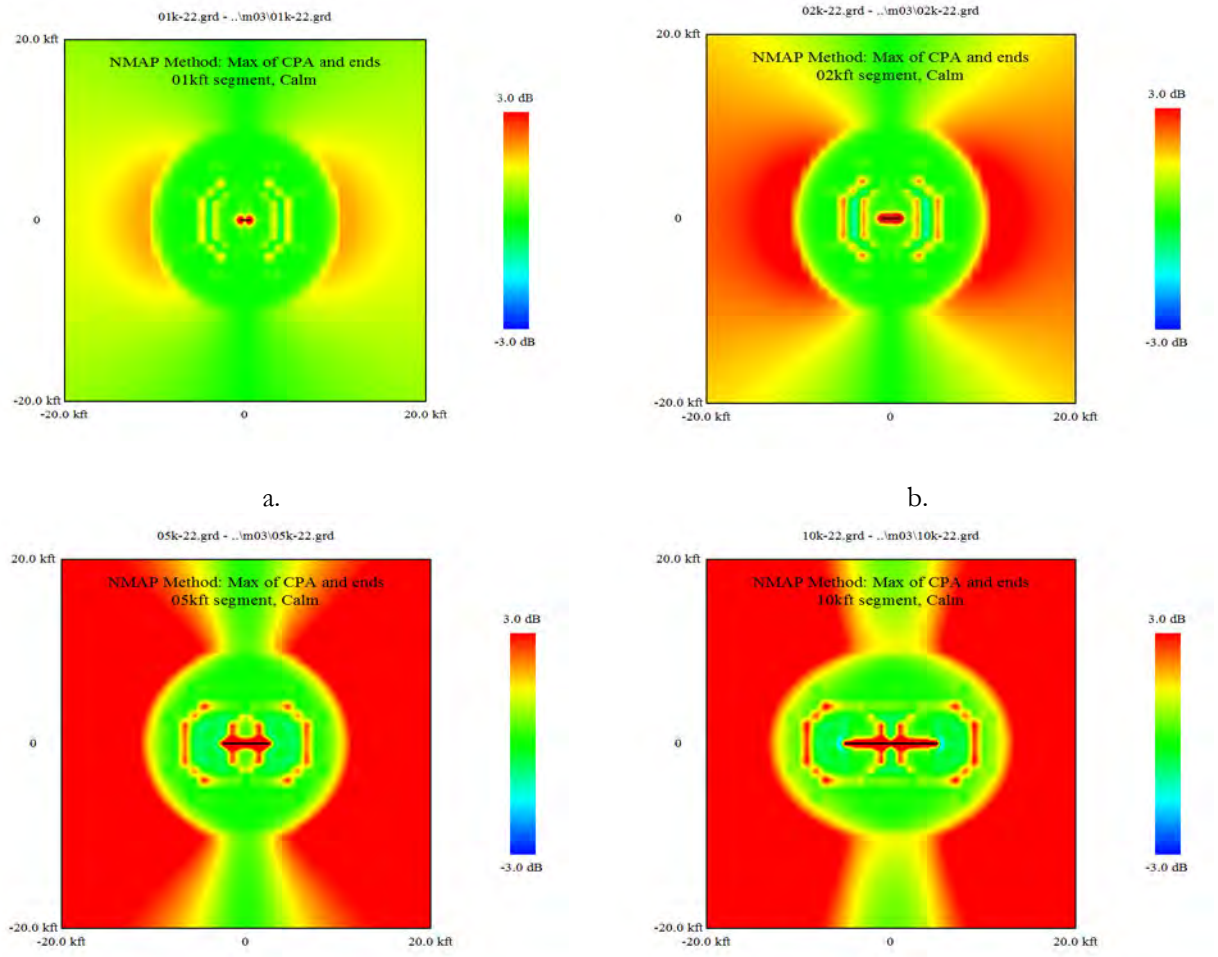

Figure 4-21. Differences, propagation based on NMAP method, calm atmosphere
(a) 1000 foot segment; (b) 2000 foot segment; (c) 5000 foot segment; (d) 10000 foot segment

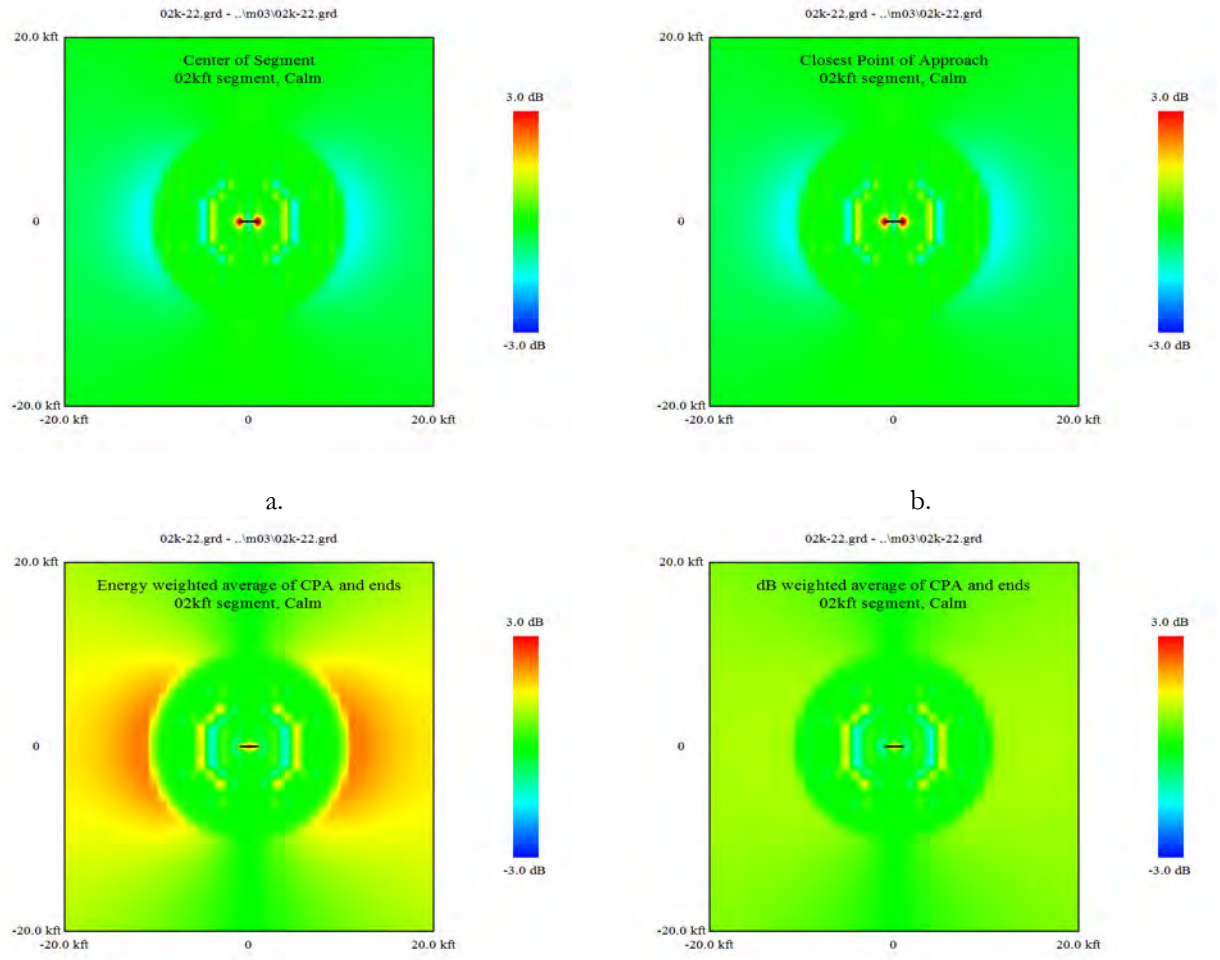

Figure 4-22. Differences, 2000 foot segment, calm atmosphere, four methods
(a) Center of segment; (b) CPA; (c) Energy weighted average; (d) dB weighted average

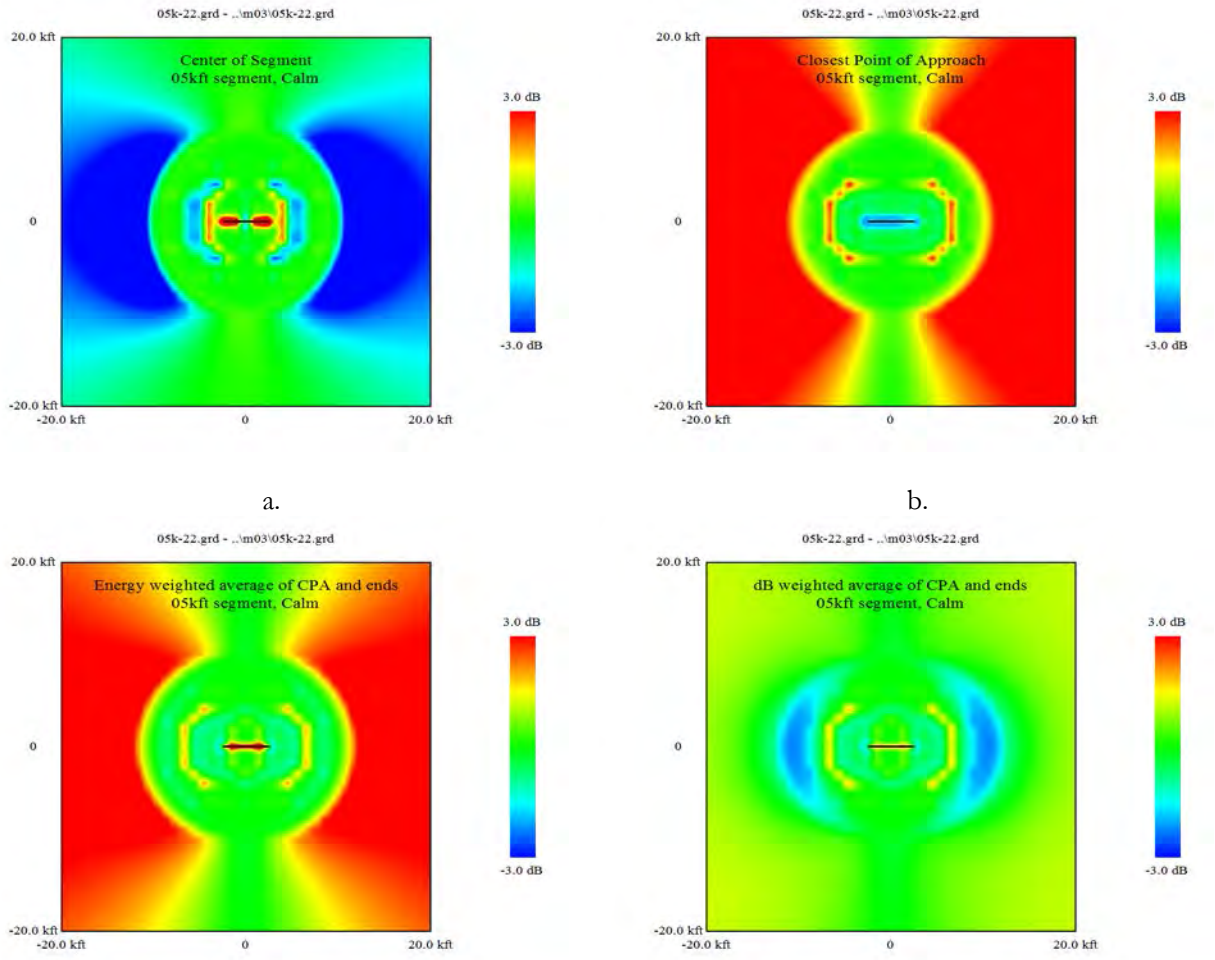

Figure 4-23. Differences, 5000 foot segment, calm atmosphere, four methods
(a) Center of segment; (b) CPA; (c) Energy weighted average; (d) dB weighted average

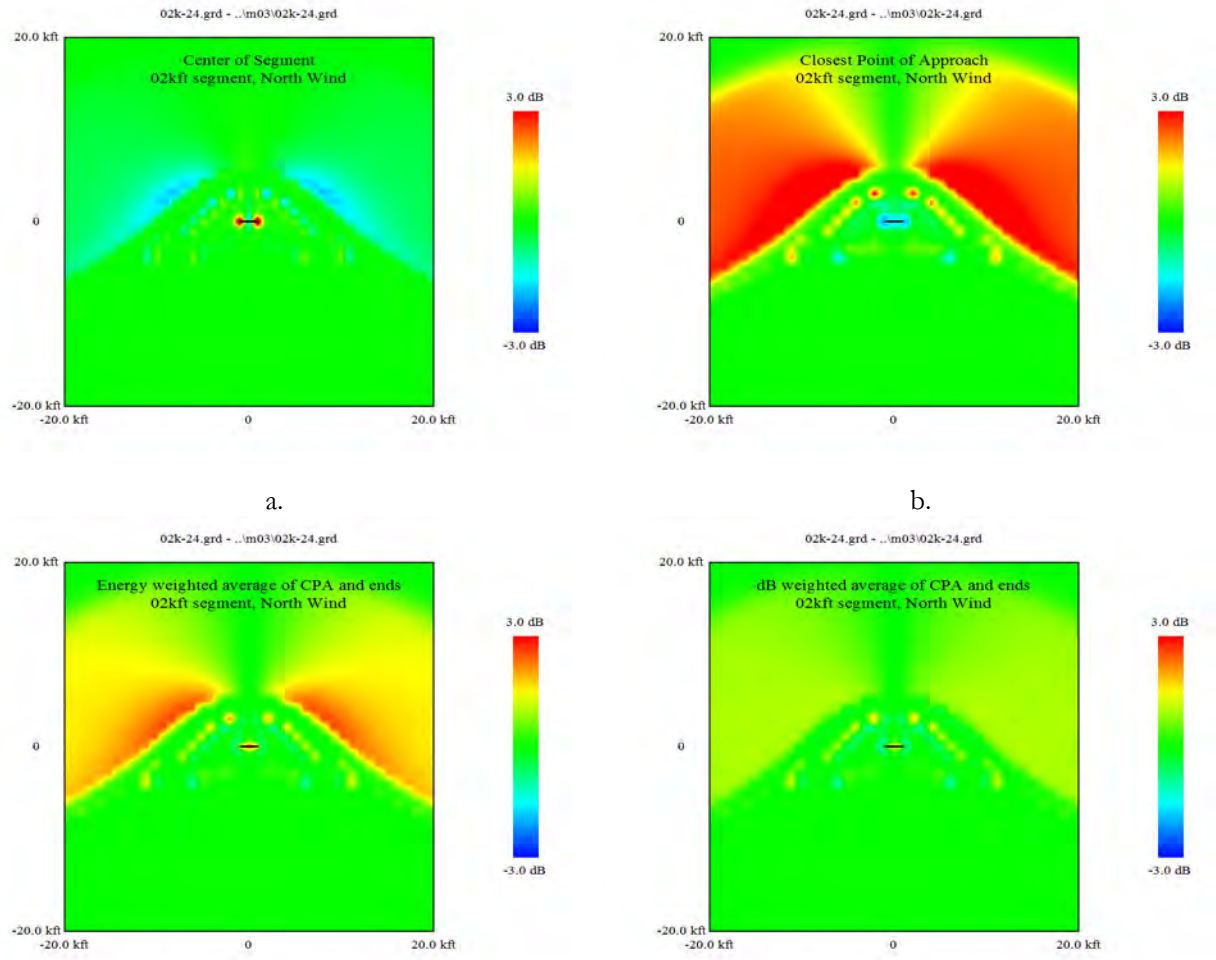

Figure 4-24. Differences, 2000 foot segment, north wind, four methods
(a) Center of segment; (b) CPA; (c) Energy weighted average; (d) dB weighted average

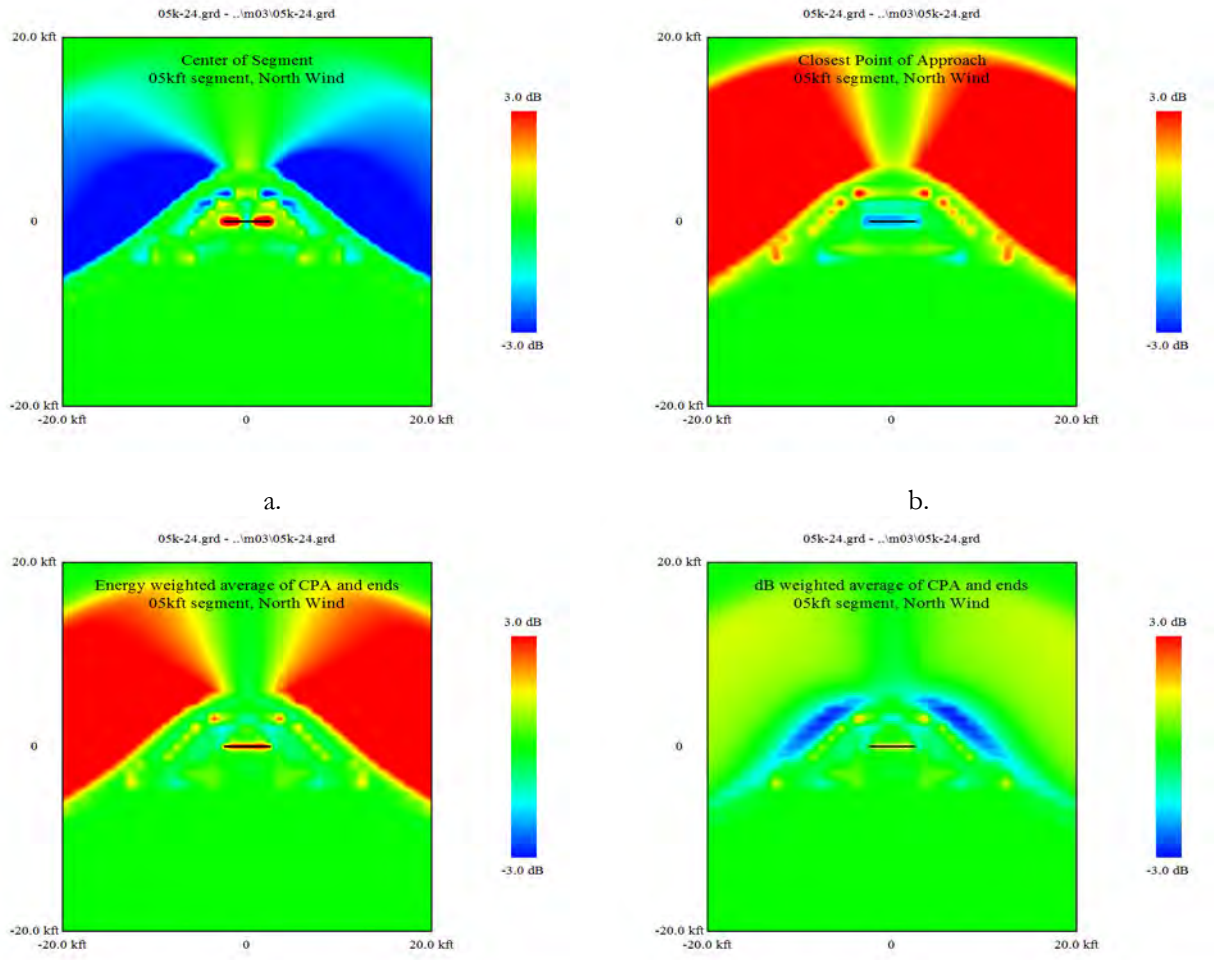

Figure 4-25. Differences, 5000 foot segment, north wind, four methods
(a) Center of segment; (b) CPA; (c) Energy weighted average; (d) dB weighted average

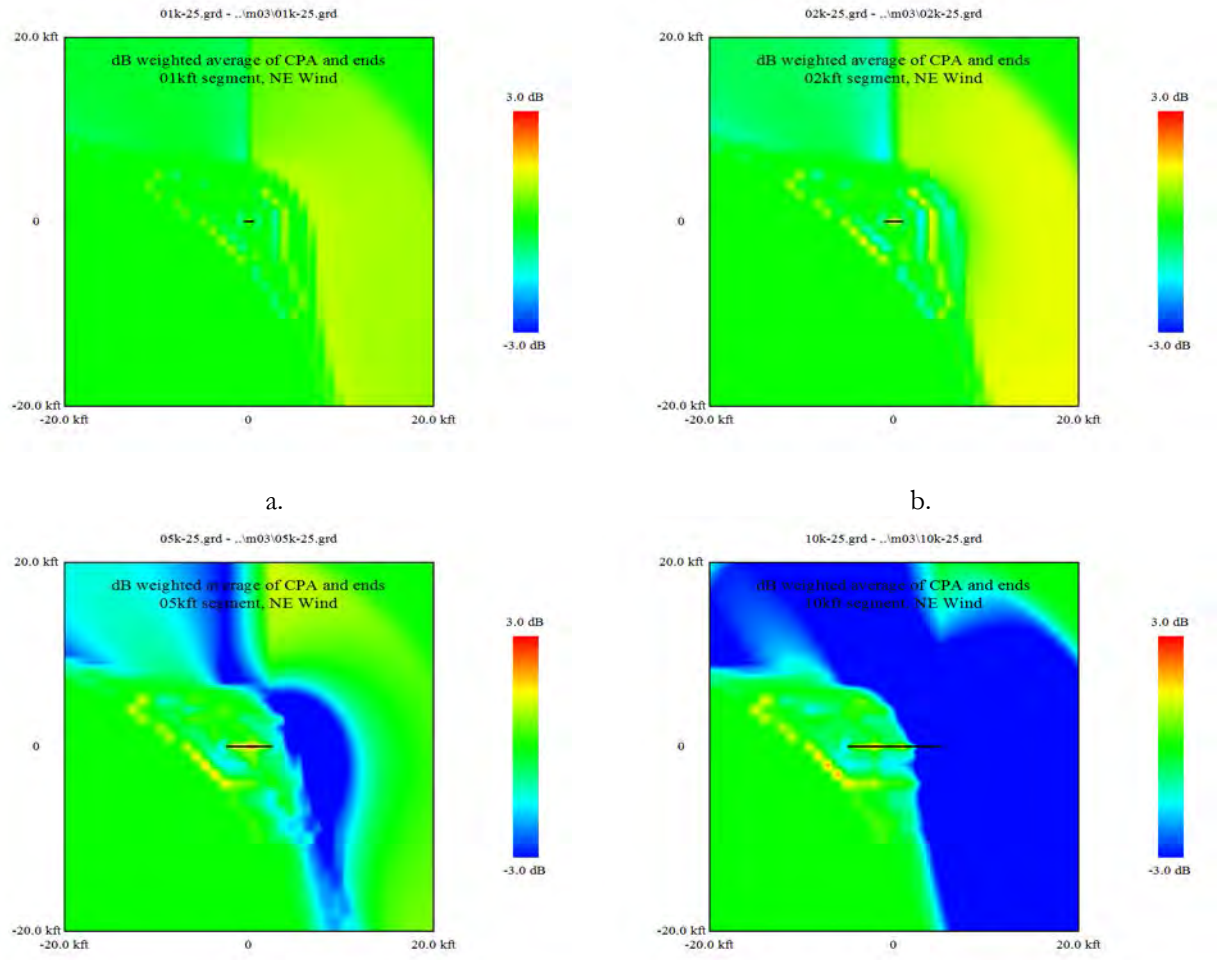

Figure 4-26. Differences, dB weighted average method, NE wind, four segment lengths (a) 1000 ft; (b) 2000 ft; (c) 5000 ft; (d) 10000 ft

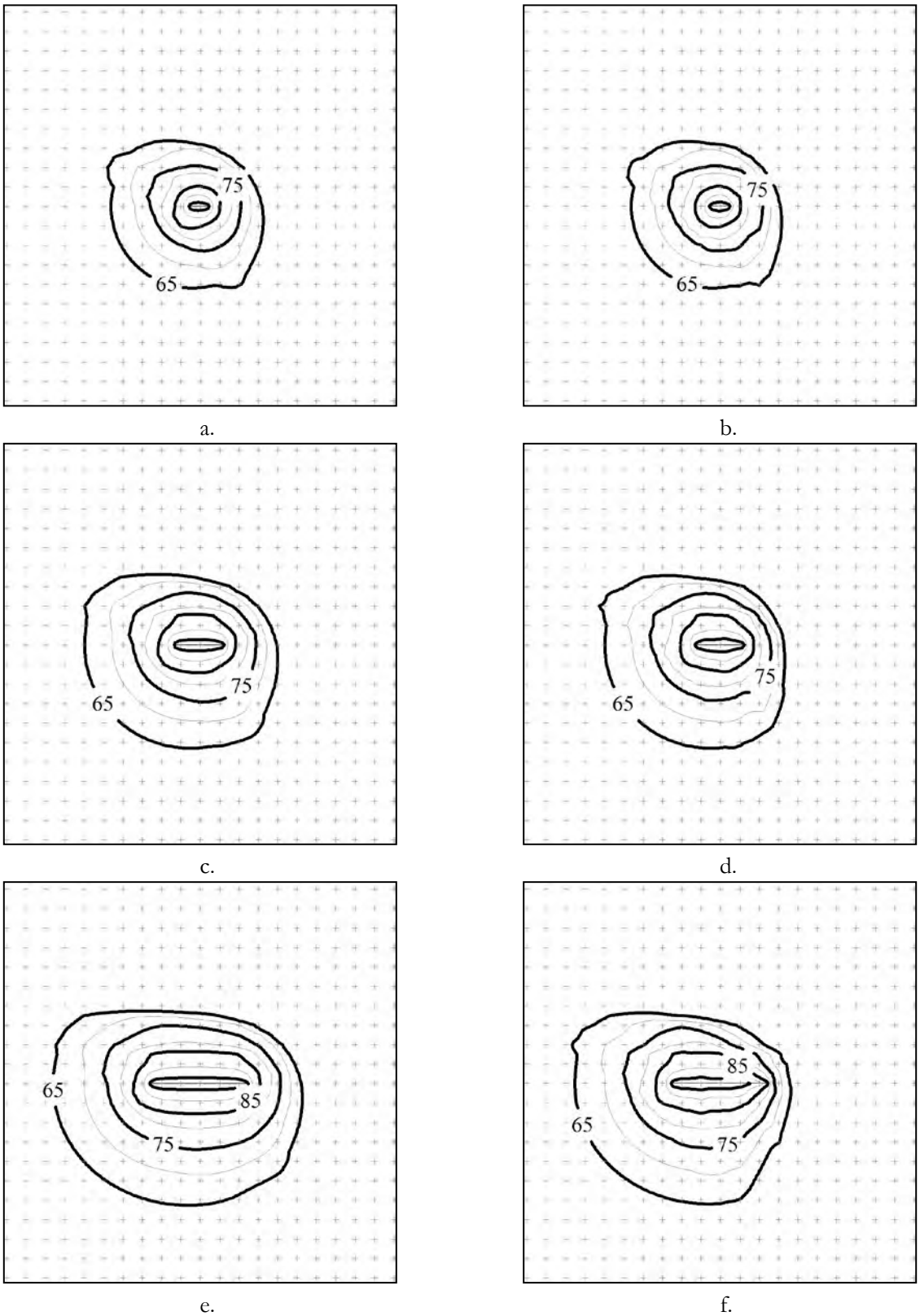

Figure 4-27.Comparison of simulation and dB average method footprints, three segment lengths (a) Full simulation, 2000 ft; (b) dB weighted average, 2000 ft; (c) Full simulation, 5000 ft; (d) dB weighted average, 5000 ft; (e) Full simulation, 10000 ft; (f) dB weighted average, 10000 ft.

References

4-1. Boeker, E., et al. 2008. "Integrated Noise Model (INM) Version 7.0 Technical Manual", FAA-AEE-08-01, January.

4-2. Koopman, J., et al. 2012. "Aviation Environmental Design Tool (AEDT) Technical Manual, Version 2a," DOT-VNTSC-FAA-12-09, November.

4-3. Society of Automotive Engineers, Committee A-21, Aircraft Noise. 1996. "Procedure for the Computation of Airplane Noise in the Vicinity of Airports," Aerospace Information Report No. 1845, Society of Automotive Engineers, Inc., Warrendale, PA, March.

4-4. Society of Automotive Engineers, Committee A-21, Aircraft Noise. 2006. "Method for Predicting Lateral Attenuation of Airplane Noise," Aerospace Information Report No. 5662, Society of Automotive Engineers, Inc., Warrendale, PA, April.

4-5. Plotkin, K.J. 2001. "The effect of atmospheric gradients on aircraft noise," JASA Paper 3aNSa2, June.

4-6. Plotkin, K.J. 2004. "Continued Analysis of the Effects of Atmospheric Gradients on Airport Noise Contours," Wyle Report WR 04-12, April.

4-7. Rosenbaum, J.E. 2011. Enhanced Propagation Modeling of Directional Aviation Noise: A Hybrid Parabolic Equation – Fast Field Program Method, Ph.D. Dissertation, The Pennsylvania State University, May.

4-8. Poulain, K. 2011. Numerical Propagation of Aircraft En-Route Noise, M.S. Thesis, The Pennsylvania State University, December.

4-9. Plotkin, K.J. 2001. "The Role of Aircraft Noise Simulation Models", Inter-Noise 2001, August.

4-10. Olsen, H., Granoien, I., and Liasjo, K. 2000. "Single Event Aircraft Noise Prediction by NORTIM," Inter-noise 2000, August.

4-11. Miller, N.P., et al. 2002. "Aircraft Noise Model Validation Study," HMMH Report No. 295860.29, June.

4-12. Fleming, G.G., Plotkin, K.J., Roof, C.J., Ikelheimer, B.J., and Senzig, D.A. 2005. "Assessment of Tools for Modeling Aircraft Noise in the National Parks," FICAN, 18 March.

4-13. Czech, J.J., and Plotkin, K.J. 1998. "NMAP 7.0 User's Manual," Wyle Research Report WR 98-13, November.

4-14. Arntzen, M., Heblij, S.J., and Simons, D.G. 2012. A weather dependent noise contour prediction concept: Calculating multi-event noise contours with ray-tracing," AIAA 2012-5412, September.

4-15. Heblij, S.J., Arntzen, M., and Simons, D.G. 2012. "A weather dependent noise contour prediction concept: combining a standard method with ray tracing," EuroNoise Prague.

4-16. Page, J., Wilmer, C., Schultz, T., Plotkin, K. and Czech, J. 2012. "Advanced Acoustic Model Technical Reference and User Manual," Wyle Report WR 08-12, February.

4-17. Plotkin, K.J. 2001. "Analysis of Acoustic Modeling and Sound Propagation in Aircraft Noise Propagation," Wyle Report WR 01-24, November.

4-18. Burley, C.L., and Pope, D.S. 2012. "APET2 User Guide," NASA Langley Research Center, Draft, May.

5.0 Airport Noise Modeling Validation Studies and Datasets

A literature search was conducted to identify noise studies incorporating both measurements and modeling at different airports and ascertain whether, if empirical datasets were to be made available, they contain sufficient detail to verify and validate propagation modeling algorithms under different airport, weather and operational conditions. While many US airports have noise monitoring and radar systems, very few articles have been published documenting comparisons between acoustic measurements and modeling for individual events. The search for suitable existing datasets was therefore broadened to include international studies.

The variability inherent in environmental conditions and operational practices dictate that accuracy and modeling validation judgments are based on statistically relevant comparisons, requiring a significant number of data points. Isolated operations can be analyzed in detail to gain understanding about physical mechanisms under a variety of conditions. They alone, however are not suitable for model "validation." The comparative results from a multitude of single-event modeling analyses must be aggregated. This concept is at the core of a multitude of INM validation studies spanning the decades.[5-1,5-2,5-3,5-4,5-5] Comparison of long term aggregated noise monitoring results with airport annual DNL contours is not sufficient for determining accuracies and limitations of propagation modeling physics, so studies which did not utilize a "summation of single events" approach and only relied on long term comparisons of DNL, or those seeking "contour calibration factors" are not included.

The data elements required to conduct a single-event acoustic modeling prediction and comparison with empirical data include the following geospatially referenced and time-synchronized data:

- Required:
  - Local meteorology (temp, humidity, wind speed and direction)
  - Vehicle position information (X,Y,Z)
  - Vehicle Configuration (Airframe / engine combination)
  - Acoustic time history (dBA)
- Bonus:
  - Aircraft weight
  - Flight Data Recorder Information
  - Engine operating state
  - Spectral acoustic time history

At a minimum the aircraft position and flight speed is required. Algorithms exist for estimation of operating state (thrust) from positional data such as the CATs code,[5-4] INM procedure step modeling[5-6] and the AEDT[5-7] thrust-from-position methodology. The ideal dataset will contain flight data recorder information indicating the engine operating state time history; however such information is very costly to obtain even for a small number of operations, and hence remains the "holy grail" in community noise acoustic empirical data.

Findings and Recommendations

A listing of the publications / datasets that were reviewed may be found in Table 5-1. The empirical datasets were not examined themselves, but assessed based on the report documentation. They are ranked (High / Medium / Low) in terms of suitability for subsequent modeling comparisons. The low priority datasets are listed in reverse chronological sequence. Table 5-1 includes the following information:

- Org – the organization responsible for data gathering or sponsoring the study.
- Location – Airport(s) where the noise measurements were conducted.
- Purpose – the intention of the original study / reasons for gathering the data.
- Measurement Dates – the older studies do not contain a relevant fleet mix.
- # Mic Sites – noise monitoring locations and/or supplemental acoustic measurement sites.
- # Noise events – correlated flight-noise event at a single microphone.
- Distance from SOTR – approximate indication of furthers microphone location.

- # Flight Ops – this was not always itemized in the reports.
- Takeoff – indicates whether takeoff data was recorded.
- Landing – indicates whether landing data was recorded.
- Tracking Data – source of aircraft position data, ARTS IIIa was frequently used.
- Op Source – Sch refers to scheduled commercial air carrier operations.
- Aircraft Types – itemized where possible, for studies with large numbers of noise events the fleet mix can be assumed to be the full fleet in operation at that airport at that time.
- Meteorology – most datasets contain airport surface data. Few have upper air balloon data, but US upper air data can be retrieved from NOAA historical databases.
- Notes – observations relevant to this study gleaned from reading the reports.
- Report date.
- Reference Citation – source of the report data.

The following paragraphs describe those ranked High or Medium priority for consideration in future modeling studies and align with the numbered datasets of Table 5-1.

1. Denver Dataset – 1997. In the US, the most comprehensive dataset was gathered in Denver in 1997 and was the source of the data used for other tasks in this study. It is unique in that synchronized tracking and acoustic data is accompanied by airline provided equipment and weight data. The high altitude operations can provide some difficulties in that aircraft performance modeling under environmental conditions at DIA is more challenging than at sea level.

The current and prior DIA studies[5-4,5-5] only considered the May 21 – 30, 1997 data. Due to funding limitations, the June 1 – 13, 1997 measurement data was neither processed nor analyzed, but has been archived for future use. The focus of the current and prior studies was primarily on departure modeling, specifically reduced thrust modeling, so the approach data was also never fully processed for May or June. Given the availability and completeness of this dataset, it should be seriously considered for future validation studies.

2 & 3. UK CAA Measurements – 1998 – 2001. The UK CAA has undertaken a series of comprehensive validation and noise monitoring system verification measurement campaigns. Many of these were triggered by expected large changes in contours due to retirement of the Concorde. The sheer magnitude of the datasets, variety of aircraft types, including the large noise monitoring distances (up to 30km from the airport) make them an attractive set for study. The potential for using UK data would best be pursued as something cooperative, to be discussed with UK partners, possibly as a funded ACRP or SAE A-21 project.

4. Wyle Boston, 2007. This dataset was gathered as part of the Boston Logan Airport Noise Study CY 2005 and 2007 Noise Modeling Analysis. The fidelity of INM modeling and hence the noise predictions was strictly controlled for that study, however the dataset could be utilized with customized profiles or thrust-from-position modeling to improve the comparisons. The dataset contains radar tracking and 1 second time history data for 5 days each in April, May and June 2007. Measurement sites were up to 20 miles from the airport. Aircraft types were varied. This dataset offers some advantages over Denver in that Boston is a sea level airport.

5. SINTEF, Oslo, Gardermoen, Norway – 2001. The Norwegian dataset was gathered to improve ground effect modeling and installation source directivity characterization in their noise model. This dataset is unique in that it includes flight data recorder information which presumably indicates the engine operating state. Unfortunately the noise monitoring locations were just beyond the runway to intentionally gather data before the aircraft have dispersed laterally. In this region the aircraft are still at a low altitude making the data less useful for assessing propagation effects and overall modeling validation at distances beyond the typical airport boundary.

6. Airservices Australia. This publication indicates that a noise and flight path monitoring system exists at eight of Australia's major airports which continuously monitors noise and records flight tracks and operational information from the airport radar systems. The Lochard system also correlates the noise with the tracking data. No other papers describing the details of the data systems or providing examples of measurements could

be located. If such correlated noise measurement and tracking / operational data could be obtained it is likely it could serve useful. This was given a medium ranking because it warrants further investigation.

Other US datasets include those gathered at Dulles in 1994, Seattle-Tacoma and Dulles and Washington National in 1978/1979, Grand Canyon in 1999, Dayton International in 2004 and Boston in 2007. However these datasets are not as comprehensive as the 1997 Denver data and lack either tracking data, aircraft weight data, detailed meteorology data and synchronized 1-second acoustic time history data.

References

5-1. Aldred, J.M., Gados, R.G. 1979. "FAA Integrated Noise Model Validation. Phase 1: Analysis of Integrated Noise Model Calculations for Air Carrier Flyovers", MITRE Technical Report MTR-79-W00095, December.

5-2. Flathers, G.W. 1982. "FAA Integrated Noise Model Validation: Analysis of Air Carrier Flyovers at Seattle-Tacoma Airport", MITRE Technical Report MTR-82W162, November.

5-3. Page, J.A., Plotkin, K.J, Carey, J.N., Bradley, K.A. 1996. "Validation of Aircraft Noise Models at Lower Levels of Exposure", NASA CR 198315, February.

5-4. Page, J.A., Hobbs, C.M., Plotkin, K.J., and Stusnick, E. 2000. "Validation of Aircraft Noise Prediction Models at Low Levels of Exposure", NASA CR 2000-21012, April.

5-5. Forsyth, D.W., and Follet, J.I. 2006. "Improved Airport Noise Modeling for High Altitudes and Flexible Flight Operations", Appendix B, Page, J.A. and Usdrowski, S., "Reduced Thrust Departures from a High Altitude Airport Using Procedure Steps with the Integrated Noise Model", NASA CR 2006-214511, October.

5-6. 2008. "Integrated Noise Model (INM) Version 7.0 Technical Manual", FAA-AEE-08-01, January.

5-7. Aviation Environmental Design Tool (AEDT) System Architecture. 2008. Document #AEDT AD-01, Section 3.7.1, June.

Intentionally left blank

Table 5-1. Noise and Operational Empirical Datasets and Studies

	Suitability for INM	Org	Study	Location	Purpose	Dates	# Mic Sites	Events	Dist from SOTR	# Flight Ops	Takeoff	Landing	Tracking Data	Op Source	Aircraft Type	Terrain	Meteorology	Notes	Report Date	Reference Citation
1	H	Wyle						modeled in detail		3685	Y	Y	Radar	Sch	Many	Flat-ish	Surface and 2/day balloon 2000		2000	
2	H	UK CAA	Validating the CAA Aircraft Noise Model with Noise Measurements Noise Mapping - Aircraft Traffic Noise	London Heathrow, Gatwick & Stansted	Adjustment of NPDs Contour Update Post-Concorde	Summer 2001	10 + 5 + 8 fixed +25 mobile	278000, 330000, 219000	Heathrow: 25-30km		Y	Y	Radar	Sch	Many	Flat-ish	Yes	Commissioned to update contours due to Concorde retirement. Noise data has 55-65 dBA recording Threshold. No indication of how the "AC mass" was estimated for determining Thrust. Internoise Report only shows arrival predictions from 25 ops.	2001-2004	Rhodes, D.P., Ollerhead, J.B., "Aircraft Noise Model Validation", Internoise 2001, The Hague, Netherlands, Aug 2001. "Noise Mapping - Aircraft Traffic Noise" ERCD Report 0306. http //archive.defra.gov uk/environment/quality/noise/environment/mapping /research/aviation/documents/aircraft-noise.pdf Rhodes, D.P., White, S., Havelock, P., "Validating the CAA Aircraft Noise Model with Noise Measurements", IoA Paper, June 2001.February 2004. http //www.caa.co.uk/docs/68/Valid_ANCON pdf Jopson, I., Rhodes, D., Havelock, P., "Aircraft Noise Model Validation - How Accurate Do We Need to Be?" http //tzone.99k org/dap_ercd_1102_modelaccuracy.pdf
3	M	UK CAA						Dep: 38460			Y	Y		Sch	22/53 types	Flat	Hourly surface			
4	M	Wyle	Modeled vs. Measured Aircraft Noise Evaluation	Boston	Pred. vs. Measurements	Apr, May June 2007 5 days /month	6	152	~20mi	n/a	Y	Y	Radar	Sch	Varies	Flat-ish	Surf	1 sec Leq, integrated metrics Compared.	2010	"Boston Logan Airport Noise Study CY2005 and 2007 Noise Modeling Analysis", Wyle Research Report WR 10-10, May 2010.
5	M	SINTEF				June 2001		70,000		155	Y	Y	FDR	Sch	Many	Flat, grass	0, 10m		2002	
6	M	ESB Australia	Noise and Flight Path Monitoring at Australian Airports	Australia	NFPMS System Description	n/a	11-Sydney to 1-Canberra	n/a	n/a	n/a	n/a	n/a	Radar	Sch	n/a	n/a	Airport	1 second data Tx for many airports. Looks like an interactive WebTrack Tool exists.	2004	Kenna, L.C., "Noise and Flight Path Monitoring at Australian Airports", Proceedings of ACOUSTICS 2004, November 2004.
7	L	Wyle				Summer 2004		n/a		1947	Y	Y	ARTS	Sch	Mix	n/a	Hourly Surface		2004	
8	L	EMPA	Modeling of directivity in FLULA	Zurich Geneva	Prediction vs. Measurements	2000	5	n/a	10km	495	Y	N	Radar	Sch	A320 RJ100 737 MD83	n/a	Surface	Used flyover to get directivity patterns (curve fits) then tested the model with commercial ops.	2002	Pirytzko, S., Butikofer, S., "FLULA - Swiss Aircraft Noise Prediction Program", Acoustics 2002 Conference, Australia, November 2002.
9	L	NPS				Sept 1999		301 hours			N	N	Video / Obs	Tour	Small	Extreme			2003	
10	L	HMMH	NM Accuracy	Denver Minneapolis	Prediction vs. Measurements	4/95-3/96 5/96-4/97 3days /month	DIA-32 MSP-24	n/a	~20mi ~8mi	46787 52927	Y	Y	ARTS	Sch	Varies	Flat-ish	Surface	Parallel effort to Wyle NM DIA. Validation study. MSP data is lower altitude, but doesn't offer much beyond current DIA.	2000	Miller, N P., Anderson, G.S., Horonjeff, R D., Kimura, S., Miller, J.S., Senzig, D A., Thompson, R.H., "Examining INM Accuracy Using Empirical Sound Monitoring and Radar Data", NASA CR 2000-210113.
11	L	Mitre/FAA				1981		58,000			Y	Y	ARTS	Sch	B727 B737 DC9 A300 DC10 L1011 B747	Flat-ish			1982	
12	L	Mitre/FAA	NM 2 Validation Study	Washington National & Dulles	Prediction vs. Measurements	May 1978 - Jan 1979	8	>6000	up to ~10 mi	n/a	Y	Y		Sch	707 727 737 747 DC8 DC9 DC10 L1011	Flat	n/a	AC position "estimated'	1979	Aldred, J.M., Gados, R.G., "FAA Integrated Noise Model Validation. Phase 1: Analysis of Integrated Noise Model Calculations for Air Carrier Flyovers", MITRE Technical Report MTR-79-W00095, December 1979.
13	L	Boeing				1977				10	N	N	Video / gyro & INS	Test	747-JT9D	Flat	Surface & Vertical		1980	

Intentionally left blank

6.0 Simplified Terrain Processing for Aircraft Noise Models

6.1 Introduction

As part of development of algorithms for propagation of sound over varying terrain,[6-1] a simple binary topography elevation file format was developed. This format, which has been standardized to a form very similar to Noisemap Binary Grid Format (NMGF)[6-2] Version 1.0 and denoted type "ELV",* is used in current DoD noise models.[6-3,6-4,6-5] The format is compact and efficient to use. A key feature is that the format is source-independent, so that the noise model itself does not require information about the original data source. That is handled by the ELV building process having two stages. The first is to import original topography source data and write it, unchanged, into an "xyz" file that consists of UTM easting, northing and elevation, in meters. The xyz file also contains zone number and the rotation angle between local true geographic east/north and UTM. The second stage is to write the ELV file, selecting the area to be covered, units, grid origin, and grid orientation.

Creating ELV files is generally done via GUI software packaged with the DoD models. That software requires manual operation and is platform-dependent. This Memorandum provides batch version of ELV building software, written in standard Fortran 90/95. This is portable to any system, and lends itself to automation. Routines for reading and using ELV files are included, along with a graphical demonstration program.

6.2 The ELV Format

This is a binary format whose basic structure is organized in blocks of four character words. Each block consists of:

- A four byte ASCII keyword.
- A one-word (4 byte) integer, specifying how many more words there are in the block. This word is denoted the "count," and has a value n.
- n words of data.

An ELV file does not have to contain all potential keywords. It can also contain keywords that a particular program does not make use of. If a keyword is unknown, the program can skip the next n words and continue.

The data are specific to the particular keyword, and can be floating point, integer or text. An ELV file contains the following keywords:

TITL specifies the format version of the file. Count is always 4. The 4 words are

'Grid'
'Vers'
1
0

which specifies that this is nominally a NMBGF Grid file, Version 1.0.

CASE allows a user comment or title. Count depends on the length of text. The content is:
number of bytes (one word)
text (count-1 words)

If the number of characters is not evenly divisible by 4, it is filled out with blanks so as to occupy count-1 words.

* NMGF is based on a "TPP" format developed under the NATO/CCMS propagation studies. Initially, TPP was replaced with NMGF 1.0. NMGF has grown well beyond terrain handling. With that growth, backwards compatibility has not been maintained, even within versions. There are thus some differences in keywords between ELV and NMGF 1.0. This report documents the ELV format.

DECM specifies the floating point numeric format. Count is always 2. The content is always 2.

FLOT
1

which specifies that data are floating point numbers, single precision. A data value of 2 means double precision.

FEET specifies that data are in units of feet. Count is always zero.

METR specifies that data are in units of meters. Count is always zero.

(Only one of FEET or METR may be specified.)

DIDJ specifies the dimensions of each cell in the grid. Count is always 2. Contents are:

dx, the x spacing between grid points
dy, the y spacing between grid points

IRJR specifies the grid point corresponding to the coordinate origin. Count is always 2. Contents are:

ir index in the x direction
jr index in the y direction

If the origin is to be the lower left corner of the grid, then ir, jr would be 1,1.

NINJ specifies the grid dimensions, points in the x and y direction. Count is always 2. Contents are:

ni number of grid points in x direction
nj number of grid points in y direction

MTRC specifies the metric represented in the grid. For ELV files, this is Zalt. The count is 2. Contents are:

Number of bytes - always 4 in this context
Either 'Zalt' or 'Flow'

The MTRC keyword in later versions of NMGF is more complex, for general use in NMPLOT. This field is not really needed for ELV application, since the program knows what the file is for.

XRYR specifies the coordinate values at IRJR. The count is always 2. Contents are:

x0 x coordinate at index ir
y0 y coordinate at index jr

UTMZ specifies the UTM zone. Meaningful if coordinates (defined either by XRYR or USER) are in meters and correspond to UTM. Count is always 1. Contents are

UTM zone number

USER specifies information relating the grid defined by XRYR† and units (FEET or METR) to geographic UTM coordinates. Count is always 4. Contents are:

xr UTM easting corresponding to the reference point at IRJR
yr UTM northing corresponding to the reference point at IRJR
userang the angle, in radians, between the grid and latitude/longitude at IRJR
ifeet code for whether units in the file are feet (1) or meters (2)

GRID precedes the grid of elevation or flow resistivity data. ZALT is a synonym for GRID in ELV files. Count is ni*nj, the number of grid points. Contents are:

† Note that X0, Y0 are the grid values at ir,jr, and are defined by keyword XRYR, while geographic reference XRYR is defined under USER. This notation has become embedded in ELV software over the years, and is kept for compatibility.

Elevation values, in C matrix order

ENDF specifies the end of the file. Count is always zero.

6.3 Importing Elevation Data: Creating an XYZ file

Stage 1 of ELV creation is to import data from original sources via program MAKEXYZ. This is run from the command line via:

makexyz inputfile

where inputfile is a text file with the following lines:

name of the output xyz file
path to source data files
number of source data files
name of each source file, followed by a code defining its type

The path must include the final delimiter, "\" on Windows PCs. The last line must be repeated corresponding to the number on the third line. The type code in the last line must be separated by at least one space. The distribution contains two sample files, ticond.ctl and float.ctl. (The extension ctl, for "control," is not required.) The file types are:

1 DLG (optional format)
2 DEM (ASCII)
3 ASCII grid
4 DTED
5 GridFloat
6 DEM (Binary)
7 APET (Tecplot as used by NASA's APET propagation code)

The sample file for GridFloat input is:

float.xyz
float\
1
93032593.flt 5

For GridFloat, the float\ directory must contain the flt and hdr files.

When makexyz is run, the name and type of each file is displayed on the screen, and a final few lines of information are written at the end.

The source files should cover the area that is desired for the ELV grid. It is strongly recommended that file types not be mixed, i.e., use only one file type. Nothing precludes mixing types, but the data sources between different types are often inconsistent.

For DLG, only optional format files are used. (The older standard format is obsolete.) DLG files obtained from USGS sometimes include line breaks, and sometimes are organized in 80 byte blocks with no line breaks. Line breaks are required. A utility, "add80cr," is included. It is run at the command line via

add80cr infile outfile

Make sure that outfile is a different name than infile.

Installing makexyz consists of copying it into an appropriate directory. There is a subdirectory "RND" (included in the distribution) that contains conversion tables from NAD27 to NAD 83 and WGS84. That must be present as a subdirectory to the program directory. If it is not, the program will halt with a warning message.

The xyz file is not necessarily of interest to the user. In the GUI versions of this software packaged with DoD noise models, it is a temporary file not preserved. In the version documented in this Memorandum, it is preserved and reviewing it may be of interest. It is also possible to manually create an xyz file, such as to create a special-purpose ELV file without delving into binary formats. The xyz file consists of the following lines:

Line 1: utmang izone nlines

where

utmang = rotation angle, radians, counterclockwise, of UTM easting and northing re: geographic east and north
izone = UTM zone
nlines = number of x,y,z lines to follow

Lines 2 through nlines+1: x y z

where

x = UTM easting, meters
y = UTM northing, meters
z = altitude, meters

Data are space delimited, and each line must contain all three specified items. The file must contain a total of nlines+1 lines.

6.4 Creating an ELV File

After an xyz file is prepared, the xyz file is generated via program xyz2elv. The command line is

xyz2elv inputfile

where inputfile is a text file that contains a single namelist block. The following are the contents of sample "float.nml":

```
&inputs
xyzfile   = 'float.xyz'
elvfile   = 'floatx.elv'
xstart    = 312000.
ystart    = 4286000.
gx        = 323000.
gy        = 4296000.
latlong   = .false.
ifeet     = 0
nx        = 201
ny        = 201
user      = .false.
xr        = 312000.
yr        = 4286000.
ir        = 1
jr        = 1
```

```
x0        =  312000.
y0        =  4286000.
userangdeg  =  0.
/
```

The definitions of each quantity in the file are in two groups: those always needed, and those needed only for user defined coordinates.

- xyzfile — the input xyz file
- elvfile — the name to assign the elv file
- xstart, ystart — coordinates of SW corner of the grid area
- gx,gy — coordinates of NE corner of the grid area
- latlong — flag set to .true. if coordinates are longitude/latitude, .false. if UTM
- ifeet — 1 if units in the ELV file are to be feet, 2 if meters
- nx,ny — grid dimensions
- user — .true. if user coordinates are to be specified, .false. if not

If user = .true., the following are needed:

- xr,yr — geographic coordinates at reference point ir,jr
- ir,jr — grid point of the reference points
- x0,y0 — user coordinates at the reference point
- userangdeg — the angle the user-defined grid is to make with longitude/latitude

The default for the ELV file is UTM, meters, with the reference position at ir,jr = 1,1. ifeet is needed only if units of feet are required, but still aligned with the UTM system.

When creating and ELV file, quantitative judgment is needed to select the grid dimensions nx,ny. These will interact with the distance between the SW and NE corners of the grid to determine mesh size dx,dy. Appropriate values will depend on the horizontal scale of the terrain, i.e., finer dx,dy values will be needed in a region with steep terrain versus smoothly varying or flat regions. A finer than necessary ELV file will take longer to generate and will occupy more memory, but will not adversely affect performance of the terrain handling routines. Program elview, described in Section 6, can be used to view and assess the results with the selected and alternate (i.e., traditional "double or halve the mesh") dimensions.

6.5 *Using ELV files*

Four subroutines are provided to read and use an ELV file. The elv file is first opened for binary access by a statement like:

```
open(unit=lunit, file=xyzfile,form='binary')
```

Routine **elsize** is then called:

```
elsize(nx,ny,lunit)
```

Pre-reads an ELV file to determine the grid size, so the main program can allocate a grid. nx,ny are the grid dimensions, and a suitable grid file is allocated, e.g

```
allocate(z(ni,nj))
```

The file is then rewound, and routine elevnm called to read the data:

call elevnm(title,ntit,ifeet,x0,y0,izone,dx,dy,z,ni,nj,ir,jr,'ZALT',xr,yr,userang,lunit)
The variables in the argument list correspond to the quantities defined in Section 2.0

The file may then be closed. Dimensional data (x, y, z, etc.) will all be in the units specified by ifeet.

Elevation data are then accessed by the following routines.

zm = ground(z,ni,nj,dx,dy,xll,yll,xm,ym)

Function that returns the elevation zm at a specified location. Input arguments are:

z	the grid
dx,dy	mesh size, as defined in Section 2.0
xll,yll	lower left corner of grid, as computed from x0,y0,ir,jr,dx,dy
xm,ym	coordinates at which elevation is needed

The algorithm is a simple interpolation between the corners of the grid cell containing xm, ym. The grid cell is found by dividing xm, ym by the grid size. A uniform grid is assumed.

call profil(z,ni,nj,dx,dy,xll,yll,x1,x2,sprof,zprof,npts)

returns equally spaced points along a terrain cut from source point x1 to receiver x2.

Inputs are:
z,ni,nj,dx,dy,xll,yll – same as for ground
x1, x2 – two-element vectors containing x,y for the source and receiver locations
npts – number of points desired in the profile

Returned quantities are:

sprof, zprof – vectors of size npts containing distance from x1 to x2 and z at each point.

The algorithm consists of dividing the line between x1 and x2 into npts equally spaced point, and calling ground at each.

call hillcut(x1,x2,prof,npts,hsrc,hrec,hillxz,nmm,imdltyp)

This routine analyzes the profile and fits and a modeled 2 to 5 point fit is generated.

Input arguments are:

x1(2)	x,y of source position, feet
x2(2)	x,y of receiver position, feet
prof(2,100)	array of x and z data for the cross-section of terrain between the source & receiver 1,* = x (radii from source) in ft 2,* = z (elevation) in ft, MSL (Same data as sprof,xprof, but re-organized)
npts	Number of points in profile
hrec	Receiver height above local ground
hsrc	Source height above local ground

Returned quantities are:

hillxz(2,5)	x,z of five points defining the model. The ends are in (i,1) and (i,5), while the middle three are the three important

	intermediate points. i,3 is the highest point: top of the hill if it's a hill, one of the ends if valley or level.
nmm	number of important points in the profile; 1=level; 2 or more=hill or valley
imdltyp	Type of propagation geometry: 1 = level, 2 = hill, 3 = valley.

The three types of propagation geometry, "imdltype," are sketched in Figure 6-1. Types 1 (level), 2 (valley) and two variations of 3 (hill) are shown. Not sketched is type 3 (hill) with one flat, which can be at either end. The algorithm consists of the following steps:

1. The end points of the profile are loaded into hillxz(:,1) and hillxz(:,5).
2. The highest point, relative to a line between the ends, is found and saved as hillxz(:,3)
3. The lowest point between hillxz(:,1) and hillxz(:,3) is found and saved as hillxz(:,2).
4. The lowest point between hillxz(:,3) and hillxz(:,5) is found and saved as hillxz(:,4).

It is possible for points 2, 3 or 4 to overlay with points 1 or 5. The following distinctions are made:

- If all of points 2,3,4 coincide with 1 or 2, then there are just two points and the profile is "level," top sketch in Figure 6-1. ("Level" is relative to a line between 1 and 5.)
- If point 3 is distinct, then the profile is a hill. If points 2 and 4 are distinct, then the hill has two flats, bottom sketch in Figure 1. If points 2 and 4 coincide with 1 and 5, there are no flats, third sketch in Figure 6-1. If one of points 2 or 4 is distinct, there is a flat on the corresponding side.
- If point 3 coincides with either 1 or 5, and one of points 2 or 4 is distinct, the model is valley, second sketch in Figure 6-1.

The relation between the original terrain cut and the modeled profile can be explored via demonstration program "elview."

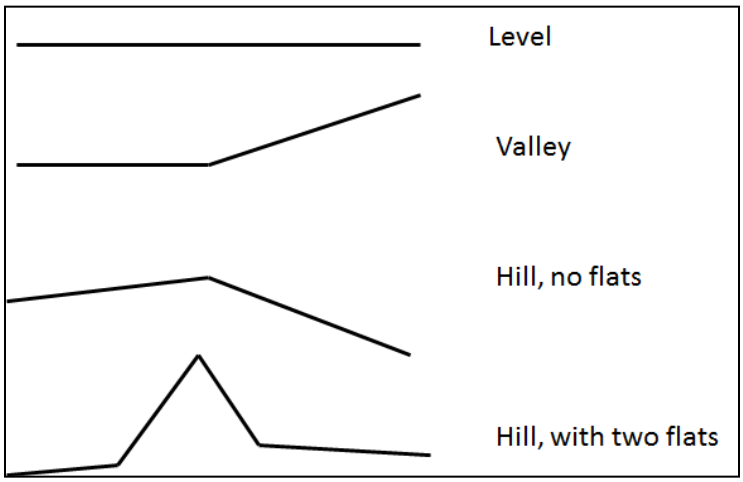

Figure 6-1. Model Propagation Geometries.

6.6 Demonstration Program

A demonstration program, elview, is included in the package. It is run from the command line via

elview elvfile

A simple contour plot of the elevation data will appear. There are ten contour levels, equally spaced between the minimum and maximum z in the file. The status bar at the bottom of the window shows the current x,y positions of the mouse, and z at that location.

Terrain cuts can be extracted:

- Press a to define a source location at the current mouse position.
- Press b to define a receiver location at the current mouse position.

Figure 6-2 shows an example screen after defining a source and receiver. Pressing "c" generates a terrain cut, which appears in a pop-up screen on top of the original contour plot. Source height is fixed at 500 feet AGL, and receiver height at 5 feet AGL. Figure 6-3 shows a typical profile plot. Figures 6-2 and 6-3 are annotated, and should be self-explanatory. Note that Figure 6-3 shows the ground angle at the receiver, a parameter used by INM.

Other active keys are:

- ESC – quit.
- Return – quit profile screen and return to contour screen.
- p – generate a png image of the current screen. A file select dialog will appear.

Source code for elview is included in the package. Graphics are done via the Winteracter library, so this is not portable. Comments in the code identify parts that are related to Winteracter and describe the use of the ELV handling routines.

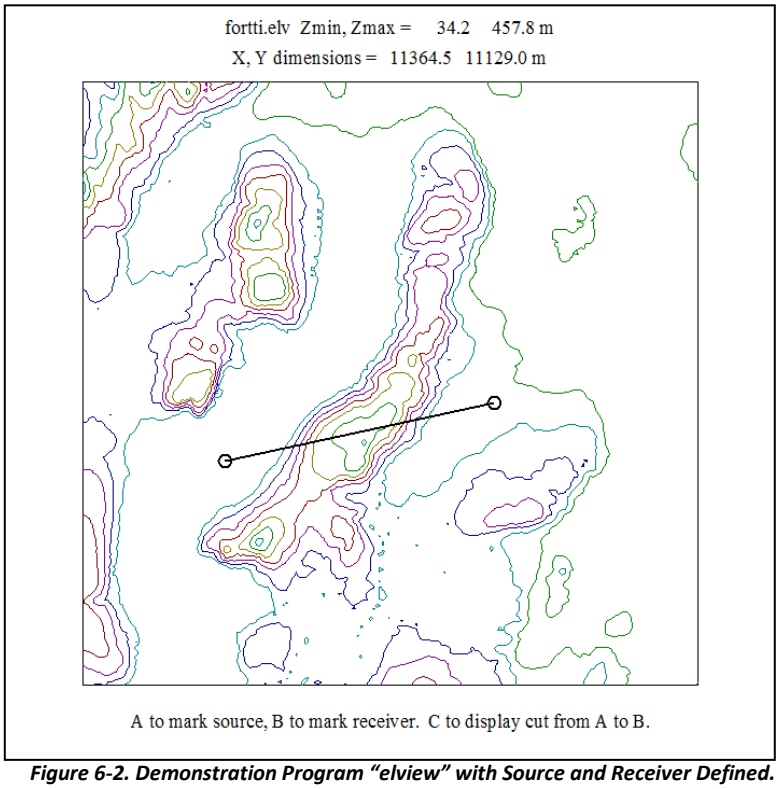

Figure 6-2. Demonstration Program "elview" with Source and Receiver Defined.

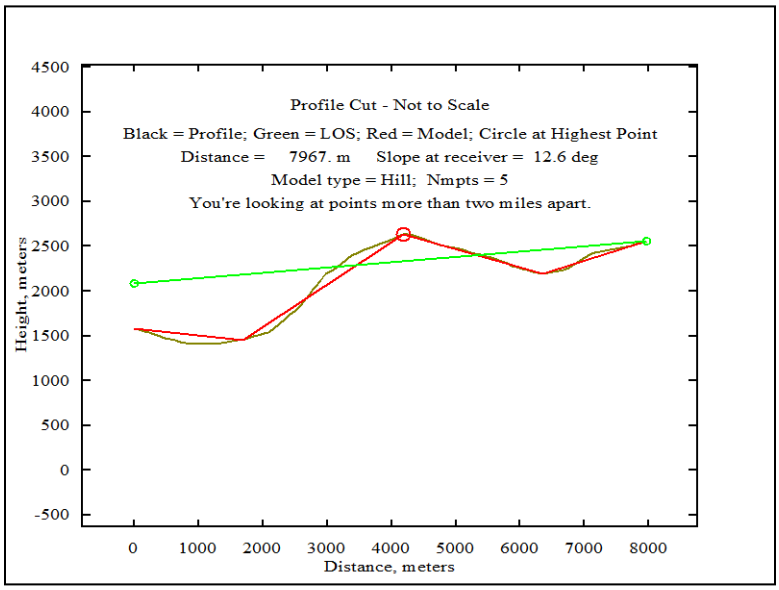

Figure 6-3. Demonstration Program "elview" Showing Terrain Cut and Model.

6.7 Software notes

6.7.1 Portability

The software has been written in Fortran 90/95, avoiding extensions as far as possible. Three items which may not be portable have been used:

1. The ELV file is "stream binary", using the form='binary' specification, which has been available in Microsoft, DEC, Compaq and Intel Fortran compilers for several decades. It is unformatted with no record markers. Fortran 2003 and later are expected to have a standard form for this.
2. Command line arguments are read via routines nargs() and getarg( ). These are extensions that have been available in the compilers noted above. Other compilers have similar functions with varying names.
3. The directory tree delimiter is taken to be "\" as in Windows. This is used to locate the RND directory, which is accessed from module nadcon.for.

elview is, of course, not portable other than across 32 bit Windows systems, but is not intended to be so.

6.7.2 USGS Software

The software uses two packages obtained from USGS. These are the General Cartographic Transformation Package,[6-6] which contains routines that convert between UTM and latitude/longitude coordinates in various datums, and NADCON,[7] which converts UTM coordinates from NAD27 to NAD83/WGS84.

6.8 Error Messages

The following error messages can appear on the console when makexyz is run:

Message: Error in DTED Datum! File rejected!
Cause: A DTED file that is not in WGS84 has been detected
Corrective action: ensure that all DTED source files are WGS84

Message: Got x instead of N
I, ID = [index] [id value]
Cause: Encountered a field type other than "node" when expecting a node. This can happen because of a corrupt file, the wrong type, or possibly a file without line breaks.

Corrective action: Check the integrity and type of the DLG files.

Message: Got x instead of L
I, ID = [index] [id value]
Cause: Encountered a field type other than "line" when expecting aline. This can happen because of a corrupt file, the wrong type, or possibly a file without line breaks.
Corrective action: Check the integrity and type of the DLG files.

Message: Failure to initialize NAD27 conversion data files.
Make sure the RND directory is in place in the program directory.
Cause: The RND directory, and/or its files, as described in Section 3.0, was not found
Corrective action: Make sure the RND directory is in place

Message: Error!!!
Cause: The program failed to open two files from the RND directory.
Correction: Make sure the RND directory is in place, and that the files have not been corrupted from the original versions. (It is unusual to get this message, rather than the general "Failure to initialize…" message.)

Message: The file [file name] is not an optional format DEM file. Please correct your choices.
Cause: The DEM file was not optional format, or was corrupt.
Corrective action: Replace the defective file.

Message: The file [file name] is not an optional format DLG file. Please correct your choices.
Cause: The DLG file was not optional format, or was corrupt.
Corrective action: Replace the defective file.

Message: Invalid File Types!
Cause: A file type in the input file is not one of the types listed in Section 3.0.
Corrective action: Use only types 1-7, and ensure that the files match the types

The following message can appear on the console when xyz2elv is run:

Message: Warning: Minval(z) =value
Cause: Defective xyz file, usually due to ignoring a failure in makexyz.
Corrective action: Review the xyz file, and correct the makexyz run.

References

6-1. NATO/CCMS Working Group Study. 2001. "Aircraft Noise Propagation over Varying Topography," September.

6-2. Wasmer, F. 2002. "A Description of the Noise Model Grid Format (NMGF)," Version 2.5, May (Version 1.0 documentation is no longer available).

6-3. Page, J.A., Plotkin, K.J., and. Downing, J.M. 2002. "Rotorcraft Noise Model (RNM 3.0) Technical Reference and User Manual," Wyle Report WR 02-05, March.

6-4. Page, J.A., Wilmer, C., Schultz, T., Plotkin, K.J., and Czech, J. 2012. "Advanced Acoustic Model Technical Reference and User Manual," Wyle Report WR 08-12, June.

6-5. Moulton, C.L. 1991."Air Force Procedure for Predicting Noise Around Airbases: Noise Exposure Model (NOISEMAP) Technical Report," Wyle Research Report, WR 91-2, September.

6-6. USGS. "General Cartographic Transformation Package," http://edcftp.cr.usgs.gov/pub/software/gctpc/.

6-7. Dewhurst, W. T. 1990. "The Application of Minimum-Curvature-Derived Surfaces in the Transformation of Positional Data from the North American Datum of 1927 to the North American Datum of 1983," NOAA Technical Memorandum NOS NGS-50, January.

Intentionally left blank

7.0 Conclusions and Recommendations

Several aspects of detailed weather and terrain analysis in aircraft noise modeling were examined in this study. The following conclusions were reached.

7.1 Improvements in Modeling KDEN Validation Data

7.1.1 Findings and Recommendations Based on INM Profile Point Analysis

INM prediction of noise from high altitude operations has improved considerably since 1998 for physics based modeling (profile point input) of reduced thrust operations. Both the absolute SEL levels (dBA) and the standard deviations of INM minus measured data comparisons have improved. An assessment of prediction accuracy for various independent parameters suggests that source noise modeling for higher altitudes, (above 15,000 ft MSL) be investigated further, both for noise prediction at larger distances from high altitude airports and for enroute noise computation. Tendencies for overprediction with conditions suggesting increase reduced thrust performance margin warrants further investigation into the assumed temperature prediction methodology (CaTS code). No other strong sensitivities with independent parameters were noted.

Analysis of the data included operations on May 21 – 30, 1997. The May 31 CaTS data was not available. Additional data for the first week of June 1997 has been recorded but was not processed during the initial DIA study and was not included here. It could be analyzed in the future if funds are available. Additionally approach data was never processed nor utilized from any of the prior DIA studies. This could provide additional insight into the accuracy of INM in approach flight modes.

7.1.2 Findings and Recommendations Based on INM Procedure Step Analysis

Comparison of INM predicted noise with measurements from high altitude operations for procedure step modeled profiles for three variants of the B737 has reduced the INM underprediction for reduced thrust high altitude departures. However due to an increase in the difference between the modeled and measured aircraft energy state at the point of closest approach, one cannot definitively credit this reduction in the predictions to improvements in the INM acoustic modeling. Differences in modeled thrust, speed and aircraft location are playing a role as well. The analysis described in Section 2.1utilized profile point trajectories, and held the aircraft location, speed and thrust constant, and was therefore able to provide a definitive indication of the INM acoustic propagation and source modeling improvements. Due to multiple variations in modeling parameters, the analysis described in this section was not able to reach a firm conclusion.

A more direct comparison of INM6 and INM7 procedure step modeling could be obtained by computing new optimal Procedure Steps for the five possible derated thrust jet coefficients using a batch version of INM, or by developing additional automated procedures which permit optimization. As noted earlier, the scope of the current effort did not permit development of new optimization procedures.

It is recommended that an additional study comparing predictions from AEDT thrust-from-position algorithms (or INM algorithms, if available) with the as-measured radar profiles be considered. An assessment of use of these algorithms with reduced thrust jet coefficients should also be explored.

7.1.3 Findings and Recommendations Based on INM Profile Point and Procedure Step Comparisons

Modeling in this study using profile points more closely matches the measured radar data and provides better agreement with acoustic measurement data than the iterative procedure step modeling process. There were considerable differences between the altitude and speed prediction of thrust based on the Assumed Temperature modeling method (CATs) and the INM prediction of thrust using modified reduced thrust jet-thrust modeling coefficients and the energy match at the point of closest approach. These differences cannot be exclusively attributed to the acoustic propagation or noise source database improvements. There are

considerable differences in the location of the point of closest approach and the aircraft operating state at that location between the two classes of profile modeling techniques.

Additional research is needed to ascertain how much of the acoustic differences are due to profile modeling effects and how much is due to INM improvements. It is recommended that the procedure step modeling process be revisited using a newer version of INM. This will likely require a batch version of INM7. The procedure step process relied on five discreet amounts of thrust reduction, however better fits to the measured radar profile might be obtained by utilizing more datasets with higher fidelity.

7.2 Simulation Modeling of KDEN Validation Data

A subset of operations from the 1997 KDEN measurements has been analyzed with three versions of INM and with simulation modeling. The 90 selected operations were departures to the east, generally straight out. INM 6 and 7 and simulation results were comparable to each other, with INM 7 performing best for this data set. NMSim results obtained in 2000 were comparable to newer AAM results. AAM results were slightly better, probably because of updates in the INM database and recent refinements in the sphere making process.

The results were found to be not sensitive to details of layering. Use of narrow band absorption at one third octave band center frequencies was adequate. The KDEN data set, with humidity of 40% and above, is in a relatively low absorption regime and did not exhibit the kind of sensitivity that would occur under dry high absorption conditions. The absorption table specified in SAE 1845 worked well for this data set, comparable to the modern INM and simulation analyses with actual absorption.

The use of SAE 866A absorption rather than the current standard ANSI S1.26-1995 does not appear to have practical adverse effects, but it would be appropriate to use the recognized standard in FAA tools.

7.3 Detailed Weather Modeling in FAA Tools

The key applying detailed propagation models, which are inhomogeneous and/or anisotropic, to FAA tools lies in minimizing the number of propagation points involved. One can always use very short segments, but at a computational cost comparable to a full simulation model but without all the benfits. An analysis was performed, simulating integrated modeling and FAA detailed tooks, via the simulation model AAM. It was found that for segments up to 2000 feet very good results can be obtained with a dB-weighted average of propagation from three points: CPA and the ends. Segments of 5000 feet or longer are not amenable to this simplification.

These results are for a particular worst-case example (low altitude, crosswind) and, in lieu of access to FAA's actual tools, relied on simulation. This analysis should be exercised within the research version of INM to establish segmentation guidelines for general cases.

For laterally homogeneous cases, e.g. propagation through a horizontally stratified atmosphere with gradients over flat terrain, calculation can be pre-computed into a table centered on the aircraft position. Application within the model is then a table lookup/interpolation rather than repeating the calculation.

Propagation over rugged terrain requires segmentation comparable to terrain lateral scale. Pre-computation is, in general, not feasible because the domain is laterally inhomogeneous.

7.4 Airport Noise Modeling Validation Studies and Datasets

A review was conducted of airport noise datasets that would be suitable for analysis similar to that presented in Sections 2 and 3 of this report. Most studies at US airports were found to be not as comprehensive as the 1997 KDEN study analyzed. It was noted that only a portion of the KDEN data was analyzed, but it is not clear that the remaining data are distinct from that which was examined. A 2007 study at Boston Logan has promise, although not as comprehensive as KDEN. The search was widened to outside the US. Several studies in Europe were identified. The conductors of those studies are participants in committee/workshop

activity with FAA (e.g., SAE A-21) and exploration of those data sets would best be accomplished cooperatively through those activities.

7.5 Simplified Terrain Processing for Aircraft Noise Models

The terrain processing routines that are used in the NMSim and AAM simulation models were extracted from their GUI interfaces, and packaged as standard Fortran subroutines suitable for incorporation into FAA tools. A variety of original data sources can be handled, and are reformatted into a standard "ELV" format. The use of a standard format means that new data sources can be accommodated with filters in the extraction process, and will not affect the user programs. Routines for efficiently reading and interpreting the ELV files are included.

Intentionally left blank

Environmental and Energy
Research & Consulting
200 12th Street S, Suite 900
Arlington, VA 22202
www.wyle.com

U.S. Department of Transportation
John A. Volpe National Transportation Systems Center
55 Broadway
Cambridge, MA 02142-1093

617-494-2000
www.volpe.dot.gov

Wyle Report 13-01
DOT-VNTSC-FAA-14-08